# DEVELOPMENT AND IMPLEMENTATION OF HIGH TEMPERATURE RESISTANT RESIN SYSTEMS THAT CAN BE USED WITH FIBER/FABRIC REINFORCEMENT FOR USE IN MISSILE/ROCKET APPLICATIONS

A THESIS SUBMITTED TO
THE GRADUATE SCHOOL OF NATURAL AND APPLIED SCIENCES
OF
MIDDLE EAST TECHNICAL UNIVERSITY

TUĞBA KAYA DENIZ

IN PARTIAL FULFILLMENT OF THE REQUIREMENTS
FOR
THE DEGREE OF DOCTOR OF PHILOSOPHY
IN
POLYMER SCIENCE AND TECHNOLOGY

FEBRUARY 2017

Approval of the thesis:

**DEVELOPMENT AND IMPLEMENTATION OF HIGH TEMPERATURE RESISTANT RESIN SYSTEMS THAT CAN BE USED WITH FIBER/FABRIC REINFORCEMENT FOR USE IN MISSILE/ROCKET APPLICATIONS**

submitted by **TUĞBA KAYA DENIZ** in partial fulfillment of the requirements for the degree of **Doctor of Philosophy in Polymer Science and Technology Department, Middle East Technical University** by,

Prof. Dr. Gülbin Dural Ünver _____
Dean, Graduate School of **Natural and Applied Sciences**

Prof. Dr. Necati Özkan _____
Head of Department, **Polymer Science and Technology**

Prof. Dr. Erdal Bayramlı _____
Supervisor, **Chemistry Department, METU**

Prof. Dr. Özdemir Doğan _____
Co-supervisor, **Chemistry Department, METU**

**Examining Committee Members:**

Prof. Dr. Halil İbrahim Ünal
Department of Chemistry, Gazi University _____

Prof. Dr. Erdal Bayramlı
Department of Chemistry, METU _____

Prof. Dr. Jale Hacaloğlu
Department of Chemistry, METU _____

Prof. Dr. Cihangir Tanyeli
Department of Chemistry, METU _____

Assist. Prof. Dr. Cemal Merih Şengönül
Department of Manufacturing Engineering, Atılım Üniversity _____

**Date:** _____

**I hereby declare that all information in this document has been obtained and presented in accordance with academic rules and ethical conduct. I also declare that, as required by these rules and conduct, I have fully cited and referenced all material and results that are not original to this work.**

Name, Last Name: TUĞBA KAYA DENIZ

Signature :

# ABSTRACT

DEVELOPMENT AND IMPLEMENTATION OF HIGH TEMPERATURE RESISTANT RESIN SYSTEMS THAT CAN BE USED WITH FIBER/FABRIC REINFORCEMENT FOR USE IN MISSILE/ROCKET APPLICATIONS

Kaya Deniz, Tuğba

Ph.D., Department of Polymer Science and Technology

Supervisor : Prof. Dr. Erdal Bayramlı

Co-Supervisor : Prof. Dr. Özdemir Doğan

February 2017, 94 pages

Motor case of a rocket/missile system is exposed to hot and high pressure gases. Its structural components such as control surfaces, outer casing are exposed to mechanical loads and aerodynamic heating due to the high velocity of the system. Therefore reinforced resin matrix polymeric composite materials are needed. These materials are applied inside and outside of the rocket/missile system in order to resist the aforementioned conditions. Considering the increasing difficulties in design criteria, rocket/missile systems that can carry its mission in harsh environments should be manufactured. This necessitates resins that possess advanced thermal and mechanical properties and high Tg than the currently used composite materials. Due to their strategic importance for the defense industry, international treaties limit importing these resins from other countries.

In this thesis, fiber/fabric reinforced composite materials were manufactured from benzoxazine derivatives. The manufactured composite materials were confirmed by accomplishing laboratory scale thermal and mechanical tests.

Synthesis of benzoxazine monomers was achieved in high yields under optimized reaction conditions by using phenol, aldehyde and amine derivatives. The characterization of these compounds was made via NMR and FTIR). Polymerization of these monomers was studied

under appropriate curing conditions. The thermal and mechanical properties of obtained thermoset materials were examined.

The composite materials were manufactured from these resins, which possessed desired thermal and mechanical properties (char yield $\geq$ %30, $Tg \geq 150^\circ$ C).

Keywords: resin, char yield, glass transition temperature, composite, benzoxazine

# ÖZ

ROKET FÜZE SİSTEMLERİNDE ELYAF/KUMAŞ TAKVİYESİ İLE KULLANILABİLECEK YÜKSEK SICAKLIK DAYANIMLI REÇİNE SİSTEMLERİ GELİŞTİRİLMESİ VE UYGULANMASI

Kaya Deniz, Tuğba

Doktora, Polimer Bilimi ve Teknolojisi Bölümü

Tez Yöneticisi : Prof. Dr. Erdal Bayramlı

Ortak Tez Yöneticisi : Prof. Dr. Özdemir Doğan

Şubat 2017 , 94 sayfa

Roket/füze sistemlerinin çalışması esnasında motor gövdesi, içerisinde oluşan yüksek sıcaklık ve basınçtaki gazlara ve sistemin yapısal bileşenleri (kanat, füze dış kaportası) uçuş esnasında ulaşılan yüksek hızlar nedeniyle mekanik yüklemelere ve aerodinamik ısınmaya maruz kalır. Bu nedenle roket füze sistemlerinin içinde ve dışında kullanılan reçine matrisli takviyeli polimerik kompozit malzemelerin söz konusu koşullara dayanması gerekmektedir. Her geçen gün tasarım isterlerinin genişlediği göz önüne alındığında daha zorlayıcı koşullarda çalışacak roket füze sistemlerinin üretimlerine ihtiyaç duyulmaktadır. Bu kapsamda, mevcut durumda kullanılan kompozit malzemeler yerine termal ve mekanik özellikleri gelişmiş yüksek Tg'li reçinelere ihtiyaç duyulmaktadır. Söz konusu reçineler savunma sanayii için stratejik öneme sahip olup yurtdışından temininde ihracat lisansı kullanımları uluslararası antlaşmalar ile sınırlandırılmaktadır.

Bu tez kapsamında benzoksazin türevi monomerler sentezlenerek elyaf/kumas takviyesi ile kompozit malzemeler üretilmiştir. Üretilen kompozit malzemelerin laboratuvar seviyesi termal ve mekanik testleri yapılarak uygunlukları doğrulanmıştır.

Monomerlerin sentezi; fenol, aldehit ve amin türevleri kullanılarak mümkün olduğunca yüksek verimde gerçekleştirilmiş ve elde edilen monomerler spektroskopik yöntemlerle (NMR,

FTIR vb.) karakterize edilmiştir. Sentezlenen monomerlerin uygun olgunlaşma koşullarında polimerleştirilmesi sonucu elde edilen termoset malzemelerin termal ve mekanik özellikleri incelenmiştir.

Termal ve mekanik özellikleri istenilen kriterleri (kül verimi $\geq$ %30, $Tg \geq 150°$ C) karşılayan reçineler kullanılarak kompozit malzeme üretimleri gerçekleştirilmiştir.

Anahtar Kelimeler: reçine, kül verimi, camsı geçiş sıcaklığı, kompozit, benzoksazin

to my love, Tansel

# ACKNOWLEDGMENTS

Firstly, I would like to express my sincere gratitude to my advisors Prof. Dr. Erdal Bayramlı and Prof. Dr. Özdemir Doğan for the continuous support of my Ph.D study and related research, for their patience, motivation, and immense knowledge. Their guidance helped me in all the time of research and writing of this thesis. I could not have imagined having better advisors and mentors for my Ph.D study.

Besides my advisors, I would like to thank the rest of my thesis monitoring committee members: Prof. Dr. Jale Hacaloğlu, Prof. Dr Cihangir Tanyeli, and Prof. Dr. Halil İbrahim Ünal, for their insightful comments and encouragement, but also for hard questions which incented me to widen my research from various perspectives.

My sincere thanks also goes to Assist. Prof. Dr. Mehmet Doğan, Dr. Ümit Tayfun, Dr. Alper Ünver, Dr. Olcay Elmalı, Türkan Güler, Vildan Sanduvaç and Osman Yaslıtaş who provided me vast support in scientific discussions. Without their precious support it would not be possible to conduct this research. Also I thank my friends Ayşegül Hisar Telli, Nehir Utku, Esra Özdemir, Halil İpek, Alinda Öykü Akar and Müberra Göktaş for their endless friendship and support.

I would like to thank my family: my parents and to my brother and sister for supporting me spiritually throughout writing this thesis and my my life in general.

Last but not the least, i would like extend my deepest thanks to my husband, Tansel, who has always been my greatest inspiration, friend and supporter.

# TABLE OF CONTENTS

ABSTRACT . . . . . v

ÖZ . . . . . vii

ACKNOWLEDGMENTS . . . . . x

TABLE OF CONTENTS . . . . . xi

LIST OF TABLES . . . . . xvi

LIST OF FIGURES . . . . . xviii

LIST OF ABBREVIATIONS . . . . . xxii

CHAPTERS

1 BACKGROUND . . . . . 1

2 INTRODUCTION . . . . . 3

2.1 Chemistry of Benzoxazine . . . . . 4

2.1.1 Synthesis of Benzoxazine Monomers in Solution . . . . . 4

2.1.2 Synthesis of Benzoxazine Monomers by Melt or High Solid Methods . . . . . 5

2.1.3 Reaction Conditions and Side Reactions . . . . . 6

2.1.3.1 Effects of Phenol Structure . . . . . 6

2.1.3.2 Effects of Amine Structure . . . . . 7

2.1.3.3 Effects of Synthesis Conditions . . . . . 7

2.2 Polymerization Mechanism . . . . . 8

2.3 Unique Properties . . . . . 8

2.3.1 Near-Zero Volume Changes . . . . . 8

2.3.2 Low Water Absorption . . . . . 10

2.3.3 Glass Transition Temperature (Tg) . . . . . 10

2.3.4 Fast Physical and Mechanical Property Development . . . . . 11

2.3.5 Very High Char Yield . . . . . 11

2.3.5.1 Burning Behavior . . . . . 11

2.3.5.2 Burning Behavior and Thermal Decomposition of Polymers . . . . . 11

2.3.5.3 Flame Retardancy Mechanism of Polymers . . . . 13

2.3.5.4 Flame Retardancy of Benzoxazines . . . . . 14

2.4 Molecular Origin of Unique Properties . . . . . 14

3 EXPERIMENTAL . . . . . 17

3.1 Materials . . . . . 17

3.2 Synthesis of the Monomers . . . . . 17

3.2.1 Solution Synthesis . . . . . 17

3.2.1.1 In Dioxane . . . . . 17

3.2.1.2 In Toluene . . . . . 17

3.2.2 Solventless Synthesis . . . . . 18

3.2.2.1 Synthesis of BA . . . . . 18

3.2.2.2 Synthesis of BP . . . . . 18

3.2.2.3 Synthesis of BZ . . . . . 18

3.3 Composite Production . . . . . 19

3.4 Characterizations . . . . . 19

3.4.1 Structural Characterizations . . . . . 19

3.4.2 Thermal Characterizations . . . . . 19

3.4.3 Rheological Characterizations . . . . . 20

3.4.4 Cone Calorimetry Characterizations . . . . . 20

3.4.5 Density Measurement of Composites . . . . . 20

3.4.6 Mechanical Characterizations . . . . . 21

3.4.6.1 Tensile Tests . . . . . 21

3.4.6.2 Compression Tests . . . . . 22

3.4.7 Thermomechanical Characterizations . . . . . 22

3.4.8 Oxyacetylene Torch Characterizations . . . . . 22

4 RESULTS AND DISCUSSION . . . . . 25

4.1 Synthesis of the Monomers . . . . . 25

4.1.1 Synthesis of BA Monomer . . . . . 25

4.1.2 Synthesis of BP Monomer . . . . . 28

4.1.3 Synthesis of BZ Monomer . . . . . 29

4.2 Polymerization Kinetics . . . . . 32

4.3 Curing of the Monomers . . . . . 34

4.3.1 DSC Analysis of Monomers . . . . . 34

4.3.2 Cure Monitoring Via DSC and FTIR . . . . . 36

4.3.2.1 Curing of BA . . . . . 37

4.3.2.2 Curing of BP . . . . . 39

4.3.2.3 Curing of BZ . . . . . 41

4.4 Properties of polymers . . . . . 43

4.4.1 Dynamic Mechanical Analysis . . . . . 43

4.4.1.1 DMA Properties of PBA . . . . . 43

4.4.1.2 DMA Properties of PBP . . . . . 44

4.4.1.3 DMA Properties of PBZ . . . . . 45

4.4.2 Thermogravimetric Analysis . . . . . 45

4.4.3 Cone Calorimetry Analysis . . . . . 51

4.5 Molecular Origin of the Differences of the Resins . . . . . 57

4.6 Properties of Composites . . . . . 60

4.6.1 Density Measurement of Composites . . . . . 61

4.6.2 Thermal Analysis of Composites . . . . . 62

4.6.3 Mechanical Characterizations . . . . . 62

4.6.3.1 Tensile Tests . . . . . 62

4.6.3.2 Compression Tests . . . . . 66

4.6.4 DMA Characterizations . . . . . 68

4.6.5 Thermomechanical Characterizations . . . . . 68

4.6.6 Oxyacetylene Torch Characterizations . . . . . 69

5 CONCLUSION . . . . . 73

REFERENCES . . . . . 75

APPENDICES

A SOLVENTLESS WITHOUT CATALYST . . . . . 81

B DSC AND TGA ANALYSIS OF PBA . . . . . 91

CURRICULUM VITAE . . . . . 93

# LIST OF TABLES

TABLES

Table 3.1 Types of Mechanical Testing . . . . . 21

Table 4.1 Optimization results for the synthesis of BA . . . . . 26

Table 4.2 Optimization table of BP monomer . . . . . 29

Table 4.3 Optimization table of BZ monomer . . . . . 30

Table 4.4 Exotherm peaks of monomers and activation energies . . . . . 34

Table 4.5 DSC analysis of monomers BA; BP and BZ . . . . . 35

Table 4.6 TGA Results of Resins in $N_2$ . . . . . 47

Table 4.7 TGA Results of Resins in Air . . . . . 50

Table 4.8 Heat Release Behavior of PBA, PBP and PBZ . . . . . 53

Table 4.9 Mass Loss Behavior of PBA, PBP and PBZ . . . . . 57

Table 4.10 Density Measurements of BA and BZ Composites . . . . . 61

Table 4.11 TGA Results of BA and BZ Composite . . . . . 62

Table 4.12 Tensile Test Results of BA and BZ Composites . . . . . 64

Table 4.13 Compressive Strength Test Results of BA and BZ Composites . . . . . 66

Table 4.14 DMA Results of BA and BZ Composites . . . . . 68

Table 4.15 TMA Results of BA and BZ Composites . . . . . 69

Table 4.16 Oxyacetylene Test Results . . . . . 70

# LIST OF FIGURES

FIGURES

Figure 2.1 Various structures of benzoxazine Molecules . . . . . 3

Figure 2.2 Synthesis of benzoxazine monomer . . . . . 5

Figure 2.3 Triazinane intermediate formation and benzoxazine formation from it . . . . 6

Figure 2.4 Dihydroxybenzylamine byproduct formation versus Benzoxazine formation . 7

Figure 2.5 Polymerization mechanism via iminium ion intermediate . . . . . 9

Figure 2.6 Fire triangle . . . . . 12

Figure 2.7 Combustion cycle of polymer . . . . . 12

Figure 2.8 Hydrogen bonding in benzoxazines . . . . . 15

Figure 3.1 Cone calorimetry . . . . . 21

Figure 3.2 Composite tensile tpecimen . . . . . 22

Figure 3.3 Instron universal tester . . . . . 23

Figure 3.4 Compression test sample of BA and BZ . . . . . 24

Figure 3.5 Oxyacetylene torch test setup . . . . . 24

Figure 4.1 Impurity BA monomer signal change with time synthesized without using catalyst . . . . . 27

Figure 4.2 Effect of catalyst amount on occurrence of by- and side products in the synthesis of BA monomer . . . . . 28

Figure 4.3 Change of BP monomer signal with time . . . . . 30

Figure 4.4 Change of intermediates of BZ monomer with time . . . . . 31

Figure 4.5 DSC thermograms of pure and crude BA monomers at different heating rates 33

Figure 4.6 DSC thermograms of pure and crude BP monomers at different heating rates 33

Figure 4.7 DSC thermograms of pure and crude BZ monomers at different heating rates 34

Figure 4.8 DSC analysis of BA, BP and BZ monomers . . . . . 35

Figure 4.9 DSC thermograms BA resin after each cure stage . . . . . 37

Figure 4.10 FTIR spectra of BA resin after each cure stage . . . . . 38

Figure 4.11 DSC thermograms BP resin after each cure stage . . . . . 39

Figure 4.12 FTIR spectra of BP resin after each cure stage . . . . . 40

Figure 4.13 DSC thermograms BZ resin after each cure stage . . . . . 41

Figure 4.14 FTIR spectra BZ resin after each cure stage . . . . . 42

Figure 4.15 DMA curve of PBA after cure cycle of 150 °C 1h180 °C 2h, 200 °C 2h, 220 °C 1h . . . . . 43

Figure 4.16 DMA curve of PBP after cure cycle of 160 °C 1h180 °C 1h, 200 °C 2h, 220 °C 1h . . . . . 44

Figure 4.17 DMA curve of PBP after cure cycle of 160 °C 1h180 °C 1h, 200 °C 2h, 220 °C 1h, 240 45min . . . . . 45

Figure 4.18 DMA curve of PBZ after cure cycle of 160 °C 1h180 °C 1h, 200 °C 2h, 220 °C 1h, 240 1h . . . . . 46

Figure 4.19 DMA curve of PBZ after cure cycle of 160 °C 1h180 °C 2h, 220 °C 1.5h, 250 °C 3h . . . . . 46

Figure 4.20 TGA curve of PBA in $N_2$ . . . . . 47

Figure 4.21 TGA curve of PBA in air . . . . . 48

Figure 4.22 TGA curve of PBP in $N_2$ . . . . . 48

Figure 4.23 TGA curve of PBP in air . . . . . 49

Figure 4.24 TGA curve of PBZ in $N_2$ . . . . . 49

Figure 4.25 TGA curve of PBZ in air . . . . . 50

Figure 4.26 Typical HRR curves for different characteristic burning behaviours . . . . . 52

Figure 4.27 Heat Release Rate Curve of PBA, PBP and PBZ . . . . . 53

Figure 4.28 Total Heat Release of PBA, PBP and PBZ . . . . . 54

Figure 4.29 % Mass Loss Curves of PBA, PBP and PBZ . . . . . 55

Figure 4.30 Mass Loss Rate Curves of PBA, PBP and PBZ . . . . . 56

Figure 4.31 Two Types of Polymers of Benzoxazine . . . . . 58

Figure 4.32 FTIR Spectra of PBA, PBP and PBZ . . . . . 59

Figure 4.33 Hydrogen Bonding of Polybenzoxazine Derivatives . . . . . 59

Figure 4.34 BA BP and BZ High Silica Composite Plates . . . . . 60

Figure 4.35 Density Measurement Samples . . . . . 61

Figure 4.36 TGA of BA Composite at $O_2$ and $N_2$ Enviroment . . . . . 63

Figure 4.37 TGA of BZ Composite at $O_2$ and $N_2$ Environment . . . . . 63

Figure 4.38 Stress strain Curves of BA Composite . . . . . 64

Figure 4.39 Stress strain Curves of BZ Composite . . . . . 65

Figure 4.40 Agglomeration of BZ . . . . . 66

Figure 4.41 Compressive Strength Test of BA Composite . . . . . 67

Figure 4.42 Compressive Strength Test of BZ Composite . . . . . 67

Figure 4.43 DMA graph of BZ High Silica Composite . . . . . 68

Figure 4.44 DMA graph of BA High Silica Composite . . . . . 69

Figure A.1 $^{1}$H NMR spectrum of monomer crude BA synthesized with 20 gr of Bisphenol A, the reaction efficiency is greater than 95 % . . . . . 81

Figure A.2 $^{1}$H NMR spectrum of monomer crude BA synthesized with 100 gr of Bisphenol A, the reaction efficiency is greater than 95 % . . . . . 82

Figure A.3 $^{1}$H NMR spectrum of monomer crude BA synthesized with 200 gr of Bisphenol A, the reaction efficiency is greater than 95 % . . . . . 83

Figure A.4 $^{1}$H NMR spectrum of monomer crude BP synthesized with 10 gr of 4,4-dihydroxybiphenyl, the reaction efficiency is greater than 95 % . . . . . 84

Figure A.5 $^{1}$H NMR spectrum of monomer crude BP synthesized with 20 gr of 4,4-dihydroxybiphenyl, the reaction efficiency is greater than 95 % . . . . . 85

Figure A.6 $^{1}$H NMR spectrum of monomer crude BP synthesized with 100 gr of 4,4-dihydroxybiphenyl, the reaction efficiency is greater than 95 % . . . . . 86

Figure A.7 $^{1}$H NMR spectrum of monomer crude BZ synthesized with gr of 4,4-dihydroxybiphenyl, the reaction efficiency is greater than 95 % . . . . . 87

Figure A.8 $^{1}$H NMR spectrum of monomer crude BZ synthesized with 20 gr of 4,4-dihydroxybiphenyl, the reaction efficiency is greater than 95 % . . . . . 88

Figure A.9 $^{1}$H NMR spectrum of monomer crude BZ synthesized with 300 gr of 4,4-dihydroxybiphenyl, the reaction efficiency is greater than 95 % . . . . . 89

Figure B.1 DSC and TGA analysis of PBA after 93 % curing indicating mass loss during cure . . . . . 91

Figure B.2 DSC and TGA analysis of PBA after 20 % curing indicating mass loss during cure . . . . . 92

# LIST OF ABBREVIATIONS

| | |
|---|---|
| BA | 6,6'-(propane-2,2-diyl)bis(3-phenyl-3,4-dihydro-2H-benzo[e][1,3]oxazine) |
| BP | 3,3'-diphenyl-3,3',4,4'-tetrahydro-2H,2'H-6,6'-bibenzo[e][1,3]oxazine |
| BZ | bis(3-phenyl-3,4-dihydro-2H-benzo[e][1,3]oxazin-6-yl)methanone |
| DMA | Dynamic mechanical analysis |
| DSC | Differential scanning calorimetry |
| TGA | Thermogravimetric analysis |
| TMA | Thermomechanical analysis |

# CHAPTER 1

# BACKGROUND

Motor case of rocket/missile systems are exposed to hot and high pressure gases and their structural components (i.e. control surfaces, outer casing) are exposed to mechanical loads and aerodynamic heating due to the high velocity of the system. These loads can cause damage in the high strength metallic alloys. In order to retain their functionality corresponding systems should be protected from temperature and pressure increase that they are exposed. For this purpose there are some thermal insulation methods one of which is ablative cooling of the system. With this system, exposed thermal or mechanical load are absorbed by the chemical and/or physical rearrangement of the protecting layer via heat or mass transfer [1, 2].

Those thermal ablative materials are composite materials which contain fiber/cloth matrix and organic binders. The reinforcement material has high mechanical strength and thermal stability with a very high temperature melting point. The organic binders on the other hand, have relatively lower melting and decomposition temperature beside their low thermal conductivity constants [3].

Ablative cooling consists of several steps depending on the characteristic of the organic binder [4]. It is known that, high char yielding materials are more resistant than the materials that can easily lose their integrity during the mass loss ablation process. The reason is the formed char layers. It can serve as a thermal protection layer for the below layers and also it is stronger than the original organic binder.

There are some special resin systems used in order to increase the char yield. This system should have some mechanical properties in addition to high char yielding and low toxic smoking properties.

As a result, polymeric composite materials applied inside and outside of the rocket/missile system, should resist the aforementioned conditions. Considering the increasing difficulties in design criteria, rocket/missile systems that can carry its mission in harsh environments should be manufactured. This necessitates resins that possess advanced thermal and mechanical properties and high Tg than composite materials that are employed at present. Due to their strategic importance for the defense industry; the import of these resins from other countries are limited by international treaties.

Due to their thermal and mechanical strength 'Phenolic resins' are used as such systems. Within the phenolics, benzoxazines exhibit some outstanding advantages besides their similarities with the traditional resins. These superiorities can be summarized as follows [5–7]:

- Zero volume shrinkage upon curing.
- Low water absorption
- No need of catalyst for curing
- Easy structural modifications
- Strong inter and intramolecular hydrogen bonding.

In this thesis; fiber/fabric reinforced composite materials were manufactured by synthesizing benzoxazine derivatives considering the developing technology about their use. The properties of manufactured composite materials were confirmed by performing laboratory scale thermal and mechanical tests.

# CHAPTER 2

# INTRODUCTION

Benzoxazine is a molecule in which a *heterocyclic six-membered ring, which contains oxygen and nitrogen atoms* is attached to the benzene ring. Depending on the heteroatoms positions, different kind of benzoxazine structures can be found (Figure 2.1).

The traditional benzoxazine which is used as a commercial thermosetting product is 3,4-dihydro-3-methyl-2H-1,3-benzoxazine.

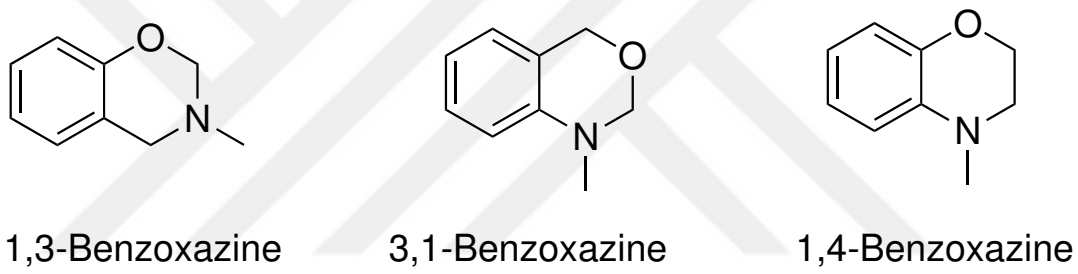


Figure 2.1: Various structures of benzoxazine Molecules

In 1944 Holly and Cope first synthesize this molecule [8] and in 1970 Schreiber patented the synthesis of small benzoxazine oligomers as a modifier for epoxy resins [9, 10]. In the 1980s Reiss et al investigated the formation reaction kinetics of monofunctional benzoxazines. They concluded that monofunctional benzoxazines result in linear manner and larger molecular weight benzoxazine resin could not be achieved with the monofunctional benzoxazine use. Another research investigate that molecular weights of the polymers from monofunctional monomers are between few hundreds to a few thousands depending on the polymerization type [11]. It is as recently as in 1994 that the study on polybenzoxazine properties was reported for the first time by Ning and Ishida [12].

At the beginning, benzoxazine were thought as attractive candidates for replacing the traditional phenolics, which are polymerized by condensation. In addition to phenolic chemistry performance, benzoxazine resin polymerization type eliminates most of the short comings results fro the condensation polymerization type of phenolics. Furthermore benzoxazine is not only an alternative to phenolics with similar thermal properties but also thay are alternatives to epoxies with much more strength in similar processing methods, or they are alternative to bismaleimides with close thermomechanical properties with easier application methods.

Extreme rich molecular structure and design flexibility gives benzoxazine a wide range of physical and mechanical properties and application abilities. The materials property balance such as thermal, chemical, electrical and physical properties are quite well and make them attractive for commercial applications.

Due to the specific and unique properties of benzoxazines such as almost zero volume shrinkage, very high char yield, fast development of mechanical properties as a function of conversion, glass transitions much higher than curing temperatures, excellent electrical properties, and low water uptake despite having many hydrophilic groups, new application areas may be developed.

In addition to formed material properties, during polymerization reactions occurs via a ring opening reaction yielding no by-product. Molecular design flexibility of benzoxazine gives opportunity for different kind and of specific applications. They are classified as alternatives to traditional phenolics, polyesters, vinyl esters, epoxies, bismaleimides, cyanate esters, and polyimides [13].

## 2.1 Chemistry of Benzoxazine

Benzoxazine resins are defined as the condensation products of primary amine, phenol and formaldehyde.

The polymerization of mono-functional benzoxazine results in linear or branched polymer with molecular weights of a few hundreds or thousands [11]. Bi functional benzoxazines oın the other hand can result in higher molecular weight cross-linked networks [14].

Depending on the reaction conditions such as time, temperature, reactants ratio, solvents used the monomenr synthesis of benzoxazines generally result in yields of 70-90 %. Ishida and his co-workers developed a highly efficient method in which no solvents are used iteIshida:1996aa, Liu:1995aa in addition to commonly adopted synthetic method using a solvent.

This melt state or solventless synthesis is applicable for precursors (amine and phenol) which may be both liquid, one of them is liquid or has a melting temperature below 150 °C, because this temperature is the starting point for the benzoxazine to polymerize. In order to avoid mixture of precursors monomers and oligomers the temperature should be kept lower than this value. Beside as oligamerization starts the viscosity of the reacting system increases which hinders the effective mixing of the reactants.

Benzoxazine can crystallize if they are pure. However these molecules tend to retain small amount of solvents and impurities, as a result purification may be difficult.

### 2.1.1 Synthesis of Benzoxazine Monomers in Solution

An example procedure for the Mannich reaction to produce 3-substituted 3,4-dihydro-2H-1,3-benzoxazines utilizes a phenol, formaldehyde, and a primary amine in a molar ratio of 1:2:1, respectively, as shown in Figure 2.2 [8, 12]. At the early stage of the reaction primary amine and formaldehyde condensed to give imine medium. The imine further reacts with phenol forming the benzoxazine structure.

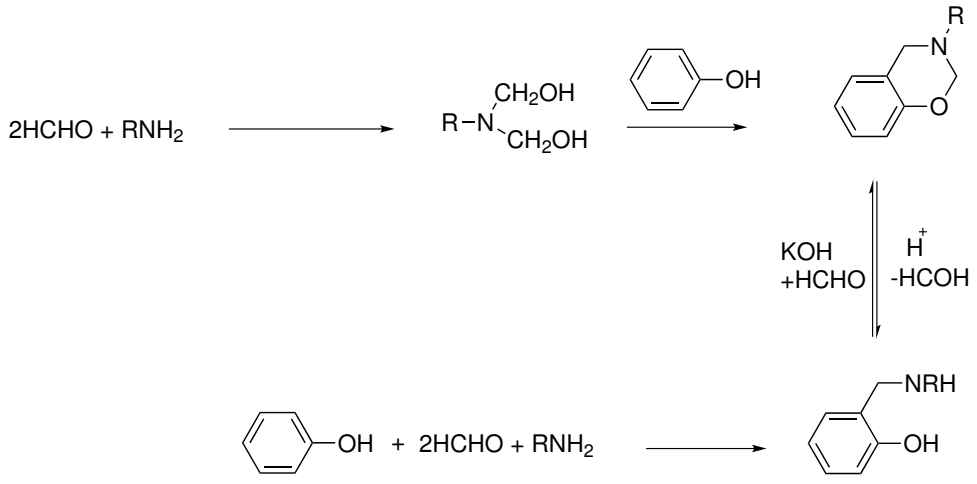


Figure 2.2: Synthesis of benzoxazine monomer

### 2.1.2 Synthesis of Benzoxazine Monomers by Melt or High Solid Methods

In solution synthesis large amount of high boiling point solvents are required and the reaction rate is so slow. In addition some precursor materials are not soluble in this high boiling point low dielectric constant solvents. Also the use of solvent increases the cost of the production method in addition with environmental problems. As abovementioned benzoxazine monomers tend to retain small amount of solvent residue, which is difficult to remove. The solventless synthesis method can overcome these shortcomings [15].

With the help of this procedure large amount of products can be produced. The reaction mechanism was proposed by Liu and Ishida [16].

Although the homogeneity of the solution synthesis is easier to control, a solution with low concentration is kinetically inefficient due to the lowered probability of the reactants to collide. Furthermore the removal of the solvent is both hard and environmentally undesirable.

With the help of the solventless synthesis, the precursors can melt at a moderate temperature. With the help of an acid base interaction, a co-melting temperature can be formed which has a value smaller than each of the precursors (eutectic systems). In the melt state reactions the oligomerization reaction is in competition with the benzoxazine ring formation. The desired temperature should be enough for benzoxazine monomer formation but should not yield oligomerization. Higher temperature or prolonged reaction times thus increase the probability of oligomer formation.

The decomposition temperature of paraformaldehyde into formaldehyde is around 100 °C, which is a typical temperature for solventless synthesis method. The decomposition of paraformaldehyde into formaldehyde plays a very important role in determining the formation of benzoxazine and side products in the melt state reactions.

In the solventless synthesis method, the system is heterogeneous consist of gas-liquid, liquid-solid, and gas-solid which requires a narrow range of temperature tolerance. The rate of reaction not only depends on the chemical structure and electronic effects of the reactants but

also to the physical state of them and also diffusion coefficients as well as on the exact nature the physical contact [17].

The main shortcoming of the melt state reaction is the fact that it is not applicable for all precursors because some phenols or amines has very high melting temperature. As a solution small amount of solvents can be added to the system but this strategy decreases the yield. For example, when the solid content is 18 % the yield of benzoxazine formation was 86 % with 36 % solid content on the other hand , the yield was increased to 90 %. For the melt state reactions on the other hand the efficiencies are dramatically increased [18]. The advantage of the addition of solvent beside the solubility problem, they may form azeotropes with water such as toluene yielding an advantegous during the purification.

In benzoxazine synthesis another possible intermediate is the formation of 1,3,5-triazinane (Figure 2.3).

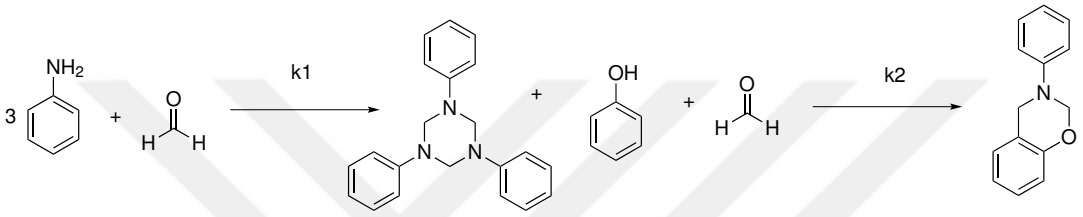


Figure 2.3: Triazinane intermediate formation and benzoxazine formation from it

If the reaction rate constant for the former reaction is lower than the latter, benzoxazine formation is favorable. In other case, triazine remains. Its stability depends on the amine forming it, phenol attacking it as well as the reaction conditions, such as temperature, concentration, acidity, and interaction frequency of the reagents.

### 2.1.3 Reaction Conditions and Side Reactions

Various reaction conditions such as nature and position of the substituents, type of the precursors used and etc, strongly effects the reaction efficiencies.

#### 2.1.3.1 Effects of Phenol Structure

The substituens of the phenol derivative on the ortho and para positions, affects both the type of the condensation reaction anf stability of the formed benzoxazine. If an N-methylol Mannicch base is considered as an reactive intermediate, a competitive reaction occurs between the ring formation and disubstituted mannich base formation (Figure 2.4).

The electron density at the free ortho position favors the by-product formation by increasing both the electrophilic character of hydroxyl group and lone pair electrons at the ortho position. Therefore by optimizing the substituents and reaction conditions the formation of the by-products can be avoided.

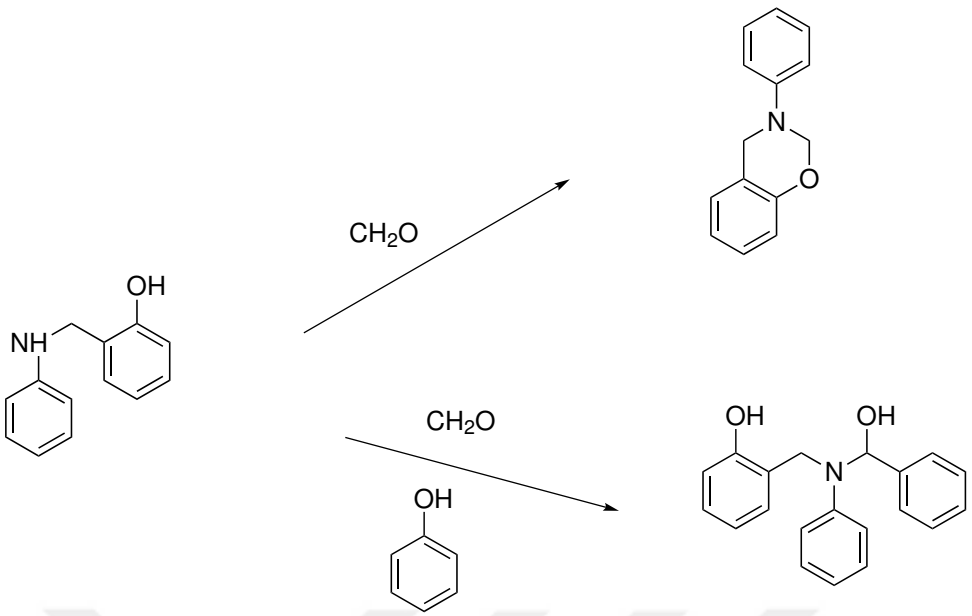


Figure 2.4: Dihydroxybenzylamine byproduct formation versus Benzoxazine formation

#### 2.1.3.2 Effects of Amine Structure

Mannich base and compound 2 shown in Figure 2.4 are favored with the use of strong amines such as methylamine etc. From mild amines like cyclohexyamine Mannich base is formed only. And finally from weak amines such as aniline only mannich base in high yield along with benzoxazine is formed.

#### 2.1.3.3 Effects of Synthesis Conditions

The benzoxazine ring formation yields are significantly depends on the solvents used. The reaction efficiencies are lowered as the dielectric constant of the solvents are increasing.

On the other hand, hydrophilic solvents, such as water and alcohol, make the ring more polar and ready to break. Oligomerization reactions start before the completion of the ring formation [19]. However in some cases the solubility in the low dielectric solvents can be overcome by mix solvent method. One solvent is low dielectric constant solvent, the other is high (such as dioxane/methanol) may be used in order to increase the solubility of the system [20]. Another example of mixed solvent may be water chloroform, one of which is hydrophobic the other is hydrophilic.

In this system the product of benzoxazine stays in the organic layer, as a result hydrolysis reaction of the benzoxazine is inhibited. Amine derivative on the other hand, can diffuse into the water layer, at the interphase of the organic and water layer actually, just after it reacts to form benzoxazine the product transform itself to the hydrophobic layer [21].

Depending on the type of the phenols and amines used for the synthesis of the benzoxazines benzoxazine derivatives can be stable at the alcohols or not. For instance if the used amine

is strongly basic and a less acidic phenol is used for the benzoxazine synthesis, the product is stable even in the hot alcohol environment [7]. It can be concluded that the substituents on the benzoxazine ring have a certain effect on the stability of the oxazine ring.

During the polymerization reaction of a benzoxazine molecule, the cleavage of the C-O bond is the primary step. Cleavage of this bond results in the formation of a carbocation and oxygen anion. The proton is transferred to the anions to form hydroxyl groups, with electrophilic attack of carbocation to the active carbon. It can be concluded that the stability and tendency to oligomerization reaction depends on the ortho carbon activity of the oxazine ring and stability of the carbon oxygen bond. In theory when the phenol has an electron donating unit as a substituent, both the oxygen anion and alpha carbon reactivity increases, resulting in easy and stable ring formation, but difficult for a polymerization reaction to initiate. The inverse situation is valid for an electron withdrawing substituent on the phenol derivative. The formation of benzoxazine ring is difficult and also the breakage and thus the polymerization is easier in this case. The reaction is thermally activates the system.

## 2.2 Polymerization Mechanism

For a benzoxazine to polymerize, the most accepted theory about the reaction is an thermally activated ring opening cationic addition reaction. The benzoxazine ring has some ring strain due to the heteroatoms on the ring. This induced strain eases the opening of the ring continues with the reaction of polymerization. Around 160 and 220 °C the polymerization reactions can take place for the purified monomers of benzoxazine [14], after a few minutes gelation take place in the absence of catalyst or initiator. The initiation reaction temperature for a benzoxazine polymerization reaction highly depends on the purity of the monomer. If the formed oligomers are purified from the reaction medium, the polymerization reaction temperature will increase because it is an cationic ring opening polymerization reaction and the formed oligomers hydroxyl groups act as an acid source, lowering the initial reaction temperature [22].

There are many theories about the polymerization depending on the type of phenols and amines used. In addition by using the same monomer, different types of polymers can be produced, depending on the initiation mode [23]. Still the iminium ion mechanism seems to explain many observed phenomena shown in Figure 2.5.

According to the iminum ion mechanism, polymerization rate depends on the stability of the iminium ion formed as well as depending on the electron density of the oxygen and alpha carbon of the phenolic moiety.

## 2.3 Unique Properties

### 2.3.1 Near-Zero Volume Changes

An important drawback about thermosetting resins is the shrinkage resulting in the residual stress for the composites because of the thermal mismatch of volume change between fiber and matrix resin. The shrinkage value for a typical epoxy or phenolic during polymerization can reach to the value about 2-10 %.

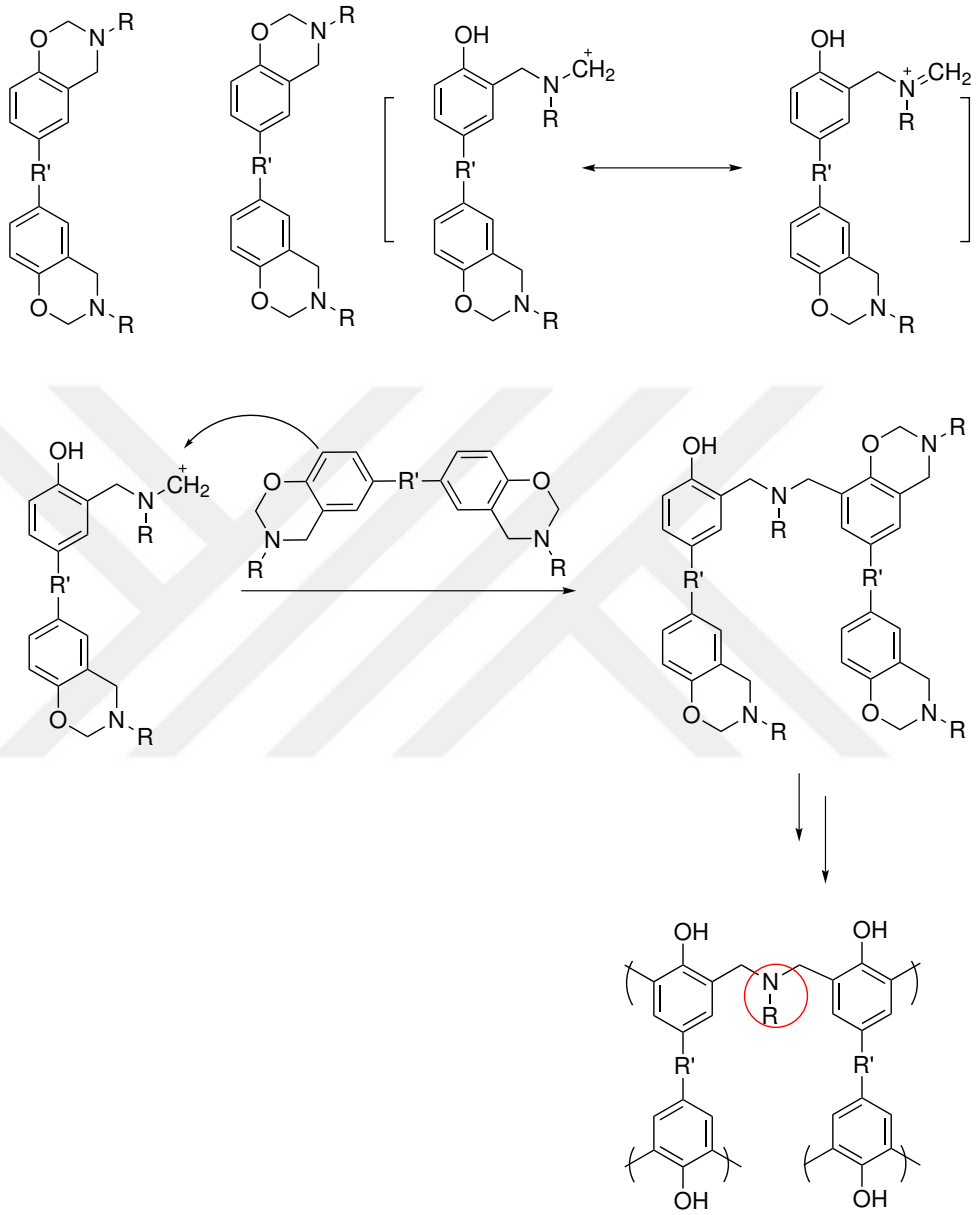


Figure 2.5: Polymerization mechanism via iminium ion intermediate

In order to achieve mechanical interlocking to a substrate with the optimal performance, the thermal mismatch between substrate and resin should be minimal and structural integrity of the resin should remain. The increase in the density of common resins creates residual stress between the substrate and the resin. For example for a composite material this residual stress may cause micro cracks or inhibit the transfer of thermal or mechanical load which lead to failure of the material.

For benzoxazine resins on the other hand, this shrinkage values are nearly zero [24–26]. The research investigate that no more than 1 % volume is changed upon polymerization of benzoxazine. It was revealed that although the volume is reduced slightly at the isothermal elevated curing temperature, the system expands upon cooling resulting in very little change in volume. This behavior of benzoxazines eliminates the risk of formation of the residual stress which in turn results in the better load transfer property.

### 2.3.2 Low Water Absorption

Common resins such as polyesters, vinylesters, phenolics, epoxies, bismaleimides, and polyimides, have relatively highe water absorption upon saturation. The reason is they all have polar groups that can interact with water. İt was investigated that the saturation by water for both epoxies and phenolics can reach to 3-20 % by weight [27]. Although benzoxazines has similar polar groups like epoxies and phenolics like phenolic hydroxyl group or Mannich base -$CH_2NCH_2$- group, the saturation by water is much less compared to these resins on the contrary to expectation.

A benzoxazine resin, which is produced from the precursors of bisphenol A, aniline and formaldehyde, can only be saturated at 1.9 % by weight. After more than 10 years [6], there was no further water absorption was observed. In addition the use of more hydrophobic precursors additionally decreases this value. This is a great advantage for benzoxazine due to the eliminated risk of water absorption which results in loss of mechanical properties, increase in dielectric properties or increase in thermal conductivity.

### 2.3.3 Glass Transition Temperature (Tg)

The apparent glass transition temperature coincides with the polymerization temperature, Tcure, if polymerization takes places under the ultimate glass transition temperature of the resin system. After a significant degree of conversion system vitrifies and inhibit the proceeding of the reaction. However if the local motion of the polymer chain allows for further reactions or geometric rearrangements, the reaction may continue and Tg can exceed Tcure. Many of the polybenzoxazine resins are within this type of materials. They exhibit high glass transition temperatures approximately from 150 to 400 °C due to active sites available to react. Thus the T$\beta$ (side chain motions) provides enough energy for the reaction to proceed [28].

Furthermore, addition reaction may also contribute to fast Tg developing. Yet another reason may be the structural rearrangements occurring at high temperatures.

### 2.3.4 Fast Physical and Mechanical Property Development

Developing good physical and mechanical properties for condensation polymers such as epoxy resins is very slow at the early stages of conversion. These type polymers need a high degree of conversion in order to achieve desired properties. As a result, if the conversion of the resin is changed due to the experimental conditions near to the end of the process, a significant amount of the properties may be changed compare to the property changes at the early stage of conversion.

For polybenzoxazines on the contrary, the properties were developed at the very early stages of conversions. The glass transition temperatures or mechanical strength values are very similar at the early stageconversion and end of the reaction. It was shownthat 80 % of Tg can be reached just by the 50 % conversion [29] for a benzoxazine of bisphenol A derivative. An epoxy derivative of the same compound can only reach 25 % of its ultimate glass transition temperature at the same conversion [30, 31]. This reveals that even at the early curing stage benzoxazine would have excellent properties.

### 2.3.5 Very High Char Yield

Federal regulations revela emerge regulation on the flammability issues from academics and industrial studies. Fire statistics [32] reveal that number of victims caused by a fire in 2011 belongs to 2349 of which 2191 sufferded injuries and 158 of them were died meaning that 16 people was passed a way in every week.

Flame retardancy is a crucial issue nowadays and there are plenty of academic studies in order to make flame retardant materials.

#### 2.3.5.1 Burning Behavior

Combustion is a chemical process in which a material reacts rapidly with oxygen and emits heat. Complicated elementary reactions take place during combustion. The fire can simply represent by a triangle shown in Figure 2.6 includes oxygen heat and fuel. If one of the three elements of this fire is removed, combustion stops. The ignition temperature is important factor at fire triangle. The fuel's temperature should be raised to characteristic ignition temperature of the material for combustion to occur and and also to continue spontaneous combustion. The precess can be divided into three main stage. At first the fuel was heated, second it decomposes into the combustibale and non-combustble compounds and finally the combustible compounds ignites upon mixing with fire resulting in the production of a fire.

After ignition proper conditions may allow flame spread and solid burning which among the others determine the heat release rate. Also heated zone should be appropriately large to overcome heat loss [33].

#### 2.3.5.2 Burning Behavior and Thermal Decomposition of Polymers

Combustion is defined as rapid, exothermic, fast chemical oxidation-reduction reaction which may be spontaneous or continuous due to ignition and heat loss. Process of combustion

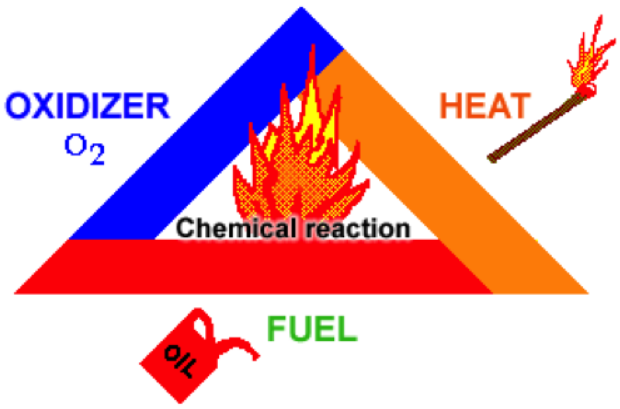


Figure 2.6: Fire triangle

for polymeric materials can be separated into stages such as heating, decomposition ignition combustion and flame propagation.

With heating, polymer's temperature is raised to its characteristic decomposition temperature and the polymer releases flammable gases which diffuse into the flame zone.

Following decomposition, if ignition source is available, combustion will begin in gas phase and release more heat for self-sustaining. Also this gas phase reaction produces combustion near solid surfaced polymeric material. Flames may occur due to polymeric material's properties and fire performance (Figure 2.7).

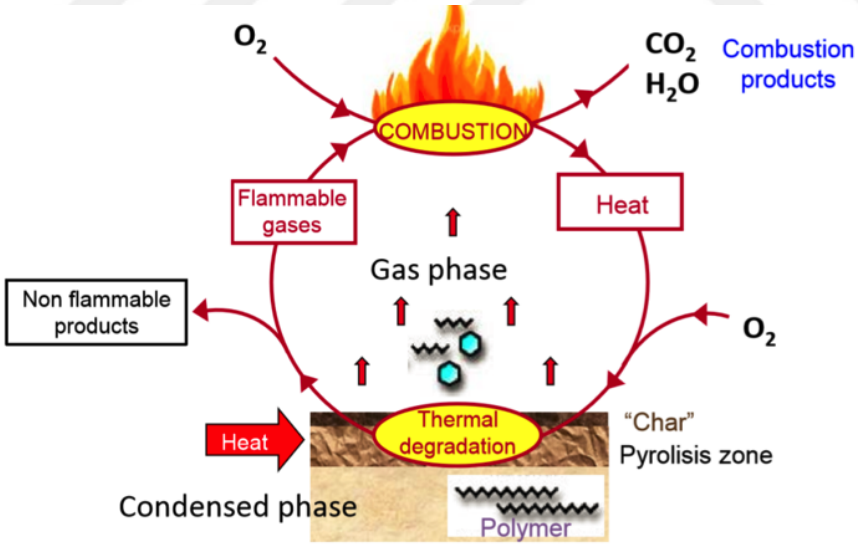


Figure 2.7: Combustion cycle of polymer

At first, polymers go pyrolysis stage. Then by the help of heat produced in pyrolysis, hot radicals react with air and volatile radicals which causes the ignition. As the temperature rises the material decomposes or thermooxidtively degrades. The small degraded combustible molecules move to the front surface and meets with the flame front. At his stage a rich supply

of the oxygen reacts with this compounds producing the flame. The reactios are exothermic and huge. These released energies turns back to the system sustaining the degraditon [34]. This cycyle continues until whole material burns (Figure 2.7.).

Flames may spread horizontally or vertically depending on the pyrolysis zone and polymeric material alignment. Horizontal flame spreads slower than vertical because flame is heated only by downward gas phase heat transfer. Vertical spread is faster because heat transfer consists of conductive, convective and gas phase [35].

Polymers can be classified according to varying thermal decomposition of their chemical composition and fire performance. Decomposition of many polymer accelerates through oxidants such as oxygen and air.

The definition of the thermal degradation of a polymer can be done that it is the case without any additional compound involve the polymer undergo chemical changes due to the high temperature environment. Thermal degradation of polymers has an importance to develop a technology in polymer processing for using polymers at higher temperature and understanding thermal decomposition mechanism for the synthesis of fire safe polymeric material.

The degradation of the polymers has two main mechanisms which are depolymerization and fragmentation of chains [36]. Polymers have different and various types of bonds. Random chain scission, chain-end scission depolymerization and elimination of pendant groups are the three main types of thermal degradation of polymers.

#### 2.3.5.3 Flame Retardancy Mechanism of Polymers

Flame retardants should block or restrain the combustion. Flame retardants can step in during specific stages of combustion like heating decomposition ignition or flame spread.

Depending on their specifications, flame retardants can defy the combustion process in their solid phase or in the flame zone physically or chemically or combination of these two mechanisms [37].

*Condensed phase*: Some of the flame retardants can form a carbon layer on surface of polymers. This layer insulates the material and acts as a physical barrier slowing down heat and mass transfer, from the flame (eg: boron or phosphate based flame retardants) [38].

*Gas phase*: With a flame retardant radical reaction mechanism of combustion can be stopped at the gas phase either by endothermic reactions or dilution of the combustible gases with halogenated flame retardants [39].

*By cooling*: The additive degrades endothermically and cools down the temperature in which degradation cannot take place anymore (eg: metal hydroxides) [40].

*By inert gas dilution*: The flame retardant additives decompose with combustion and produces large volumes of non-combustible inert gases which dilute oxygen supply or fuel below the flammability limit (Talc, chalk, Aluminum hydroxide, which produces CO and $H_2O$) [41].

*By dilution*: In this mechanism the additive behave as a thermal sink which results in increase of the heat capacity of the system, or it reduces the concentration of the flammable products below the limit of flammability at the condensed phase (eg: microglass sphere , fibers or

minerals) [42].

#### 2.3.5.4 Flame Retardancy of Benzoxazines

One of the two basic mechanism of flame retardancy is the char formation capability. Char reduces the evoparation of the flammable gases to the flame zone and diffusion of the oxygen to the decomposition zone. İt also act as a thermal barriers inhibiting the direct thermal radition of the underlyin material.As a result a high char yield is a desired property for a flame resistant material.The prelemineier analysis about the char forming capability can be achieved by using thermogravimetric dynamic analysis. The char yields for the epoxies with this technique is around 5-15 % for phenolic resins on the other hand the values can reach to 30-55 % [43, 44]. These phenolic resins are one of the highest char yield resins in which processing is easy. İnvolment of aromatic units in the structure of the resin increases the char yield capability in spite of the fact that there is no a direct correlation between char forming ability and benzene ring. For example polybenzoxazine has higher percent of aromatic units compare to traditional phenolics but their char yields are away better than the phenolics. The char yields of benzoxazine are in the range of 35-75 % [45]. Walter and Lyon's theory states that, polar group contribution to char forming ability for benzoxazines are quite high [46].

## 2.4 Molecular Origin of Unique Properties

Polybenzoxazines has outstanding properties compared to phenolics, epoxies and bismaleimides. The very fast development of the advanced properties of the benzoxazines such as high char yield, high Tg, high mechanical properties and low diffusion abilities can be explained by various and complex nature types of hydrogen bonding abilities of the benzoxazine. In the literature it was investigated that almost all type of hydrogen bondings can be formed by benzoxazines. They are OH-OH inter and intramolecular hydrogen bondings, OH-N six-membered intramolecular hydrogen bondings or OH-$\pi$ . These interactions were investigated by X-ray crystallographic study of model dimer [47], molecular modeling study [48], high resolution solid-state $^{1}$HNMR with double quantum technique [49] and FTIR study of model oligomers all strongly support the formation of both inter and intra-molecular hydrogen bonds. The very stable six-membered hydrogen bond shown in Figure 2.8 can explain the hydrophobicity, low dielectric constant, high char yield, and high modulus.

The excellent mechanical, thermal and physical properties of the benzoxazines are believed to result from the hydrogen bonding capability. The hydrogen bonding capability and type of formed hydrogen bonds depends on the electronic character of the benzoxazine molecule. Researches investigate that, a local helical structure can be formed due to the complex hydrogen bonding capability of benzoxazines. A particular interest in understanding the type and strength of the helical formation give information about the design of the monomer synthesis. The ratio of intermolecular hydrogen bonding compare to intramolecular hydrogen bınding depends on the electronic characters and acidities of the phenols or amines used. A higher basicity and electron density amine such as methyl amine has higher tendency to form intermolecular hydrohgen bonding than a lower basicity end electron density amine derivative such as aniline. Similarly more acidic phenol forms higher ratio of intramolecular hydrogen bonding rather than intermolecular hydrogen bonding. The design crtieria should involve an optimum ratio of intra and intermolecular hydrogen bonding capability. The intrsmolecular hydrogen

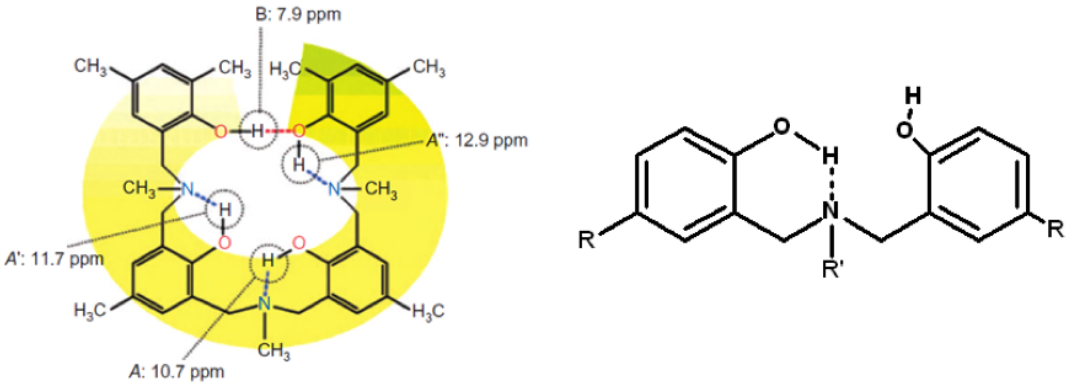


Figure 2.8: Hydrogen bonding in benzoxazines

bonding is very stable upto 300 °C [50] although if the glass transition temperature is higher than this value. However the interaction with other additives depends on the strength of the intermolecular hydrogen bonding capability.

# CHAPTER 3

# EXPERIMENTAL

## 3.1 Materials

Bisphenol-A received from Sigma Aldrich. Aniline (99 %) and paraformaldehyde were received from Merck Company. 4,4-dihydroxybiphenyl and 4,4-dihydroxybenzophenone are received from ABCR GmbH & Co. KG company. Epoxy structural adhesive received from HENKEL with the commercial name of Hysol EA 934NA. High silica fabrics are received from CPMIEC Company. All materials are used as received without further purification

## 3.2 Synthesis of the Monomers

### 3.2.1 Solution Synthesis

#### 3.2.1.1 In Dioxane

Stoichiometric amount of paraformaldehyde was dissolved in 1:2 methanol:dioxane solvent system via heating. After the dissolution of formaldehyde, the reaction flask was cooled below 10 °C. Then stoichiometric amount of aniline was dissolved in dioxane and added dropwise with automatic syringe for 1 h. The mixture was stirred for another hour at room temperature. Then first catalytic amount of base (5-10 % wt. with respect to phenol) and bisphenols were added respectively. The mixture was stirred under reflux for 5-10 h.

#### 3.2.1.2 In Toluene

Stoichiometric amounts of aniline (0.02 mol, 1.86 g), aqueous formaldehyde solution (0.04 mol,from 37 % solution), and bisphenol (0.01 mol) were dissolved in toluene (5 mL) in a 250-mL three-necked flask. The mixture was stirred and refluxed for 5-10 h. After evaporation of toluene the crude product was dissolved in ethyl acetate or chloroform and washed with 3 N NaOH (3-5 times), brine and deionized water respectively.

### 3.2.2 Solventless Synthesis

#### 3.2.2.1 Synthesis of BA

Bisphenol-A (2 g, 0.009 mol) and paraformaldehyde (1.41 g 0.044 mol) were mixed in a mortar for approximately 15 minutes. Then NaOH (1.5 % wrt bisphenol A) was added and mixed for another couple of minutes. The reagents were taken into a 25 ml reaction flask and (1.65 g 1.57 ml 0.018 mol) aniline was added and stirred for 3-4 minutes. Physical appearance of the mixture when no formaldehyde remains should be as homogenous as possible. Otherwise oligomers start to form. The mixture was heated in a preheated oil bath at 80 °C with a condenser. After 20 minutes condenser was removed, the system was opened to atmosphere and the temperature was raised to 150 °C. After heating at this temperature for 70-80 minutes reaction flask was allowed to cool to room temperature. Same synthetic procedure was repeated using 20, 100 and 250 g batches of Bisphenol A. $^1$H NMR spectra of crude products are given in Appendix A.

For further purification, BA was dissolved in diethyl ether and washed with brine (3-5 times). Organic layer was dried over $Mg_2SO_4$ filtered and concentrated using rotary evaporator to some extent. Then the mixture was dumped over thick aluminum foil (thick, industrial one) The purpose of doing this process is to increase surface and remove as much solvent as possible from the product. The aluminum foil with the product was taken into a vacuum oven at 120 °C and kept for two hours. The product was obtained as yellow transparent chunks.

#### 3.2.2.2 Synthesis of BP

Stoichiometric amount of 4,4-dihydroxybiphenyl (2 g 0.011 mole) and paraformaldehyde (1.61 g 0.053 mol) were mixed in a mortar for approximately 15 minutes to get fine powders. Then NaOH (2.5 % wrt bisphenol) was added and mixed for another couple of minutes. After adding aniline (2 g, 1.96 ml, 0.021 mol) the mixture was liquidified. Then it was taken into a preheated oil bath at 80 °C with a condenser. After 15 minutes, the condenser was removed, system was opened to atmosphere and the temperature was increased to 140 °C. After heating at this temperature for 65 minute it was brought to room temperature. The reaction was also repeated by using 10, 20, and 100 g of bisphenol. $^1$H NMR spectra are shown in Appendix A.

For further purification of the monomer it was precipitated from acetone/methanol, or ethyl acetate/methanol, or chloroform/methanol solvent systems. Purified product was allowed to stay in a vacuum oven for two days at 45-50 °C and 100 mmHg.

#### 3.2.2.3 Synthesis of BZ

Stoichiometric amount of 4,4-dihydroxybenzophenone (2 g 0.009 mol), paraformaldehyde (1.40 g 0.047 mol) and aniline (1.74 g, 1.71 ml, 0.019 mol) were mixed in a mortar for approximately 15 minutes to get a fine powder. Then NaOH (1% wrt bisphenol) was added and mixed for another couple of minutes. Then the mixture was taken into a 25 ml reaction flask and heated with a preheated oil bath at 110 VC with a condenser. After 15 minutes condenser was removed and system was open to atmosphere. After heating the mixture for 65 min open atmosphere at 135 °C it was cooled to room temperature.

The reaction was also repeated by using 5, 20, and 200 g of bisphenol. $^1$H NMR spectra are shown in Appendix A.

For further purification of the monomer it was precipitated from acetone/methanol, or ethyl acetate/methanol, or chloroform/methanol solvent systems. Purified product was allowed to stay in a vacuum oven for two days at 45-50 °C and 100 mmHg.

### 3.3 Composite Production

In the preparation of the composites high silica cloth was chosen because of thermal performance of the fiber ($SiO_2$ content $\geq$ 95 %, areal weight: 300±30 g/m$^2$, fracture strength: 89±10 N/cm$^2$).

The composites were prepared by resin powder molding model [51]. About 8 g of the well-grounded resin was distributed between the fabric layers. 9, 20 and 40 layers of plies were used according to specified analysis.

On the basis of DSC analysis of the materials defining melting and curing behaviors, processing procedure of BA and BZ silica cloth composites was determined as follows.

The sandwiches were first preheated to 150 °C in order to melt and liquefy the resin under the pressure of 2 ton (0.5 MPa). When the excess resin stops flowing from the mold, the temperature and pressure were increased to their corresponding curing values. Such as;

Applied curing cyles for BZ; 170 °C 2 hour, 190 °C 2 hour and 220 °C 2 hour.

Applied curing cyles for BA; 160 °C 2 hour, 180 °C 2 hour and 200 °C 2 hour.

### 3.4 Characterizations

#### 3.4.1 Structural Characterizations

FTIR measurements in attenuated total reflectance (ATR) mode were performed by using IR-spectrometer (Bruker VERTEX 70) at a resolution of 2 cm$^{-1}$ with 32 scans between 600-3800 cm$^{-1}$ wavenumbers.

$^1$H NMR spectra were obtained in $CDCl_3$-$CCl_4$ (1:1) solvent system, recorded in a Brucker Spectrospin Avance DPX-400 Ultra shield instrument at 400 MHz and 100 MHz respectively. The $^1$H NMR data was reported as chemical shifts ($\delta$, ppm) relative to tetramethylsilane ($\delta$ 0.00), peak multiplicity (abbreviations are as follows: s, singlet; d, doublet; t, triplet; q, quartet; m, multiplet; br, broad) and coupling constants in Hertz integrated number of protons.

#### 3.4.2 Thermal Characterizations

In order to analyze exothermic and endothermic physical or chemical events of the composites, neat resins and monomers, Differential Scanning Calorimetry (DSC) analysis was used. The

thermograms were recorded with a TA DSC 2920, ranging from room temperature to 400 °C, with different heating rates of 5 °C/min 10 °C/min, 15 °C/min and 20 °C/min under a nitrogen and oxygen atmosphere.

TGA measurements were carried out using a TGA/DSC analyzer with varying heating rates 5 °C/min, 10 °C/min, 15 °C/min and 20 °C/min under nitrogen environment.

### 3.4.3 Rheological Characterizations

Change in the mechanical property with dynamic heating for neat resins and composites were analyzed by Dynamic mechanical analysis (DMA). The samples had rectangular dimensions of 54x10x3; length x width x thickness. The analyses were conducted in three point bending configuration at 1 Hz using a DMA Q800 of TA Instruments. Tests were performed at a constant amplitude using sinusoidal oscillation and under dynamic conditions in the interval T = $-100 \ldots 400$ °C at a heating rate of 5 °C/min.

### 3.4.4 Cone Calorimetry Characterizations

The combustion behavior of the neat resins were examined by using a Fire Testing Technology mass loss cone calorimeter (according to ISO 5660). Mass loss cone calorimeter was used in order to investigate time to ignition (TTI), rate of heat release (HRR), the maximum rate of heat release (PHRR) of the cured resins. A 50 kW/m$^2$ heat flux was used on the resin surface. The specimens' dimensions were 50 mm x50 mm x 3 mm. Edge burning effects were reduced by covering the samples with heavy duty aluminum foil leaving an exposed area of 80 mm$^2$.

The device consists of a radiant electric heater in a conic shape, an electric spark for ignition, and a load cell to measure the weight loss (3.1). All tests were ended after 600 s exposure of the incoming heat radiant.

### 3.4.5 Density Measurement of Composites

Water displacement method according to ASTM D 792 (Method A) was used in order to measure the density values of the composite samples. The weight of the samples were recorded before and after immersing method. And displacement of the water was the measuring criterion.

The dimension of a specimen is 30x30x3 mm3. mm$^3$. The densities were calculated by equation:

$$\rho = \frac{A}{A - B} \times \rho_0 \tag{3.1}$$

where $\rho$ and $\rho_0$ are densities of the specimen and water at a given temperature (g/cm$^3$), A and B are weight of the specimen in air and in water (g).

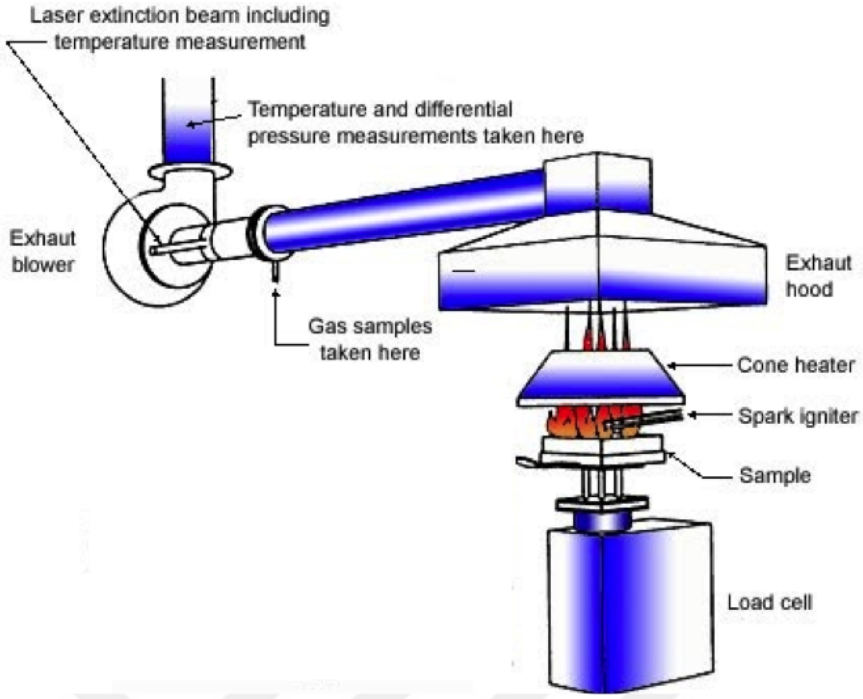


Figure 3.1: Cone calorimetry

### 3.4.6 Mechanical Characterizations

After fabrication the test specimens were subjected to various mechanical tests as per ASTM standards. The mechanical tests that we carried out are tensile test, compression and bond in tension test-2. The specimen size and shape for corresponding tests are as shown in Table 3.1.

Table3.1: Types of Mechanical Testing

| **Test** | **ASTM Standart** | **Specimen Size** |
|---|---|---|
| Tensile Test | ASTM D 3039 | 250x25x3 |
| Compression Test | ASTM D 3410 | 150x25x1 |

#### 3.4.6.1 Tensile Tests

Tensile tests are used to measure the force needed to permanently deform a sample and to locate the extent of elongation at fracture point. ASTM D3039 is employed to define in plane tensile properties of high modulus fiber reinforced polymer matrix composite materials.

Fiber reinforced composites were cut to appropriate dimensions (as per ASTM D3039, see Figure 3.2) by a saw cutter after they were dried. The specimens had a rectangular cross section with 25 mm width and 250 mm length. Test specimens were mounted on the grips of Instron universal test device with 10 mm gauge length (Figure 3.3). Stress – strain curve was obtained after the test to locate elastic modulus and ultimate tensile strength. An average of

two tests were taken to determine these properties.

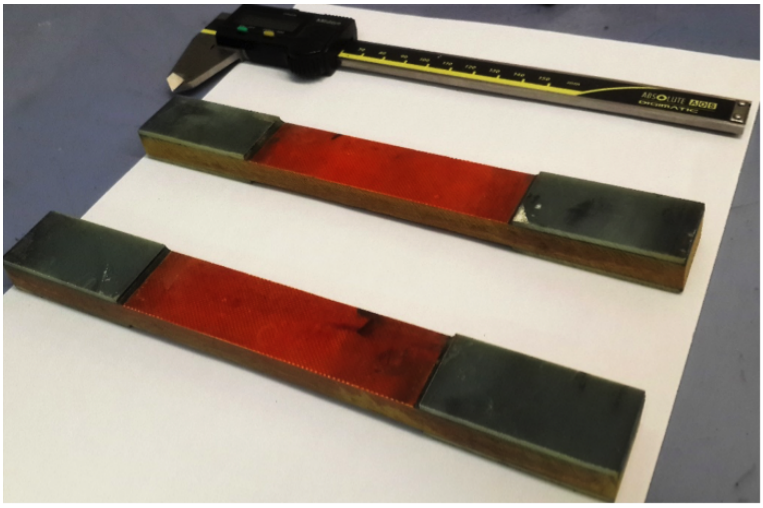

Figure 3.2: Composite tensile tpecimen

#### 3.4.6.2 Compression Tests

Fiber reinforced composites were cut to appropriate dimensions (as per ASTM D3410, see Figure 3.4) by a saw cutter after they were dried. The specimens had a rectangular cross section with 25 mm width, 250 mm length and 1 mm thickness. Test specimens were mounted on the grips of Instron 44 81 test device with 10 mm gauge length. Tests were carried in room temperature with a 1.5 mm/min constant head speed. Stress – strain curve was obtained after the test to locate ultimate strength. An average of three tests were taken to determine mechanical properties.

### 3.4.7 Thermomechanical Characterizations

In order to investigate the thermal expansion behavior of the composites Thermomechanical Analyses (TMA) were conducted according to ASTM D696. By using Rheometric Scientific TMA 500. The sharp change in the thermal expansion behavior can be named as the glass transition temperature of the composite. The thermal expansion coefficents before and after glass transitions were detected from the slope of the curves of Height increase vs temperature. The analyses were conducted in the temperature range of room temperature to 400 °C with a heating rate of 5 °C/min.

### 3.4.8 Oxyacetylene Torch Characterizations

The ablation behavior of the composite under the exposure of oxyacetylene torch was characterized according to ASTM E 285-80 standard. This characterization technique is a preliminary analysis, which is widely used for the investigation of the materials ablation behavior [11].

Figure 3.3: Instron universal tester

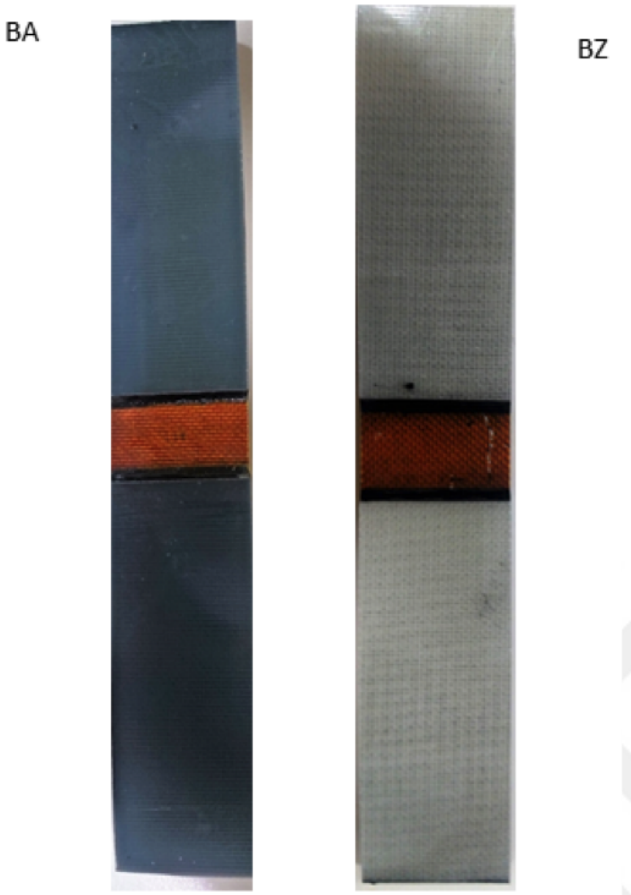


Figure 3.4: Compression test sample of BA and BZ

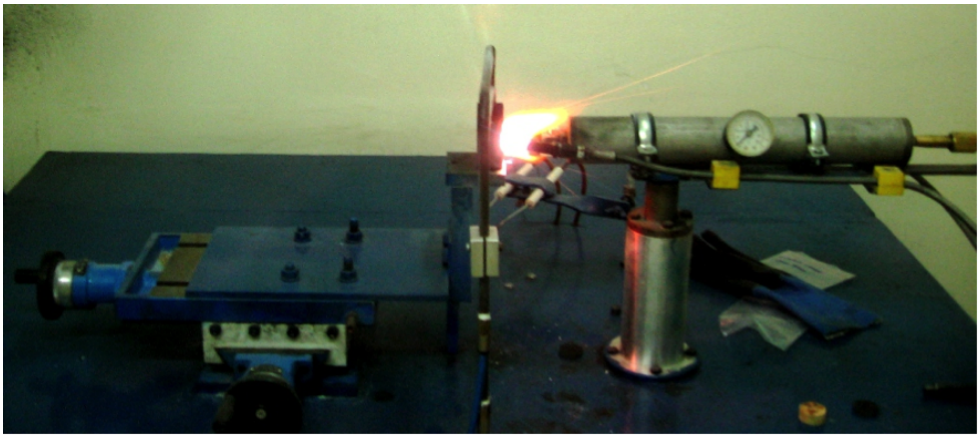

Figure 3.5: Oxyacetylene torch test setup

# CHAPTER 4

# RESULTS AND DISCUSSION

## 4.1 Synthesis of the Monomers

In order to synthesize BA, BP and BZ; both solution and melt state reactions were carried out. While designing the reaction parameters for solution synthesis; it was decided to employ low dielectric constant, high boiling point and aprotic solvents are used. The reasons are;

- benzoxazines can form at high temperatures,
- C-O bond on the oxygen ring should be stable, should not be protonated or polarized.

In order to increase the solubility of the precursors, small amount of polar, protic solvents were used. Within the context of these decisions, efficiencies of the reactions were below desired levels.

For the melt state synthesis; it was intended to have a melt mixture by mixing precursors below 150 °C. This was established for BA; while, for BP and BZ, since starting phenols for BP and BZ synthesis have very high melting temperatures, it couldn't be performed. In order to avoid this situation, a base catalyst was employed and by screening the reaction parameters, efficiencies close to full conversion were achieved for all of the monomers.

### 4.1.1 Synthesis of BA Monomer

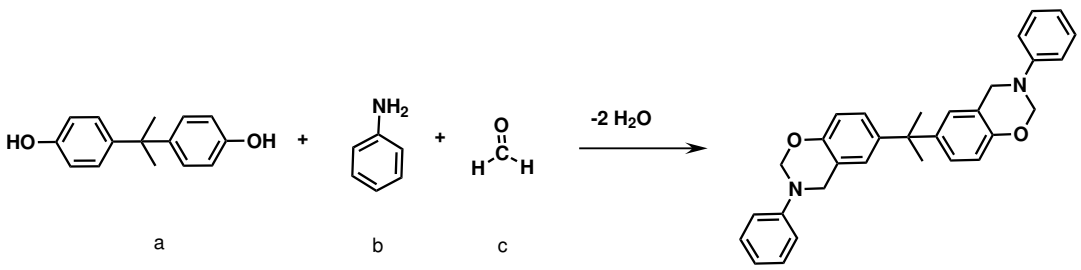


For the synthesis of this monomer; the reaction temperature, stoichiometry of the reactants and the amount of the catalyst were optimized. The results of these studies are summarized in Table 4.1.

As can be seen from Table 4.1, when there is no catalyst (entry 4-8), two extra signals were

Table4.1: Optimization results for the synthesis of BA

| **Entry** | **Rxn Type** | **a:b:c Ratio** | **Rxn Time min** | **% Cat (NaOH)** | **Temp (°C)** | **Efficiency (%)** |
|---|---|---|---|---|---|---|
| 1 | In Dioxane | 01:02:04 | 480 | - | Reflux | 0 |
| 2 | In Dioxane | 01:02:04 | 600 | 10 | Reflux | 65 |
| 3 | In Toluene | 01:02:04 | 480 | - | Reflux | 59 |
| 4 | Melt | 01:02:04 | 5 | - | 110 | 44 |
| 5 | Melt | 01:02:04 | 8 | - | 140 | 61 |
| 6 | Melt | 01:02:05 | 10 | - | 85 | 78 |
| 7 | Melt | 01:02:05 | 15 | - | 95 | 90 |
| 8 | Melt | 1:2:4.5 | 15 | - | 95 | 80 |
| 9 | Melt | 1:2:4.5 | 95 | 0.5 | 10 | 78 |
| 10 | Melt | 1:2:4.5 | 95 | 0.5 | 10+10 | 80 |
| 11 | Melt | 1:2:4.5 | 85+95 | 0.2 | 10+5 | 67 |
| 12 | Melt | 1:2:4.5 | 85+95 | 0.2 | 10+20 | 73 |
| 13 | Melt | 1:2:4.5 | 85+95 | 0.2 | 10+35 | 80 |
| 14 | Melt | 1:2:4.5 | 85+95 | 0.2 | 10+60 | 82 |
| 15 | Melt | 1:2:4.5 | 95 | 0.2 | 10+10 | 72 |
| 16 | Melt | 1:2:4.5 | 95 | 0.2 | 10+30 | 79 |
| 17 | Melt | 1:2:4.5 | 95 | 0.2 | 10+20 | 78 |
| 18 | Melt | 1:2:4.5 | 95 | 0.2 | 10+20 | 80 |
| 19 | Melt | 1:2:4.5 | 95 | 0.4 | 10+40 | 82 |
| 20 | Melt | 1:2:5.5 | 95 | 0.2 | 10+10 | 74 |
| 21 | Melt | 1:2:5.5 | 95 | 0.2 | 10+30 | 78 |
| 22 | Melt | 01:02:05 | 95 | 0.5 | 15+65 | 81 |
| 23 | Melt | 01:02:05 | 95 | 0.5 | 15+45 | 85 |
| 24 | Melt | 01:02:05 | 95 | 0.5 | 15+65 | 88 |
| 25 | Melt | 01:02:05 | 100 | 0.2 | 10+50 | 88 |
| 26 | Melt | 01:02:05 | 100 | 0.2 | 10+70 | 88 |
| 27 | Melt | 01:02:05 | 95 | 0.5 | 10+70 | 88 |
| 28 | Melt | 01:02:05 | 95 | 1 | 10+70 | 84 |
| 29 | Melt | 01:02:05 | 95+110 | 1.25 | 15+45 | 81 |
| 30 | Melt | 01:02:05 | 95+110 | 1.25 | 15+65 | 87 |
| 31 | Melt | 01:02:05 | 110 | 1.5 | 20+10 | 81 |
| 32 | Melt | 01:02:05 | 110 | 1.5 | 20+40 | 83 |
| 33 | Melt | 01:02:05 | 110 | 1.5 | 20+70 | 96 |

observed on the $^{1}$H NMR (Figure 4.1). The signal at ~4.1 ppm corresponds to the side product (compound 4) mentioned on page 7. The second signal at ~4.8 ppm corresponds to triazinane (compound 3) on page 6. This signal increases after 15 min but decreases significantly after 20 min. The product formation is mainly taking place over this compound.

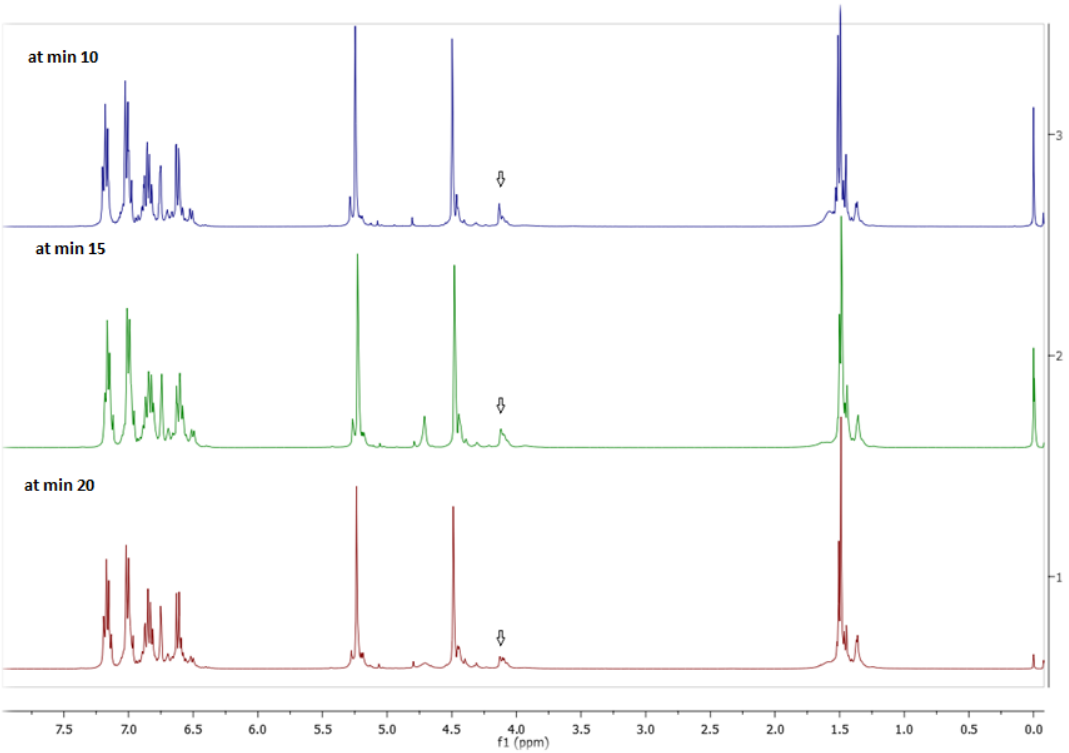


Figure 4.1: Impurity BA monomer signal change with time synthesized without using catalyst

When the reaction was done by using NaOH as the catalyst, the signal at 4.09 ppm corresponding to byproduct decreased depending on the catalyst amount. By keeping all other parameters the same but changing the catalyst from 0.2 to 1.5 %, formation of byproduct was eliminated completely (Figure 4.2).

Such a signal was not observed for BP and BZ monomers. The electron density on the $\alpha$ carbon of bisphenol A molecule compared to other phenols is relatively high. This increases the possibility of byproduct formation. By adding base catalyst to the system, labile proton of the phenolic moiety makes the oxygen attack more possible than the $\alpha$-C attack. This may be the reason of the disappearance of the signal.

In a similar way, the signal 4.81 ppm was decreased with increase of base used. Increase in the reactivity of phenolic oxygen leads to enhanced attack to triazine. With the use of base catalyst, phenoxide ion was formed which has higher nucleophilicity than phenol itself resulting in more efficient cleavage of triazinane ring.

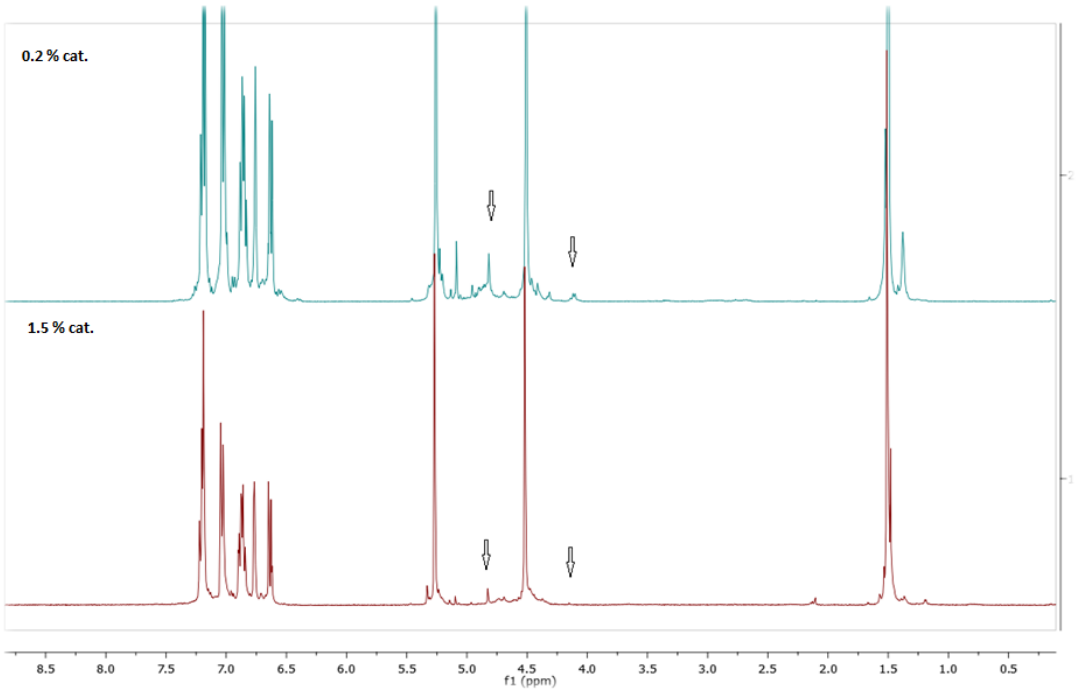


Figure 4.2: Effect of catalyst amount on occurrence of by- and side products in the synthesis of BA monomer

### 4.1.2 Synthesis of BP Monomer

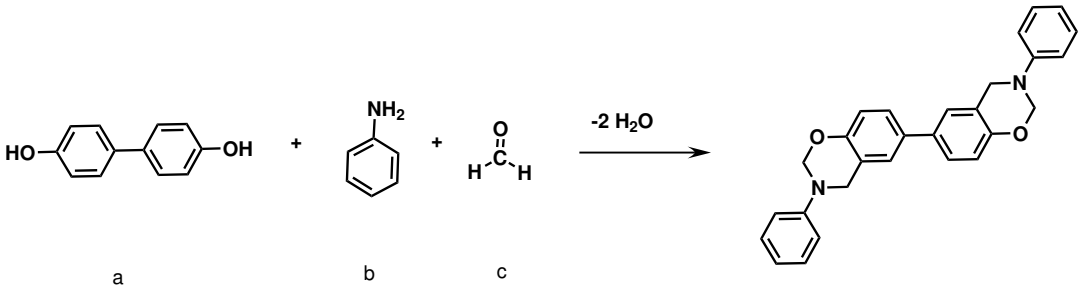


4,4-Dihydroxybiphenyl phenolic compound used for the synthesis of BP monomer has a melting point of 280 °C. For this synthesis temperature; stoichiometry and catalyst have been screened in the solventless and solution reactions. The results are summarized in Table 4.2 below.

For the synthesis of this monomer, previous studies in literature state that synthesis of this compound can be achieved by solution method such as in toluene or in dioxane [52,53]. Similar experiments were conducted at the laboratory but the efficiencies were too low and purification could not be achieved. As a result, melt state reactions were tried even though the phenol used for this synthesis did not melt before 150 °C which is a characteristic temperature for benzoxazines above which oligomerization reactions can start. The system did not show melt state within available temperature scan range. But unexpectedly, the product has shown characteristic signals oxazine. The product has remaining some insoluble residue. Those may be unreacted reagents or some oligomeric products having enough degree of polymerization to

Table4.2: Optimization table of BP monomer

| Entry | Rxn Type | A:B:C Ratio | Rxn Time min | % Cat (NaOH) | Temp (°C) | Efficiency (%) |
|---|---|---|---|---|---|---|
| 1 | Melt | 01:02:05 | 6h | - | 120 | 0 |
| 2 | Melt | 01:02:05 | 45 | - | 110 | 18 |
| 3 | Melt | 01:02:05 | 45 | - | 120 | 51 |
| 4 | Melt | 01:02:05 | 20 | - | 135 | 64 |
| 5 | Melt | 01:02:05 | 40 | - | 150 | 84 |
| 6 | Melt | 01:02:05 | 80 | - | 145 | 84 |
| 7 | Melt | 01:02:05 | 12+40 | 0.5 | 145 | 90 |
| 8 | Melt | 01:02:05 | 10+30 | 0.5 | 140 | 88 |
| 9 | Melt | 01:02:05 | 15+45 | 0.5 | 140 | 92 |
| 10 | Melt | 01:02:05 | 10+40 | 0.5 | 145 | 89 |
| 11 | Melt | 01:02:05 | 10+40 | 0.5 | 145 | 88 |
| 12 | Melt | 01:02:05 | 15 | 0.5 | 140 | 55 |
| 13 | Melt | 01:02:05 | 15+25 | 0.5 | 140 | 76 |
| 14 | Melt | 01:02:05 | 15+65 | 0.5 | 140 | 92 |

not to dissolve. The highest efficiency can be achieved with this system was accomplished at 145 °C.

For the melt state reaction, base catalyst was used and the amounts were screened. With the use of 2.5 % base catalyst wrt phenolic moiety, a liquid mixture at room temperature can be achieved. The resultant product had no remaining insoluble parts and the NMR spectrum of the product is shown in Figure 4.3.

### 4.1.3 Synthesis of BZ Monomer

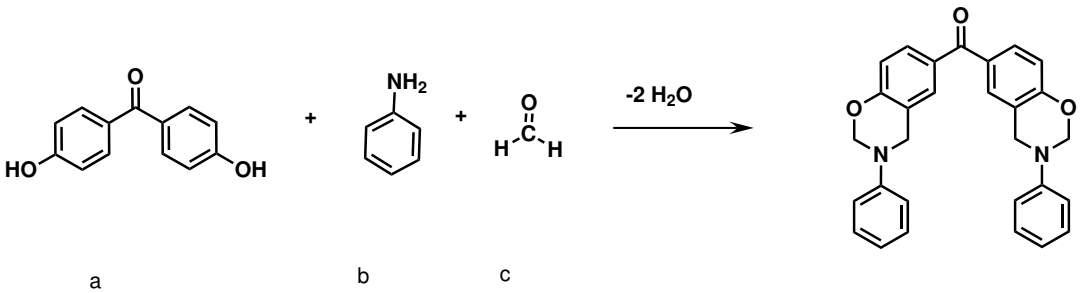


4,4-Dihydroxybenzophenone phenolic compound used for the synthesis of BZ monomer has a melting point of 200 °C. For this synthesis temperature, stoichiometry and catalyst have been screened in the solventless and by solution reactions. The results are summarized in Table 4.3 below.

As similar with the BP molecule; researchers used in solution method for the synthesis of

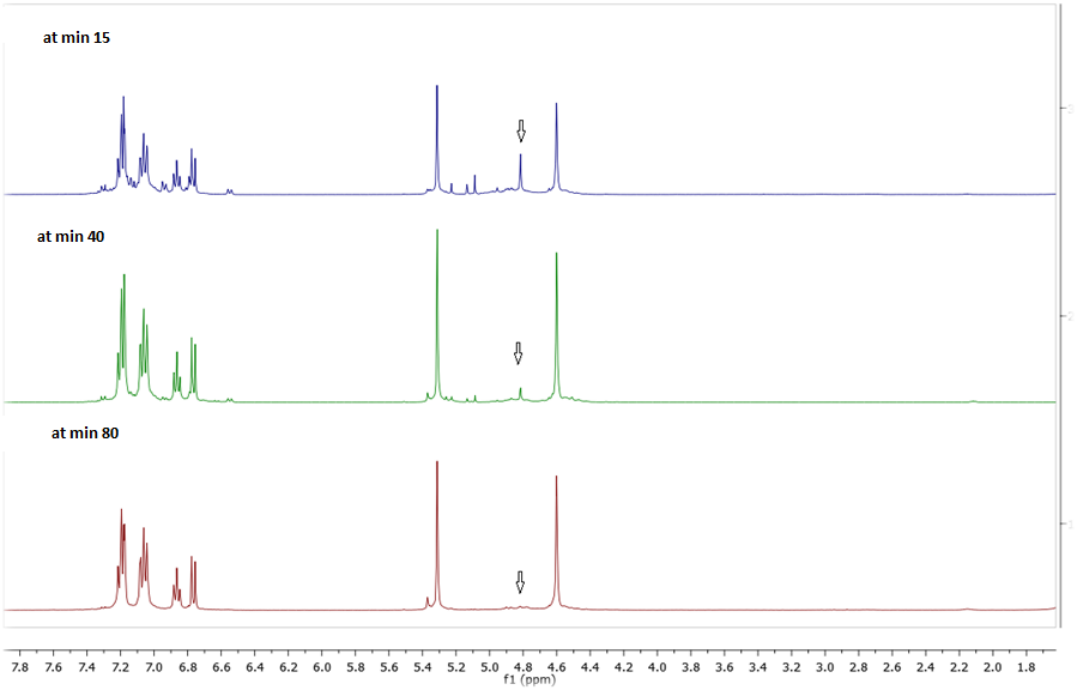


Figure 4.3: Change of BP monomer signal with time

Table4.3: Optimization table of BZ monomer

| **Entry** | **Rxn Type** | **A:B:C Ratio** | **Rxn Time min** | **% Cat (NaOH)** | **Temp (°C)** | **Efficiency (%)** |
|---|---|---|---|---|---|---|
| 1 | Melt | 01:02:05 | 60 | - | 140 | 55 |
| 2 | Melt | -1:2:5 | 60 | - | 100 | 39 |
| 3 | Melt | 01:02:05 | 60 | - | 90 | 26 |
| 4 | Melt | 01:02:05 | 60 | - | 135 | 64 |
| 5 | Melt | 01:02:05 | 60 | - | 135 | 62 |
| 6 | Melt | 01:02:05 | 60 | - | 135 | 40 |
| 7 | Melt | 01:02:05 | 20 | - | 85 | 25 |
| 8 | Melt | 01:02:05 | 8+20 | - | 135 | 57 |
| 9 | Melt | 01:02:05 | 15+30 | - | 135 | 88 |
| 10 | Melt | 01:02:05 | 135 | 0.5 | 15+25 | 53 |
| 11 | Melt | 01:02:05 | 135 | 0.5 | 15+45 | 63 |
| 12 | Melt | 01:02:05 | 135 | 0.5 | 15+45 | 77 |
| 13 | Melt | 01:02:05 | 135 | 0.5 | 15+65 | 85 |
| 14 | Melt | 01:02:05 | 110+135 | 1 | 15+45 | 60 |
| 15 | Melt | 01:02:05 | 110+135 | 1 | 15+65 | 90 |

this monomer. The reaction time is changed within 6 to 24 hours. Also the efficiency of the reaction is quite low (60 %) [52, 53].

The solventless method for this molecule did not work at first. This phenolic derivative is the least reactive among the two due to the strong electron withdrawing bridge, which decreases the reactivity of the phenolic oxygen from the electronic point of view. The product could not be gathered within the low temperatures (80-120 °C). When the temperature was increased the system flooded and effused from the reaction balloon and filled the condenser. This may be due to the reason that when the reaction conditions were not sufficient for the reaction to take place, decomposition of paraformaldehyde to gaseous formaldehyde evaporates, bringing the melt state reactants with it. Even the product could be produced with this system; the efficiencies were too low making the purification nearly impossible. The product had a significant percent of insoluble residue.

The solventless experiments were repeated with the use of a base. As a result of temperature and base quantity screening best result was achieved with a total conversion. Corresponding characteristic $^{1}$H NMR is shown in Figure 4.4.

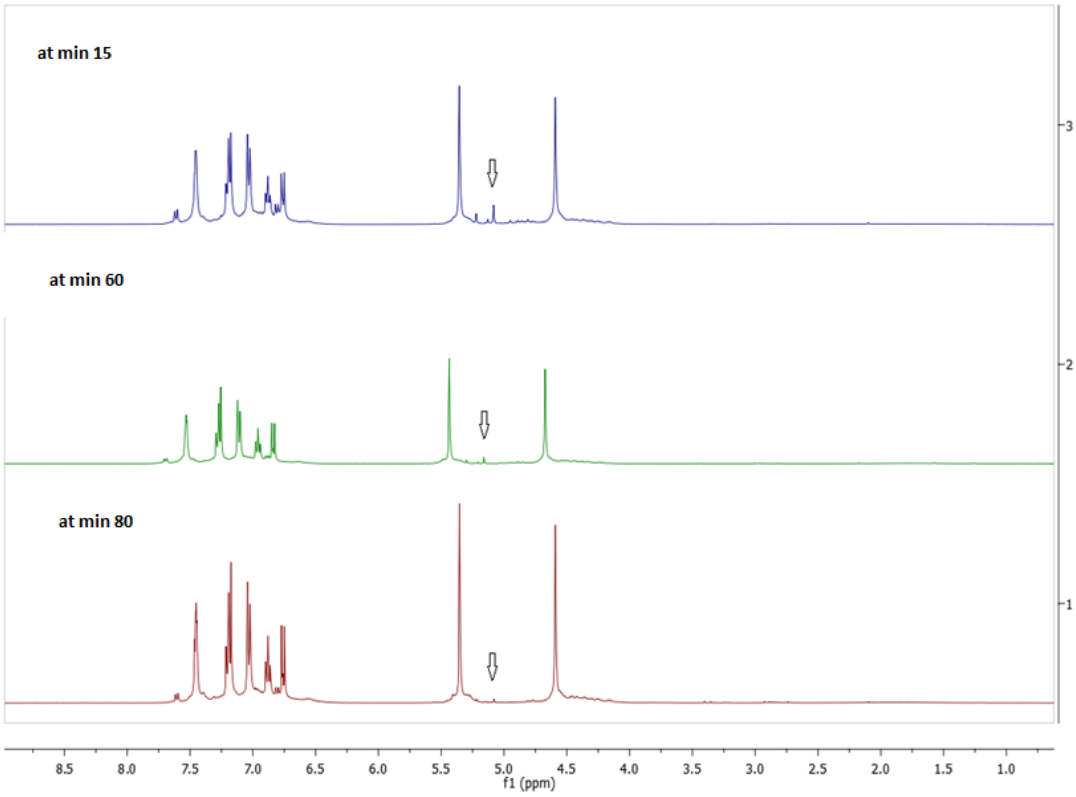


Figure 4.4: Change of intermediates of BZ monomer with time

In general; in the melt state reactions, decomposition of paraformaldehyde is the rate determining step. In addition to this, for an in solution system, the solvents used are either mixed solvents one of which can dissolve water and the other dissolves the product (e.g. dioxane: methanol) or type of solvents that can make azeotrope with water (e.g. toluene). These systems remove the produced water from the reaction medium and shift the reaction towards the

product side. The dilution of the reaction medium makes the reaction proceed slower and it provides sufficient time for side reactions and thus the efficiency is decreased. Besides removal of those high boiling solvents are not easy and desire time and effort.

While designing our melt state reactions, two-step heating was used. First the system was condensed in order make sure that, decomposed formaldehyde should not leave the system and take place in the reaction medium. Beside by avoiding the escape of the produced water, dissolution of the paraformaldehyde and phenol precursor is increased and enhances the reaction with amine like in the case of solution synthesis using mixed solvent systems for better solubility. In the literature it is shown that for an amine formaldehyde condensation reaction, amines are totally consumed after 15-20 min above 100 °C [53]. As a result; after making the reaction take place, the condensation was stopped and open the system to the atmosphere, let the water escape and shift the equilibrium to the right and also let the excess formaldehyde to leave the system which is difficult to purify.

## 4.2 Polymerization Kinetics

Polymerization reactions for benzoxazine involves several steps which results in complex kinetics. As the polymerization reactions proceeds the physical medium of the reaction environment drastically has changed. At the initial state of the reaction the medium is a mixture of low molecular weight oligomers or monomers with low viscosity. As the reaction proceeds the molecular weight of the resulting chains increase which in turn increase in the molecular interaction, viscosity. On the other hand molecular mobility decreases. The decrease in the molecular mobility becomes more dramatic when the formed chains crosslinks. The crosslinked chains lose the ability to move and past one another. At this step the system becomes a high viscous medium from easy flowing medium. Up to this stage the reactions are kinetically controlled and benzoxazines undergo autocatalyzed polymerization like epoxies. Trace amount of oligomeric benzoxazine hydroxyl group act as an acid source. As the reaction proceeds newly formed OH groups are the new catalyst sources. After transition to rubbery state reaction becomes diffusion controlled and finally it solidifies.

As the polymerization proceeds due to increase in molecular weight, the thermal energy provided by that specific temperature would not be sufficient for further reactions and the chains freezes. At this stage vitrification of the material occurs, and this temperature would be the glass transition temperature of the material. As the molecular mobility decreases the reaction becomes diffusion controlled rather than kinetic controlled.

The reaction occurring at high temperature ranges for thermosetting resins are competing with the decomposition of the structure as well. It is nearly impossible to get fully converted structures but every molecule its characteristic ultimate degree of conversion, depending on its properties.

In order to understand the primary curing behavior of the monomers BA, BP and BZ, DSC thermograms of each were examined at different heating rates (Figure 4.5,4.6 and 4.7). Crude BA and BZ show significantly lower melting temperature compare to purified ones. Similarly their curing onsets have lowered compare the pure products. However, decrease in the melting temperature is much faster than curing temperature. This gives a wider processing window, i.e. more time to prepare desired shapes while it melts before curing starts.

For the BP monomer however, the decrease in the curing onset is faster than the melting temperature. The decreases are small, and the material reveals similar behavior with the purified one.

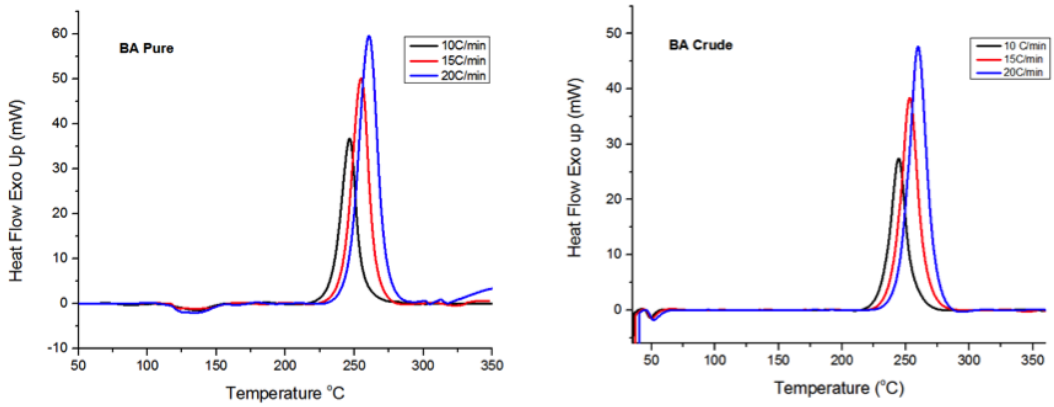


Figure 4.5: DSC thermograms of pure and crude BA monomers at different heating rates

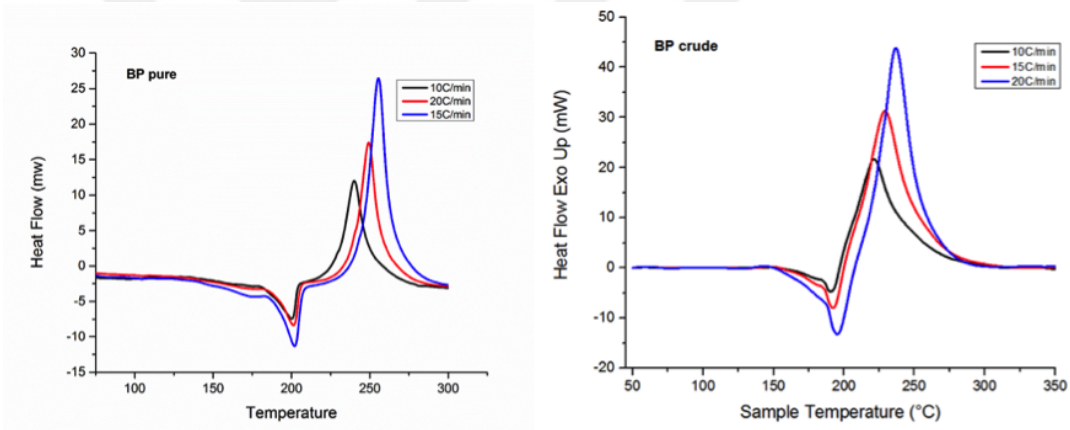


Figure 4.6: DSC thermograms of pure and crude BP monomers at different heating rates

Curing activation energies of uncured material are examined with Kissinger [11] method, which assumes reaction activation energy constant during curing independent of curing degree which is not correct as abovementioned. Maximum curing peaks of crude and purified monomers and their reaction activation energies which are calculated according to 4.1 are shown in Table 4.4.

$$-ln\left(\frac{\beta}{T_p^2}\right) = \frac{Ea}{R} \times \frac{1}{T_p} - ln\left(\frac{AR}{Ea}\right) \tag{4.1}$$

In 4.1; $\beta$ is the heating rate, $T_p$ is the peak temperature of the exotherms at each heating rate, Ea is the activation energy, R is the universal gas constant and A is the preexponential factor.

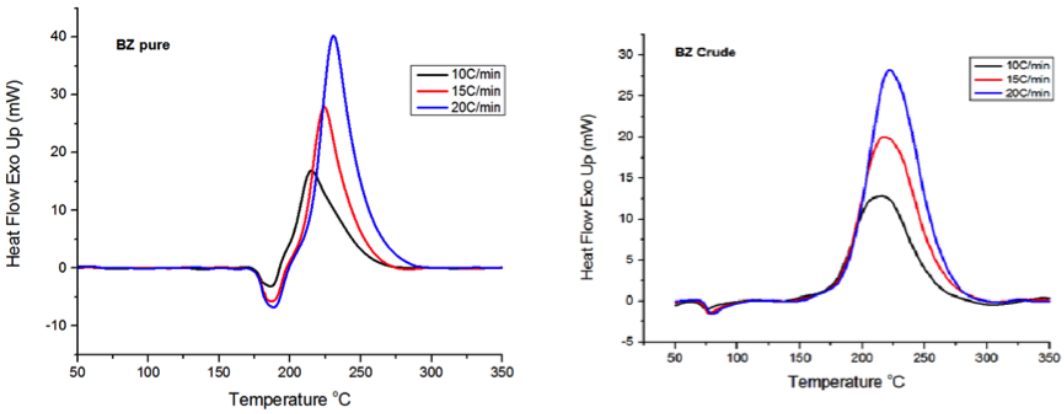


Figure 4.7: DSC thermograms of pure and crude BZ monomers at different heating rates

Table4.4: Exotherm peaks of monomers and activation energies

| °C/min | BA (°C) | BP-pure (°C) | BP-crude (°C) | BZ-pure (°C) | BZ-crude (°C) |
|---|---|---|---|---|---|
| 10 | 244.55 | 240.08 | 221.47 | 215.19 | 213.38 |
| 15 | 253.26 | 249.27 | 229.32 | 224.40 | 220.72 |
| 20 | 259.82 | 255.55 | 236.98 | 230.88 | 226.21 |
| Ea (kJ/mol) | 98.56 | 95.48 | 85.52 | 92.204 | 82.05 |

As mentioned in the Section 2.2, polymerization tendency is higher for the lower electrophilic character rings. As expected, BZ has the lowest activation energy and BA has the highest. For the crude monomers, activation energies decrease further, due to catalytic amount of phenolic moieties.

## 4.3 Curing of the Monomers

### 4.3.1 DSC Analysis of Monomers

Polymerization reactions of benzoxazine monomers are exothermic. DSC analysis proves this information while giving an exothermic peak around the polymerization temperature depending on the dynamic heating rate. As a consequence, the energy under the exothermic peak is proportional with the energy release during cure.

Curing characteristics of benzoxazine resins **BA**, **BP** and **BZ** were studied by a differential scanning calorimeter (DSC) at a heating rate 10 °C/min as shown in Figure 4.8. The stepwise decreases in heat of the samples are melting temperatures of the monomers. The thermal transition located between 150 and 275 °C are attributed to the thermal curing characteristics of benzoxazine ring opening reactions. The characteristic transitions of the monomers are collected in Table 4.5.

BA has a melting temperature of 48 °C, BZ has a melting point of 75 °C and BP has a melting

Table4.5: DSC analysis of monomers BA; BP and BZ

| | $T_{onset}$ (°C) | $T_{peak}$ (°C) | $T_{end}$ (°C) | $T_{melting}$ (°C) |
|---|---|---|---|---|
| **BA** | 210 | 249 | 270 | 48 |
| **BP** | 191 | 226 | 264 | 195 |
| **BZ** | 152 | 218 | 256 | 75 |

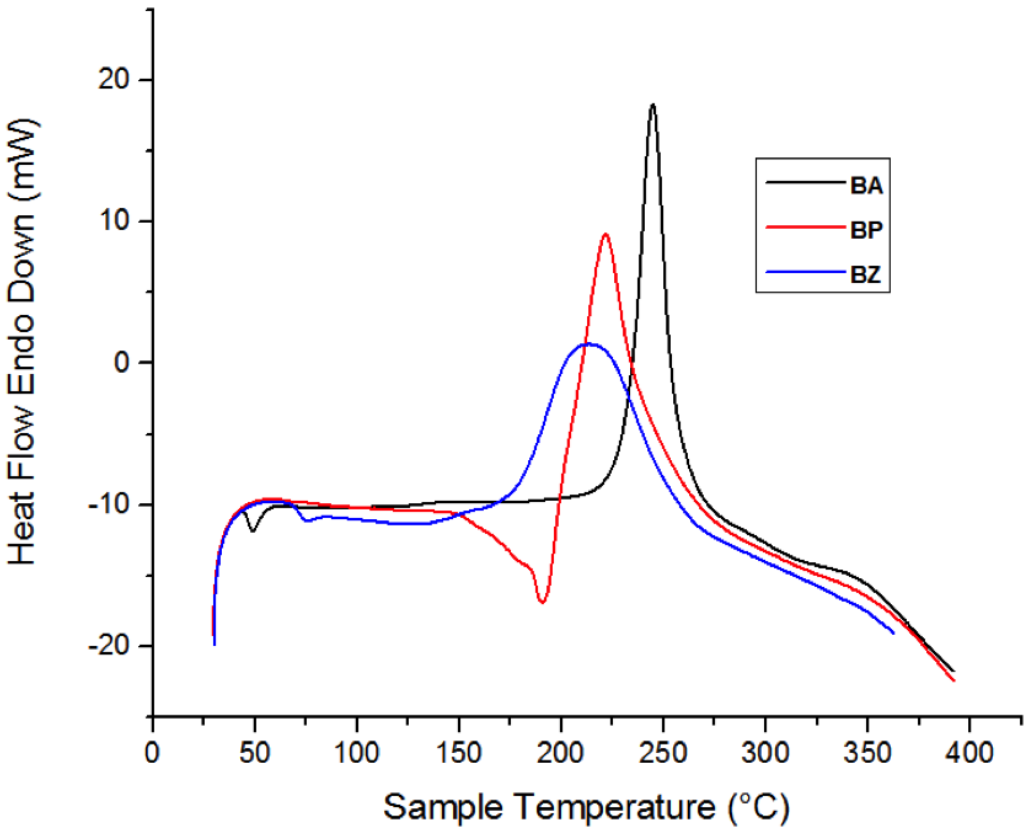


Figure 4.8: DSC analysis of BA, BP and BZ monomers

temp of 195 °C. The lowest melting temperature of BA can be attributed to the alkyl units on the bridge, which provides free rotation and prevents compact packing of crystallites. BP has the highest melting behavior, which may be due to the strong interaction resulting from the $\pi$-$\pi$ stacking of the aromatic units.

The polymerization rate is affected mainly from two contributions. First one is the electronic effect of the monomers and the second one is the interactions between the molecules determining the viscosity of the system. At the beginning of the reaction even though BA has the lowest viscosity, the initiation of the reaction is the slowest compared to the others due to electronic effects. As shown in Figure 2.5 the oligomerization or polymerization starts with the breakage of the -O-C- bond at the oxazine ring. The reason of the latest reaction start of BA may be the electron donating bridge substituents on the molecule. The electron donating alkyl units at the para position of oxygen increases the charge density of it [54]. The increasing charge on the oxygen atom makes the bond more stable and this retards the initiation of the reaction.

Similarly BZ has the lowest onset of polymerization due to the decreasing effective electronic charge on the oxygen, which eases the breakage of the bond. BP has nothing on the bridge and should show an average behavior, which is in agreement with the DSC results.

At the second step of the reaction (Figure 2.5), the alpha carbon of the benzoxazine ring attacks to the iminium ion via electrophilic substitution reaction. The effective charge density on the alpha carbon of benzoxazine increases the rate of reaction. As a result BA has the highest rate for the second step of polymerization. BZ on the other hand has the lowest charge density on $\alpha$ carbon. Therefore, the rate of reaction decreases from BA to BZ due to this electronic effect. Another factor affecting the retardation of polymerization proceeding is the viscosities of the systems. The viscosity enhancement is the lowest for BA due to weak intermolecular interactions compare to BP and BZ. These reasons explain the exothermic peak shapes. For BA ring opening is retarded but once it opens the reaction proceeds more quickly than the others. For BZ on the other hand, ring opening is enhanced but electrophilic substitution is retarded.

The difference between melting temperature and curing onset gives the processing window of the material. Thermograms reveal that the highest processing window belongs to BA and the lowest belongs to BP.

### 4.3.2 Cure Monitoring Via DSC and FTIR

As mentioned in 4.2 Polymerization reactions depend on both electronic effects and reaction medium viscosity. During polymerization of thermosets the material transfer itself from liquid to first rubbery phase then glassy phase. Therefore, while deciding the reaction temperatures, some certain consideration should be accounted beside the DSC thermograms.

- High temperatures are needed for curing to occur. As a result, degradation of the material is inevitable in competition with the polymerization during thermal treatment (shown by the Appendix B). In order to minimize the degradation rate, the reaction should be conducted at the lowest possible temperature for reaction to occur with a slow rate.
- The reaction at constant (relatively) low temperature can proceed to some extent due

to the increased viscosity and molecular weight. The energy given by the constant relative low temperature will not be sufficient to continue the reaction due to the formed secondary forces via molecular weight increase. This results in freezing the reaction, ie. vitrification.

As a result, for the polymerization to occur with a minimum material lost, proper step heating process were conducted. The degree of conversions are calculated according to Equation 4.2

$$\%Curing = \left(1 - \frac{\Delta Hi}{\Delta Hmonomer}\right) * 100 \tag{4.2}$$

Where $\Delta Hi$ is the amount of exothermic energy of the material after the thermal treatment. $\Delta Hmonomer$ is the amount of the heat of the heat of the untreated monomer.

#### 4.3.2.1 Curing of BA

The optimal curing conditions of BA monomer were determined from the partial disappearance of the area under the curve of the exothermic peak in the DSC experiment. Corresponding curves are shown in Figure 4.9.

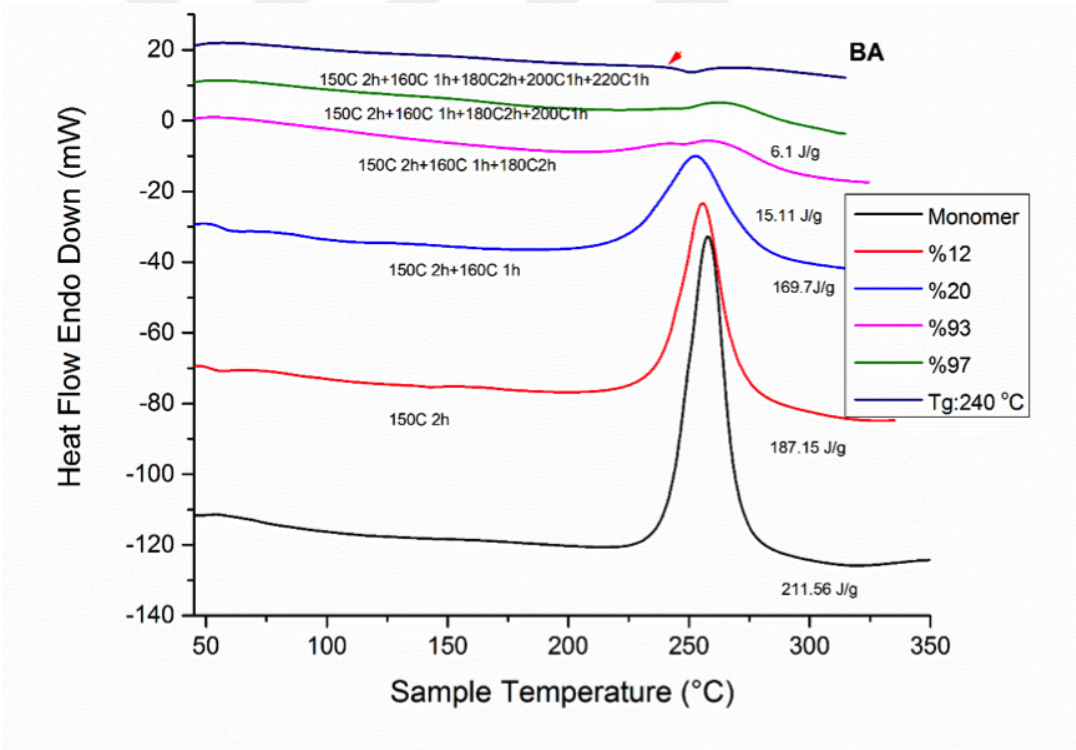


Figure 4.9: DSC thermograms BA resin after each cure stage

The heat of reaction of the uncured sample was measured to be 211.6 J/g. After a step curing at 150 °C/2 h, 160 °C/1 h, 180 °C/2h, 200 °C/1h and 220 °C/2 h, the values decreased to 187.2, 169.7, 15.1 and 6.1 J/g, respectively, which corresponded to the degree of conversion of

12, 20, 93 and 97 %. The decrease in the heat capacity around 220 °C can be interpreted as glass transition.

The curing exotherm shifts to lower temperature for the first two thermal treatment step, and then shifts to higher temperatures for the two last steps. This behaviour is in agreement with abovementioned idea which explains that, polymerization intiation is difficult for BA with stable oxazine ring structure. Once it is broken, the second step which is the electrophilic substitution reaction is more convenient for BA. After some extent of course the viscosity reaches a critical value with incresed molecular weight, the probability of the reaction to occur decreases and needs more energy input. Chemical structure of benzoxazine resin BA, its network formation with the abovementioned curing schedule was studied by FTIR spectroscopy. Figure 4.10 shows corresponding FTIR spectra.

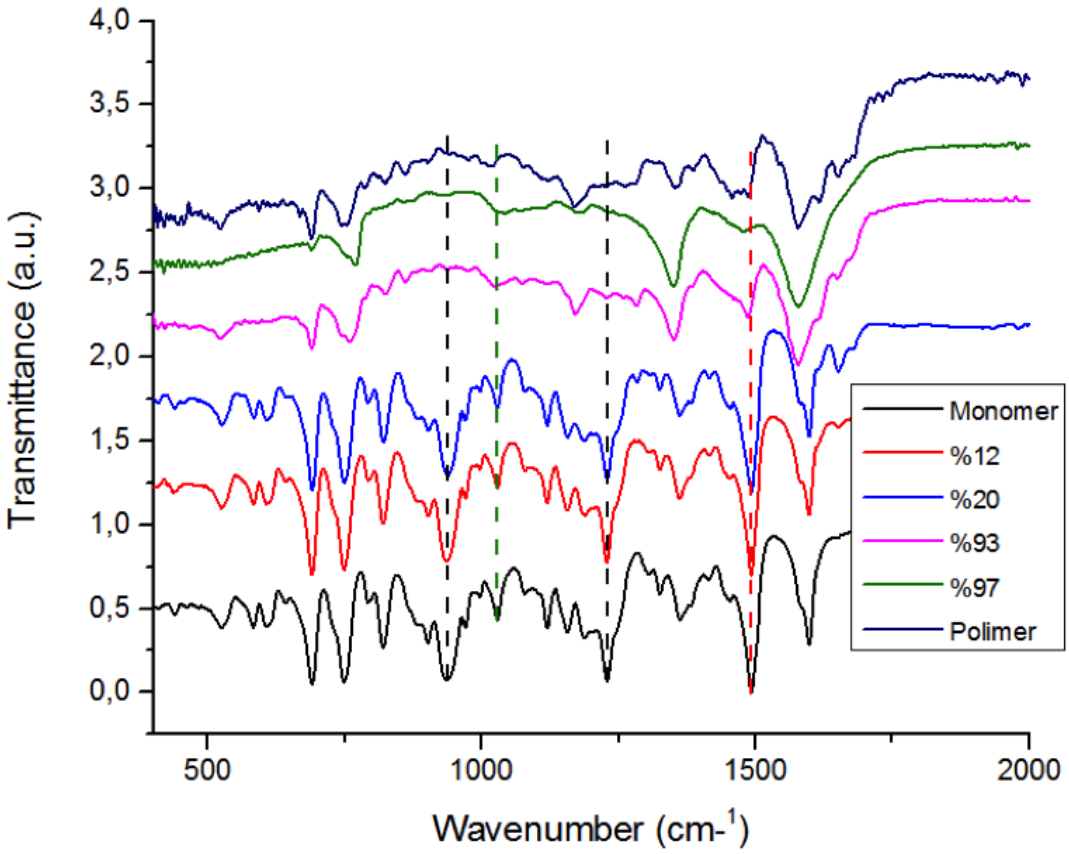


Figure 4.10: FTIR spectra of BA resin after each cure stage

IR absorption band found at 1230 $cm^{-1}$ can be at assigned to C–O–C stretching mode of benzene ring and 1493 and 938 $cm^{-1}$ assigned to tri-substituted benzene ring as shown in Figure 4.10 bottom curve.

The oxazine ring was broken by the breakage of C–O-C bond of the ring. With the initiation of polymerization the BA molecules were transformed from a ring structure to a network structure. While this process occuring tri-substituted benzene ring transforms into a tetra-substituted benzene ring [55–57]. The polymerization reaction of the BA can be monitored from the decrease of the absorption bands at 1493, and 938 $cm^{-1}$ and the appearance of the

new absorption band at 1476 $cm^{-1}$ of the tetra-substituted benzene ring.

#### 4.3.2.2 Curing of BP

The network formation of BP after thermal cure was also monitored by DSC thermogram. Figure 4.11 shows DSC curves of BP after each stage.

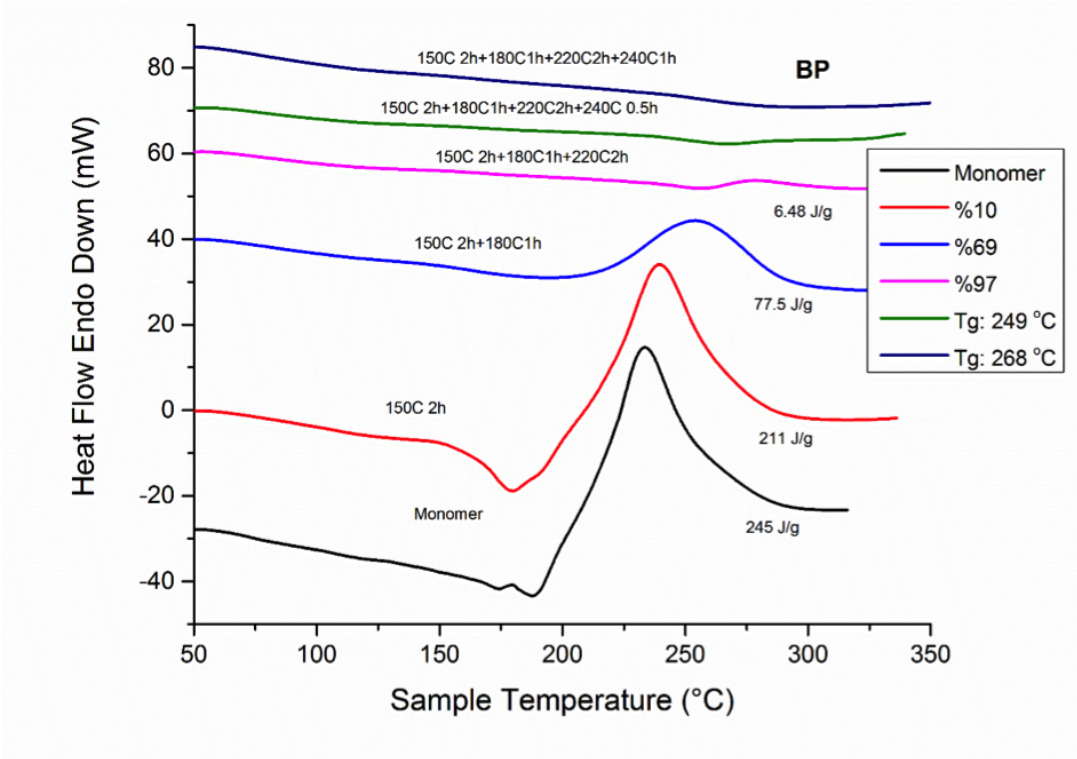


Figure 4.11: DSC thermograms BP resin after each cure stage

The heat of reaction of the uncured sample was measured to be 245 J/g. which is higher than needed for BA. After a step curing at 150 °C/2 h, 180 °C/1 h, 2200 °C/2h and 240 °C/1 h, the values decreased to 211, 77.5 and 6.5 J/g, respectively, which corresponded to the degree of conversion of 10, 69, and 97 %.

Although it is seen that 30 min at 240 °C is sufficient for ultimate conversion, the step heat capacity increases with the increase in thermal treatment. This can be due to the immobilization of dangling segment with thermal annealing.

FTIR spectra of BP after each cure stage, as shown in Figure 4.12.

With the increase of curing temperature, the absorption bands of C–O–C stretching mode of benzene ring at 1230 $cm^{-1}$ and tri-substituted benzene ring at 1484 and 928 $cm^{-1}$ decreased and finally disappeared after the curing at 240 °C. Additionally, a new band is formed at 1450 $cm^{-1}$ which can be attributed to four membered benzene ring signal.

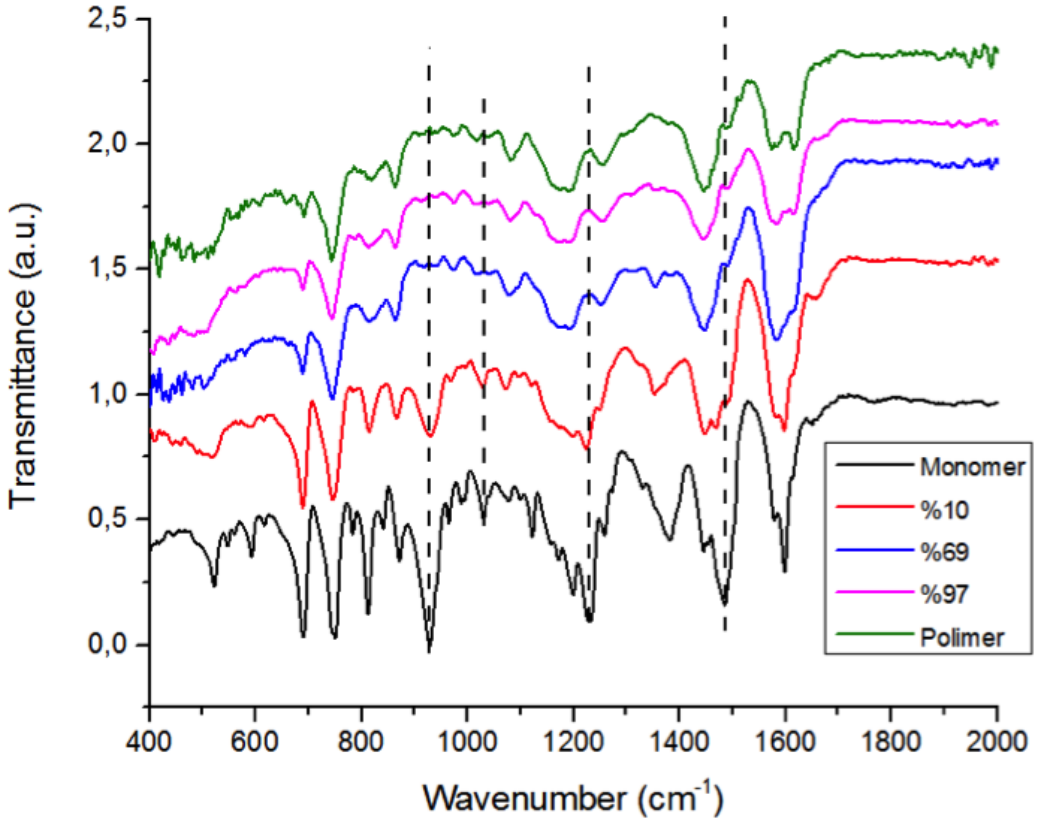


Figure 4.12: FTIR spectra of BP resin after each cure stage

#### 4.3.2.3 Curing of BZ

In order to maintain minimum time and lowest temperature curing schedule, step heating temperature program was applied to BZ monomer. Figure 4.13 shows respective responses of the material after each thermal step.

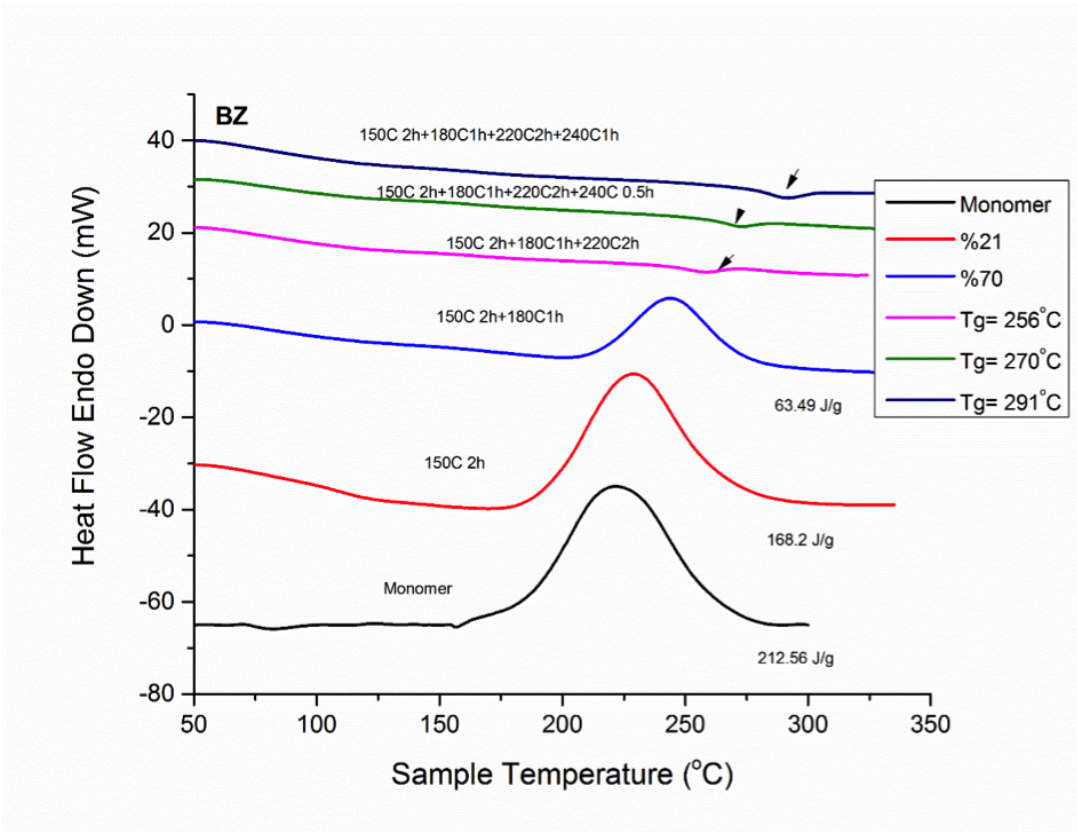


Figure 4.13: DSC thermograms BZ resin after each cure stage

The heat of reaction of the uncured sample was measured to be 212.6 J/g. The decrease of the exothermic amount is clearly observed with the increase of curing temperature. After a step curing at 150 °C/2 h, 180 °C/1 h, the values decreased to 168.2 and 63.5 J/g, respectively, which corresponded to the degree of conversion of 21 and 70 %. The exotherm disappeared after curing at 220 °C/2h indicating the completion of cross-link reaction. However after thermal treatment at 240 °C/1 h, the glass transition shifts to higher temperature.

As indicated in 3.1.1, the polymerization gets harder for both BP and BZ as the reaction proceeds. The curing exotherms shifts to right with the increase in conversion.

FTIR spectra of BZ after each cure stage is shown in Figure 4.14.

With the increase of curing temperature, the absorption bands of C–O–C stretching mode of benzene ring at 1227 $cm^{-1}$ and tri-substituted benzene ring at1494 and 933 $cm^{-1}$ decreased and finally disappeared after the curing at 240 °C. Additionally, a new band is formed at 1484 $cm^{-1}$ which can be attributed to four membered benzene ring signals.

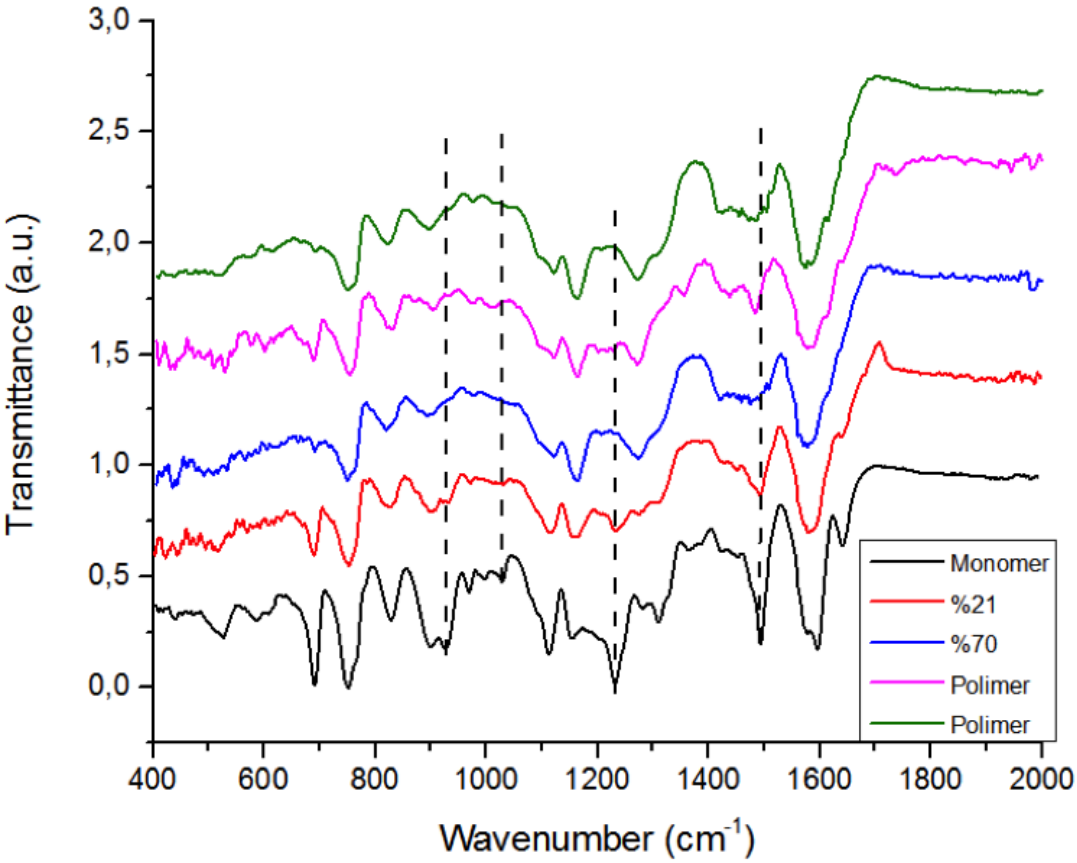


Figure 4.14: FTIR spectra BZ resin after each cure stage

## 4.4 Properties of polymers

### 4.4.1 Dynamic Mechanical Analysis

*The dynamic storage modulus (E' )* is defined as the stress in phase with the strain in a sinusoidal shearing deformation divided by the strain. *Loss modulus (E")* is defined as the stress with a phase lag with the strain divided by the strain. It is a measure of the energy dissipated as heat per cycle under deformation, i.e., the viscous response of the material. The ratio between the loss modulus and the storage modulus is called the *mechanical loss factor*, or tan $\delta$. The damping properties of the material give the balance between the elastic and viscous phases in a polymeric structure [58].

As the temperature increases, E' decreases for all resins which is attributed to the increase in the molecular mobility of the polymer chains [59]. In the glassy region before glass transition however the decrease in the modulus is faster compare to other thermosetting resins. This may be due to the weakening of the intermolecular forces of the benzoxazine structures in which hydrogen bonding has significant effects on properties. Absorption of the load with the relaxation of these intermolecular forces retards the glass transition.

#### 4.4.1.1 DMA Properties of PBA

Change in storage modulus loss modulus and damping factor with temperature increase is shown in Figure 4.15 for PBA.

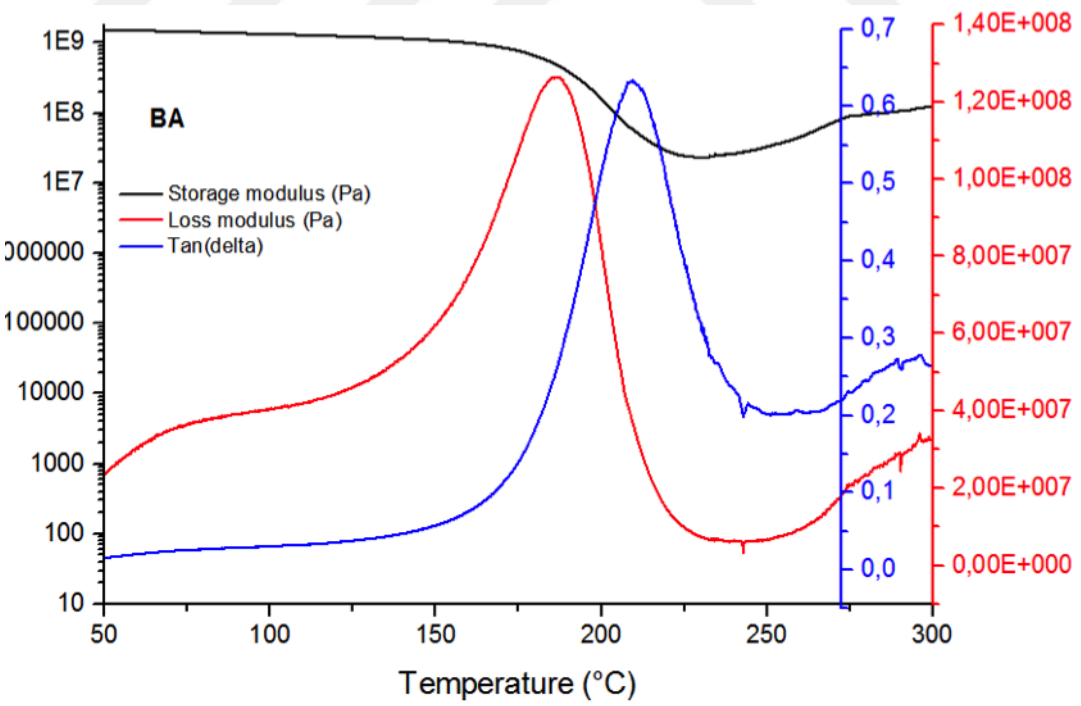


Figure 4.15: DMA curve of PBA after cure cycle of 150 °C 1h180 °C 2h, 200 °C 2h, 220 °C 1h

Mechanical integrity is lost at 168 °C for PBA. This temperature can be addressed as Tg of E'. Loss modulus on the other hand exhibits a peak at 187 °C in which the real relaxation occur before which the molecules cannot move and after which the molecules are free to move and thus maximizes at the glass transition which has the highest friction value. The ratio of loss modulus to elastic modulus (tan $\delta$) peaks with a value of 0.63 and its half height width is 40.13 °C.

The properties of resulting polymer are compared with the commercial product properties of Huntsman Company. Their final products with similar curing conditions have similar properties [51].

#### 4.4.1.2 DMA Properties of PBP

Effect of different curing cycles on the properties of PBP is shown in Figure 4.16 and 4.17.

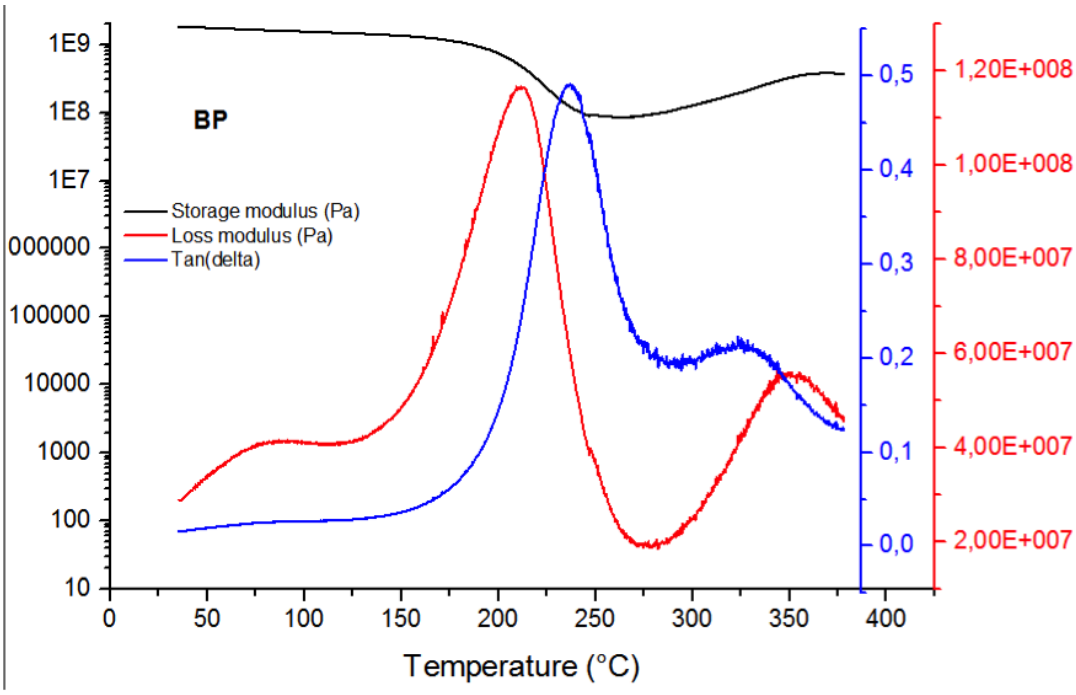


Figure 4.16: DMA curve of PBP after cure cycle of 160 °C 1h180 °C 1h, 200 °C 2h, 220 °C 1h

The increase in the thermal treatment rises glass transition temperature from 202 °C to 235 °C. In adition, tan $\delta$ value decreases from 0.49 to 0.38. Half height width of damping parameter on the other hand increases from 63.2 °C to 76.0 °C. It can be concluded that additional thermal treatment makes the material harder and limits and broadens the molecular mobility. Room temperature storage modulus on the other hand decreases significantly with the application of additional thermal treatment from 1750 Mpa to 999 MPa. Increase in glass transition temperature and decrease in modulus seems contradictory ideas. This attitude can be explained with the idea that, increase in crosslinking reduces the secondary molecular interactions and increases the free volume of the polymer [60, 61].

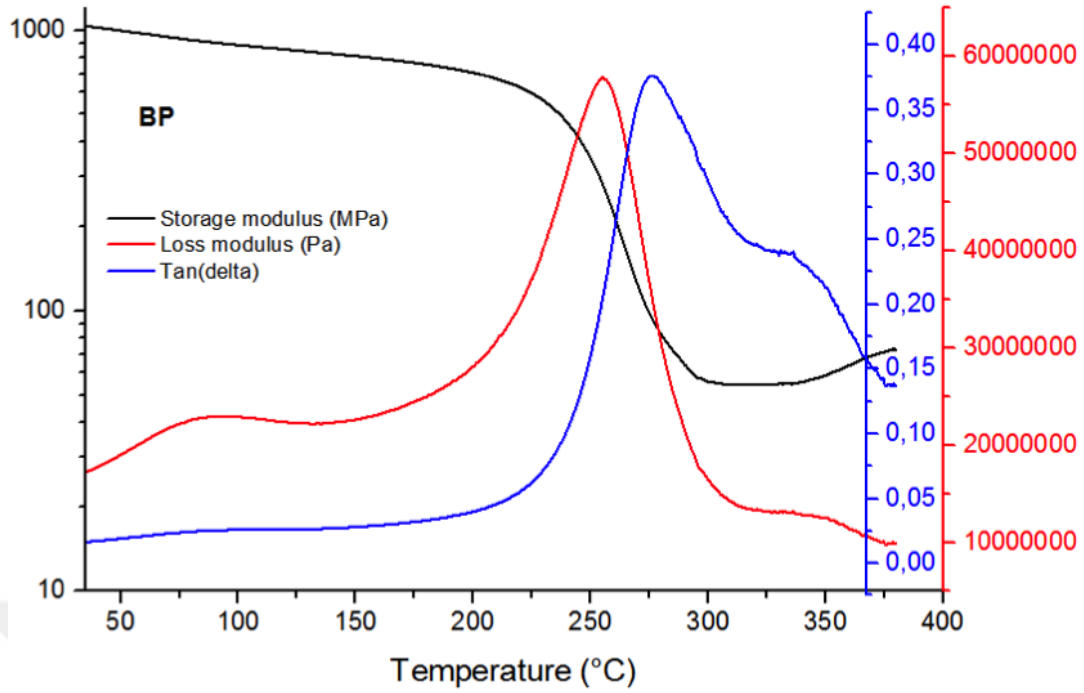


Figure 4.17: DMA curve of PBP after cure cycle of 160 °C 1h180 °C 1h, 200 °C 2h, 220 °C 1h, 240 45min

#### 4.4.1.3 DMA Properties of PBZ

Effect of different thermal treatment on the properties of PBZ resin is shown in Figure 4.18 and 4.19.

As can be seen from Figure 4.18, storage modulus shows a sudden increase after decreasing at 208 °C. This behavior can be explained with the incomplete curing. By applying thermal treatment during the test, the material first reaches the rubbery region and continues to reaction to reach complete curing by the additional uncured sites of the chain. In the Figure 4.19 on the other hand, additional thermal treatment diminishes this behavior. The mechanical integrity can be preserved up to 323 °C which is the ultimate glass transition temperature of PBZ.

As similar with PBP the damping factor for PBZ is decreased and the material gets harder as the curing treatment is applied. The storage modulus of the material is decreased with the same reasons for PBP.

The significant decrease in room temperature storage modulus can be explained with free volume values. X-linking stiffness decreases which will be explained later in detail.

### 4.4.2 Thermogravimetric Analysis

Thermogravimetric analysis is a technique in which at inert atmosphere or oxidative atmosphere, the mass loss of a substance is measured with the temperature increase or time increase

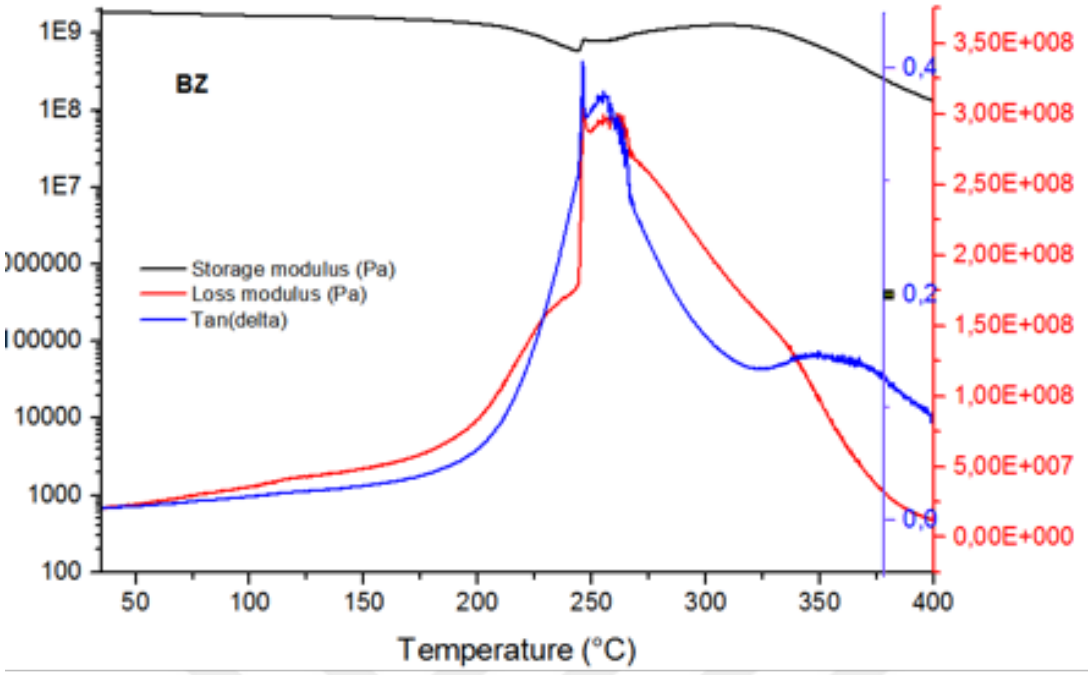


Figure 4.18: DMA curve of PBZ after cure cycle of 160 °C 1h180 °C 1h, 200 °C 2h, 220 °C 1h, 240 1h

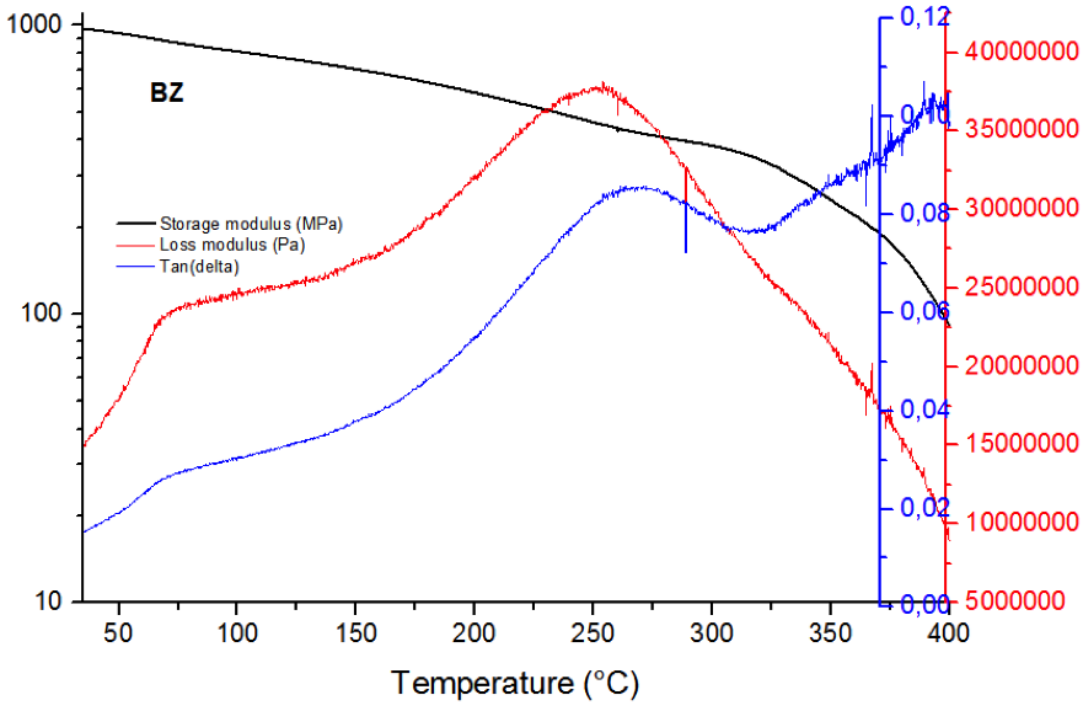


Figure 4.19: DMA curve of PBZ after cure cycle of 160 °C 1h180 °C 2h, 220 °C 1.5h, 250 °C 3h

at constant temperature with a controlled temperature program. The decomposition process is affected from the decomposition environment. This technique is generally used for investigating the decomposition and corresponding mass loss mechanism of polymers.

Thermogravimetric analysis of the cured PBA, PBP and PBZ resins in air and $N_2$ were conducted in order to understand the thermal performance of the resins. Corresponding TGA graphs measured in air and $N_2$ were shown in Figure 4.20 to Figure 4.25. The temperatures at which a significant percent of weight loss occurred with the information of char yields at 800 °C for inert atmosphere and at 600 °C are summarized in Table 4.6 and in Table 4.7.

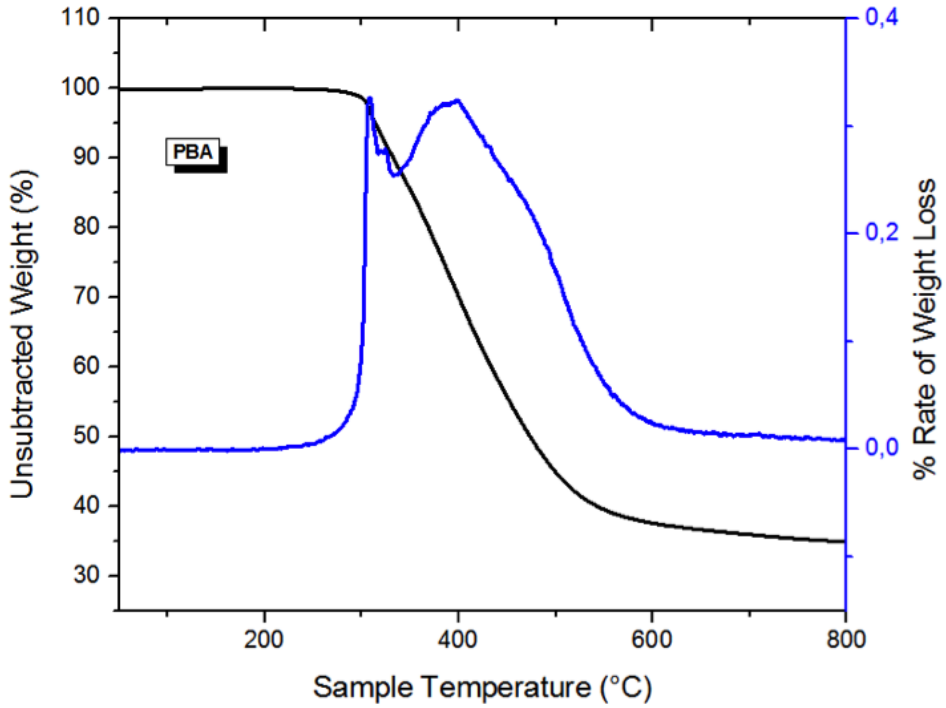


Figure 4.20: TGA curve of PBA in $N_2$

Table4.6: TGA Results of Resins in $N_2$

| | 5% | 10% | Rate1 | Rate2 | char |
|---|---|---|---|---|---|
| PBA | 316 | 327 | 307 0.32 | 400 0.32 | 35 |
| PBP | 355.5 | 381.5 | 411.3 0.22 | 487 0.12 | 61 |
| PBZ | 402 | 426 | 435 0.19 | 511 0.25 | 59 |

The thermal degradation mechanism of benzoxazine exhibits that the Mannich Bridge is the first degraded part predominantly releasing the primary amine as volatile. Depending on the nature of the amine used the first degradation products will be Schiff base or Mannich base degrade. If basicity of the amine is strong former case is favorable, for the low basicity is true for the later degradation. Within the early degradation of the Mannich Bridege, methylene bridge formation was detected [62]. Benzoxazines are also known to form strong hydrogen

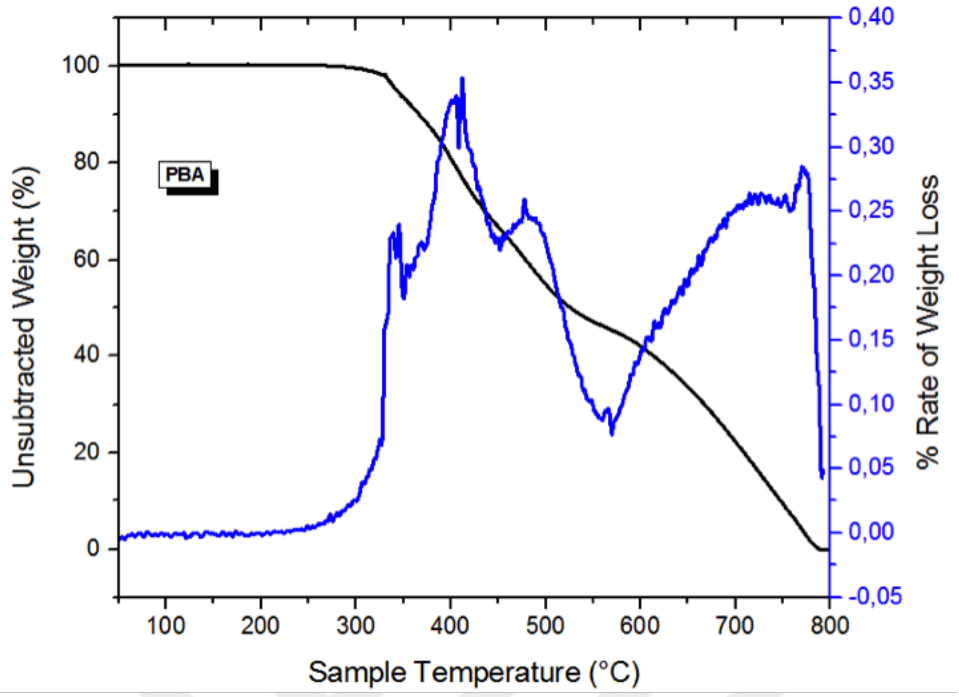


Figure 4.21: TGA curve of PBA in air

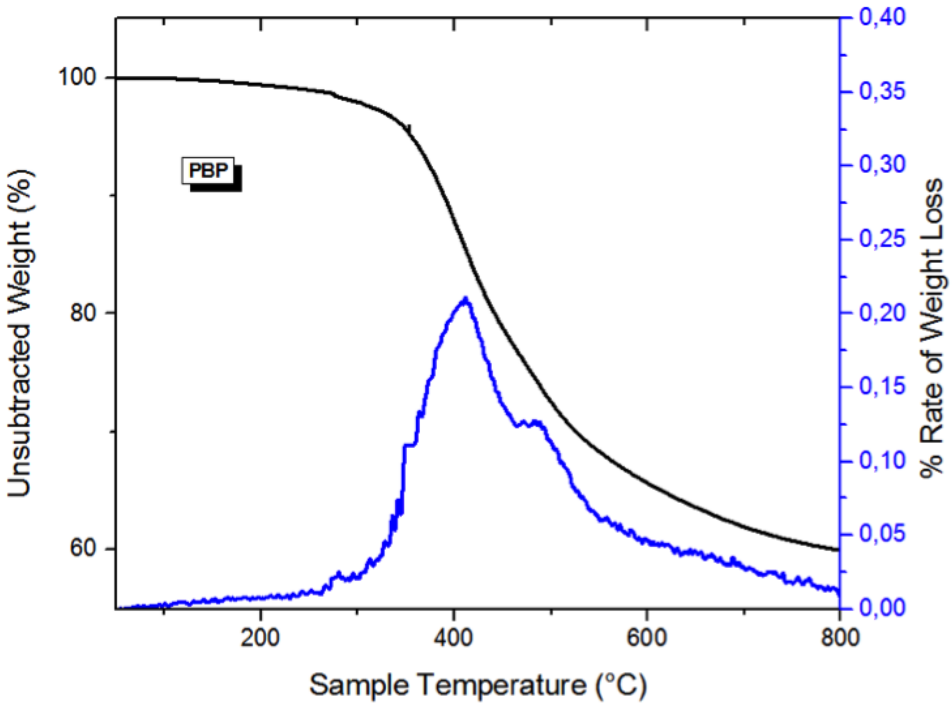


Figure 4.22: TGA curve of PBP in $N_2$

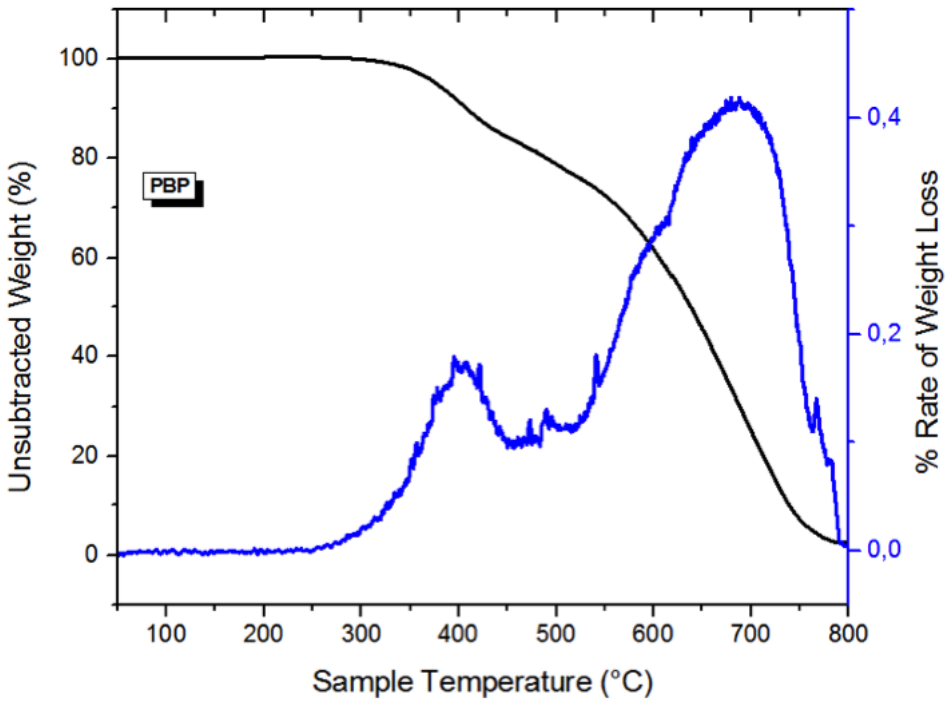


Figure 4.23: TGA curve of PBP in air

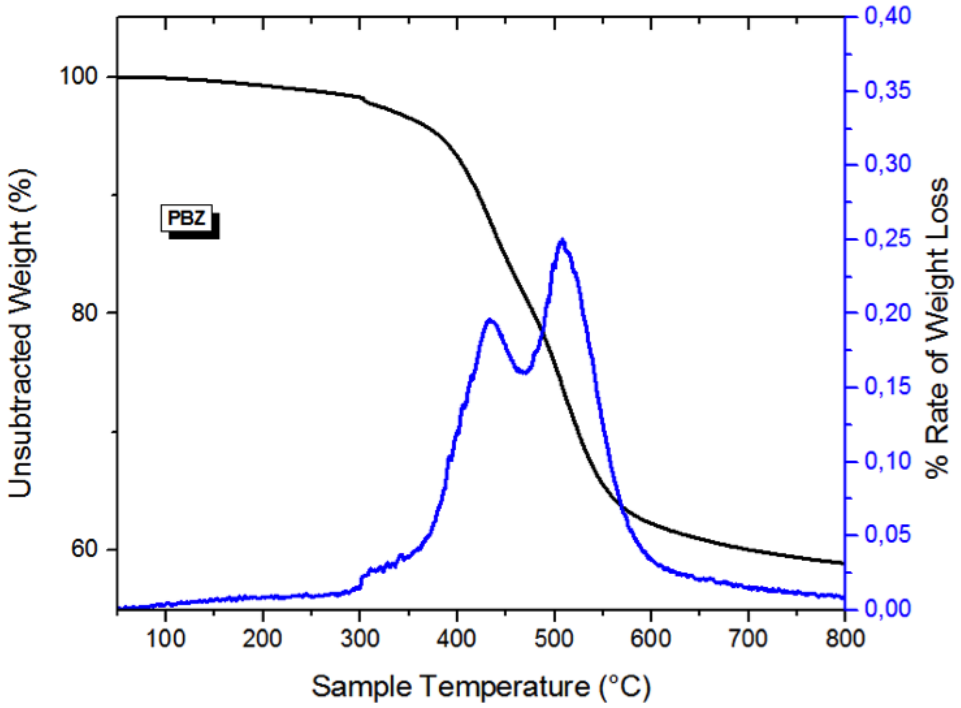


Figure 4.24: TGA curve of PBZ in $N_2$

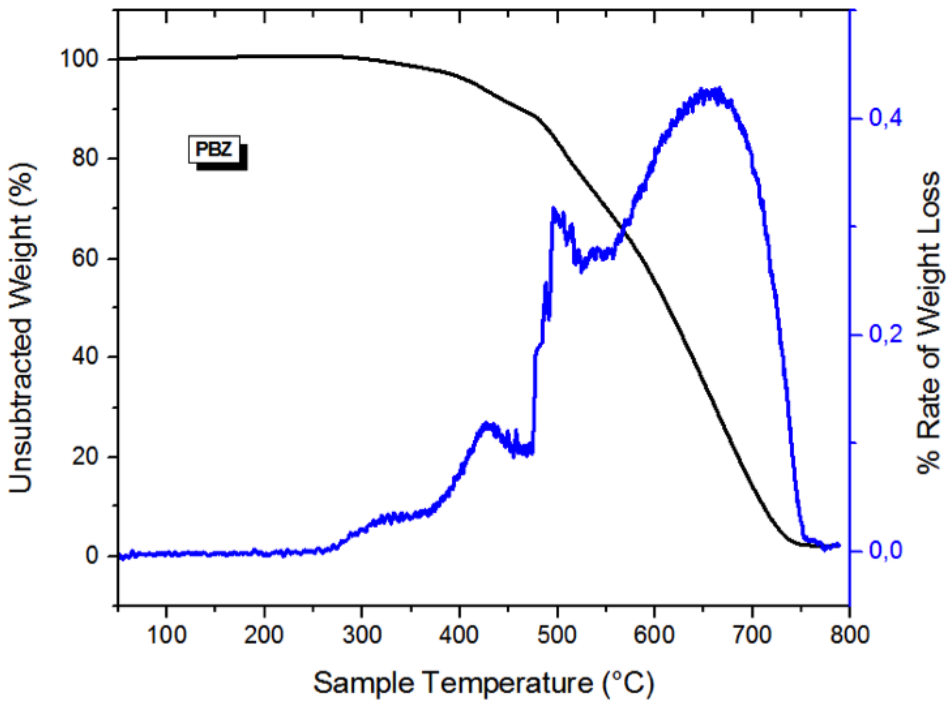


Figure 4.25: TGA curve of PBZ in air

Table4.7: TGA Results of Resins in Air

| | 5% | 10% | Rate1 | Rate2 | char |
|---|---|---|---|---|---|
| PBA | 345 | 369 | 411 0.34 | 720 0.26 | 42 |
| PBP | 379 | 409 | 401 0.17 | 692 0.41 | 62 |
| PBZ | 435 | 465 | 426 0.11 | 658 0.43 | 56 |

bonds. Strength of the hydrogen bond can delay the initial degradation temperature. The type of the hydrogen bonds depends on phenol acidity and amine basicity. More acidic phenols yield higher fraction and stronger intramolecular six membered hydrogen bonding as OH—N. The strength of this hydrogen bonding affects the primary decomposition and it is highest for PBZ and lowest for PBA. The isopropyledene unit in PBA also has similar decomposition temperature as the mannich bridge. As a result the first decomposition for PBA is very fast. For the degradation of the remaining phenolic moiety, the degradation temperature is highest again for PBZ than PBP, however the rate is also higher. At the end the char yield of PBP exceeds PBZ slightly.

Under inert atmosphere the polymer show mainly two step degradation. The first step is abovementioned respective amine group degradation, and the second is the phenolic backbone degradation. PBA starts to degrade first and PBZ starts as the last. Although PBZ has highest degradation temperature as at the inert atmosphere, the overall rate results in highest char yield for PBP. The thermograms show that three of the polymers show thermoxidative stability till 500 °C.

### 4.4.3 Cone Calorimetry Analysis

The complexities in the reproducibility and chemistry of the fire, there are different methods to analyze different characteristics of combustion process. Limiting Oxygen Index (LOI) UL-94 dripping tests are some common used examples of these methods. Cone Calorimeter is a bench-scale flame retardancy test in which different levels of thermal radiation can be simulated. Heat release rate, time to ignition, mass loss rate, effective heat of combustion are some characteristics results of the material defining their fire behaviors [63, 64].

*Time to Ignition (s):* When surface of the material is exposed to fire, it is heated to about the endothermic decomposition temperature of the material. Decomposition produces flammable gases flow from material to fire. When the mass loss rate of the decomposed product reaches a significant value with an effective heat of combustion sufficient to make them to spark with fire, ignition occurs. TTI can be measured from the onset on an HRR curve. TTI depends on; amount of thermal irradiance, oxygen availability, temperature, thermophysical and themochemical properties of the material.

*Heat Release Rate ($kW/m^2$):* A quantitative measure of the amount of oxidative exothermic thermal energy released by a material per unit are when exposed to fire radiating a constant heat flux. HRR is not constant but varies with exposure time. The most characteristic parameters are the *Peak Heat Release Rate* and *Average Heat Release Rate*. The heat released by a burning material can provide additional thermal energy for the growth and spread of fire. As a consequence it is the most important characteristic of a material defining its flammability.

*Mass Loss:* Measurable amount of the material when it is exposed to fire. It depends on the ignition time, combustion energy, char formation or transformation from thermally thick material to thermally thin material [64].

*Effective Heat of Combustion (MJ/kg):* For cone calorimetry measurement effective heat of combustion is defined as the ratio of heat release rate to the mass loss rate.

*Total Time of Burning:* It is the time elapsed from the beginning of the test to the flameout.

*Fire Grow Index:* Ratio of PHRR to TTI. It is a way of describing the flame spread rate. The unit is kW/m$^2$s.

*Fire growth Rate:* The ratio of PHRR to time to PHRR. It is another definition of flame spread rate. The unit is kW/m$^2$s.

In order to have better flame retardancy, heat release rate, total heat release and mass loss should be lower with an increase in time to ignition value.

*Heat release behaviour of polymers:* Heat Release Rate profile of a material fluctuates considerably over time due to various chemical and physical thermal events occurs to the sample exposes to the fire. First the material does not release any heat because the thermal loads are insufficient to heat the material to the decomposition temperature.

When external heat flux heats the surface to thermal decomposition temperature, an immediate heat release occurs from the initial surface volatiles. They immediately form a protective layer which is not so strong. Then the heat release shows a sudden decrease due to the first formed protective layers. Since the initial layer is not strong enough the rate starts to increase but steadily this time. After a while due to the formation of an effective char layer, the rate starts to decrease after it peaks. Here the char functions in two ways; first, it behave as a barrier preventing the release of flammable volatiles to the flame zone and diffusion of oxygen to the decomposition zone. Second, due to its porous structure, it behaves as a thermal barrier inhibiting the direct exposure of the flame to the material.

By these two mechanisms the decomposition rate and thus the heat release rate slows down. In Figure 4.26 typical burning behaviours of different materials heat release rate graphs are shown.

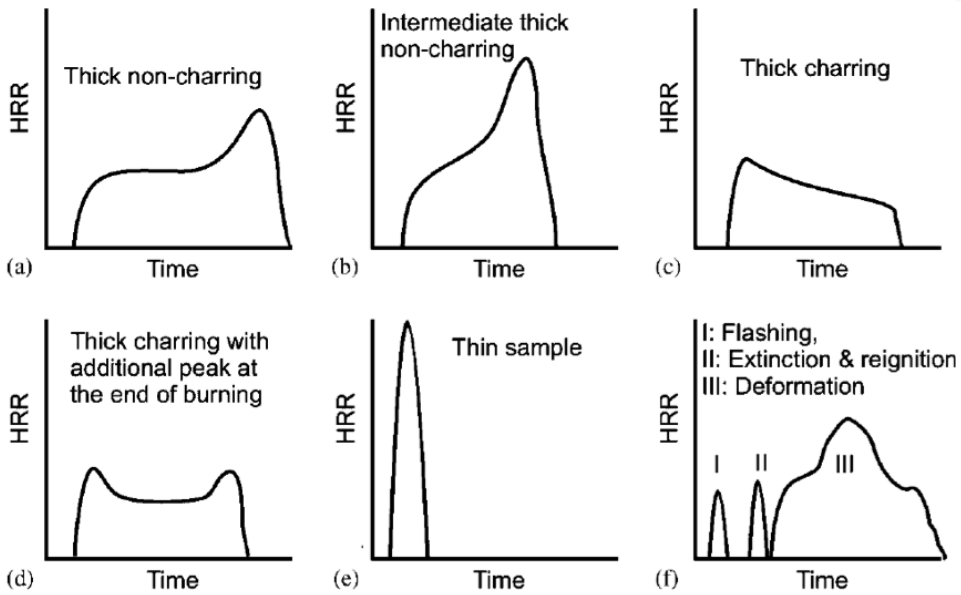


Figure 4.26: Typical HRR curves for different characteristic burning behaviours

Under 50 kW/m$^2$ heat flux, the heat release rate heat, total release curve, mass loss curve and

mass loss rate and with time is shown in Figure 4.27 and Figure 4.28.

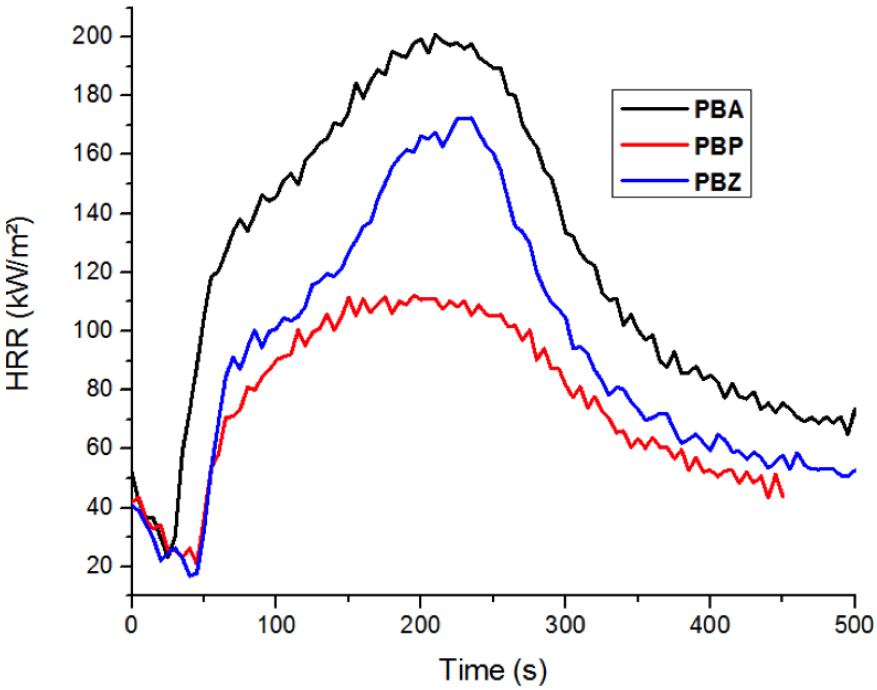


Figure 4.27: Heat Release Rate Curve of PBA, PBP and PBZ

Table4.8: Heat Release Behavior of PBA, PBP and PBZ

| Sample | TTI (s) | PHRR ($kW/m^2$) | THR ($MJ/m^2$) | PEHC (MJ/kg) |
|---|---|---|---|---|
| BA | 23 | 201 | 62 | 69.47 |
| BP | 43 | 122.22 | 32 | 77.31 |
| BZ | 47 | 172.57 | 42 | 71.7 |

Time to ignition which is the x-intercept of first increase in the heat release rate is lowest for PBA and highest for PBZ. This result is consistent with TGA at inert atmosphere results in which initial thermal degradation temperature are in the same order. Heat release rate first increases for three of the polymers due to first flammable products evaporate from the virgin material. For PBA the rate increases nearly linearly and faster than the other two polymers. The rate starts to decrease after peaking at 200 s. for PBP on the other hand the increase in the rate after first peak is slower and the rate in this zone is nearly constant. The rate of heat release starts to decrease before the others, indication of better flame retardancy. For PBZ a more complex behavior is observed. The rate increase after first increase is slower first but after 175 second it accelerates as if it is a non-charring thermally thin material.

The results indicate that, PBP has lowest total heat release and peak heat release. The highest heat of combustion value of PBP shows that better flame retardancy is occurred in

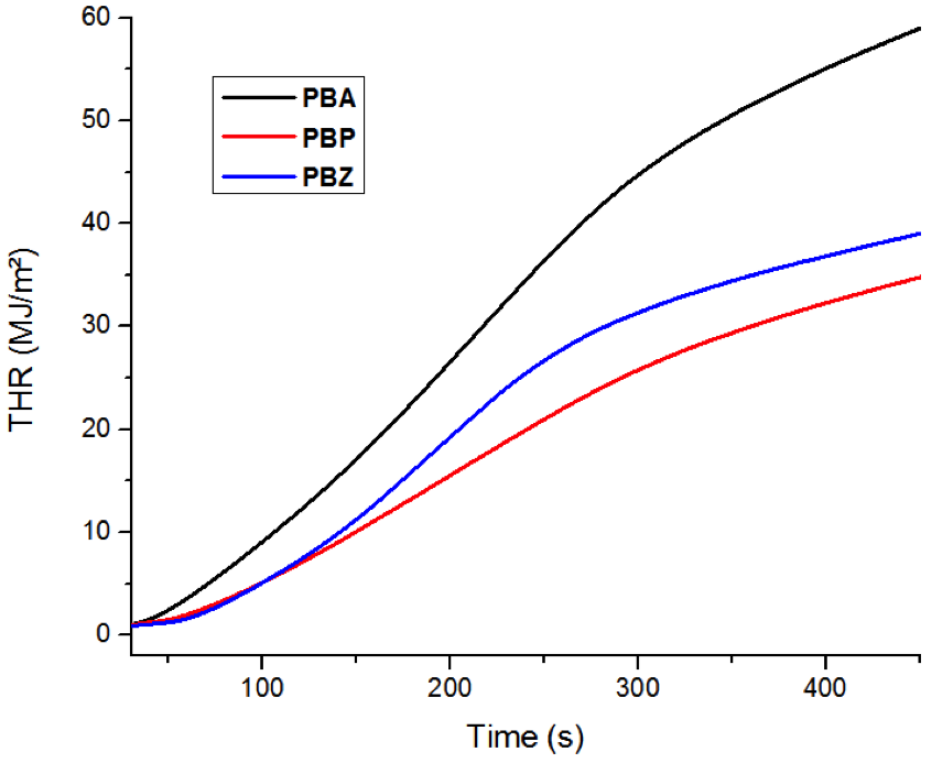


Figure 4.28: Total Heat Release of PBA, PBP and PBZ

the condensed phase rather than in the gas phase.

*Mass loss behavior of polymers:* In the first part of mass loss, material shows a delay because the surface temperature has not reached to the decomposition temperature. Than a rapid loss in mass is observed as the endothermic decomposition starts. In this step the rate increases rapidly. After this, step rate of mass loss slows down due to the increase in thermal insulation, provided by the growth of char surface layer. As mass loss proceeds the material becomes thermally thin with time and decomposition rate again increases. At last, step rate again decreases and drops to zero as the last remains of the polymer was degraded.

Under 50 kW/m2 heat flux, mass loss curve and mass loss rate curve are shown in Figure 4.29 and Figure 4.30 and the results are summarize in Table 4.9.

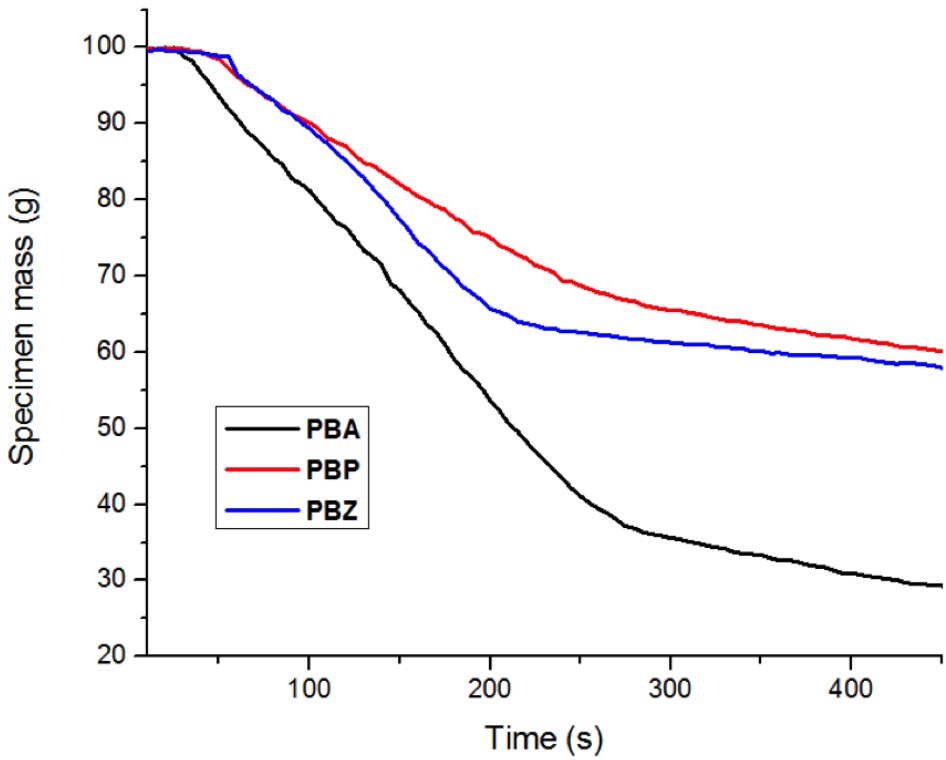


Figure 4.29: % Mass Loss Curves of PBA, PBP and PBZ

Comparing with TGA results both BP and BZ are good char forming materials around 60 % of the residue remaining at 800 °C in an inert atmosphere. The char yield for cone calorimetry measurement for the material at 820 °C for with an exposure time of 450 s are very similar with the TGA results at 800 °C in the inert atmosphere. This indicates that degradation occur below the pyrolysis zone is inert.

The rate of weight loss is higher for PBA and its char residue is the lowest among the three of the polymers. Still it has an char yield above 30 % with an exposure time of 450 second and 820 °C. PBP has the highest char yield and lowest rate of mass loss. After an initial increase in the rate of mass loss, the rate steadily decreases and after a point it has formed a stable residue that does not allow continuing of fire.

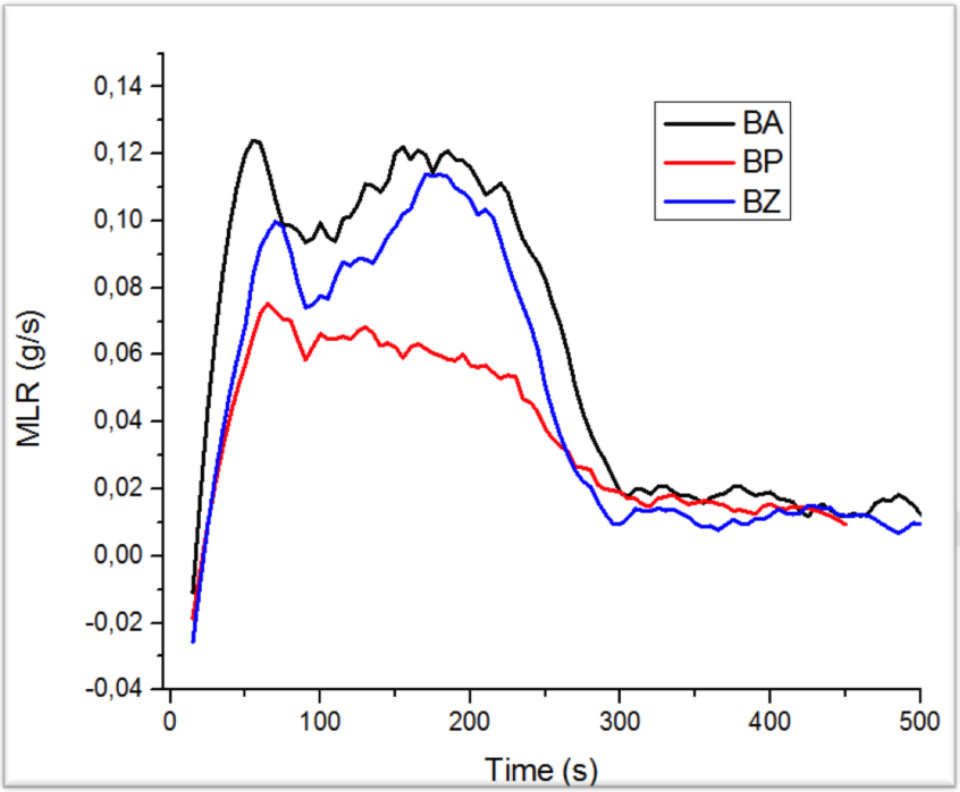


Figure 4.30: Mass Loss Rate Curves of PBA, PBP and PBZ

For PBZ the initial rate of weight loss is higher than PBP but lower than PBP. The acceleration of mass loss is on the other hand is highest among three. It behaves as if it is a non-charring material, although it has a significant amount of residue when fire ends.

In general the flame retardancy can be achieved with three mechanisms all of which are functions of each other. First one is the thermal insulation capability of the material, second is the structural integrity and the third one is the burn through resistance.

In general the condensed phase can be divided into three regions. At the top layer, initial degradation products form a char layer. Below the char layer, second layer can be named as the decomposition layer, in which the material is decomposing at a temperature above the decomposition temperature but below the char formation temperature. At this region the polymer partially degraded producing high molecular weight segments which are too heavy to vaporize to the flame zone. In addition, due to the incomplete decomposition, the material can not produce char or combustion gases. Below the decomposition zone of the material, the region can be named as virgin material, This region may contain cracks but the temperature is too low for a decomposition to occur. When the temperature at the bottom zone is low and the rate of heat transfer to this layer is slow, the material can be named as thermally thick material.

While continuing to heat the sample the char layer proceeds to move towards to the virgin zone. As a result heat transfer rate to the virgin zone increases. The material eventually becomes a thermally thin material.

For PBZ the sample cracks during the repeated experiments, the sample broken from different sides. This may result in the ease of heat conduction to the back surface and decreases the efficiency of formed char as a barrier to inhibit the escape of the flammable gaseous products into the fire zone. It behaves as if it is thermally thick although it has a considerable amount of char residue due to the occurrence of these cracks. In order to be effective char, the structural integrity of the char zone is very important.

Table4.9: Mass Loss Behavior of PBA, PBP and PBZ

| Sample | Char @ 300 (s) | Char @ 450 (s) | Time to peak (s) | Peak MLR (g/s) | Mean MLR |
|---|---|---|---|---|---|
| BA | 36 | 29 | 57 | 0.12 | 0.089 |
| BP | 66 | 60 | 65 | 0.075 | 0.049 |
| BZ | 63 | 59 | 177 | 0.11 | 0.069 |

### 4.5 Molecular Origin of the Differences of the Resins

The reason of the lowest glass transition temperature for PBA can be explained with the lowest crosslinking density of it. The crosslinking density is highest for PBZ on the other hand. The modulus value at room temperature is highest for PBA and lowest for PBZ. The values at 50 °C are; BA: 1530 MPa, BP: 998 MPa, BZ: 935 MPa. This can be explained that increasing crosslinking density increases the free volume of the material and thus decreases the modulus. The modulus values in the rubbery region show an opposite trend in the rubbery

region. At Tg+50 °C modulus values are: BA: 32.85 MPa, BP: 69.76 MPa, BZ: 177.31 MPa. We can conclude that dependency of modulus to molecular stiffness is more important than its' crosslinking density before Tg, after Tg on the other hand crosslinking density dominates the storage modulus property.

The reason of the higher crosslinking density of PBZ can be explained with the polymerization mechanism shown in Figure 4.31.

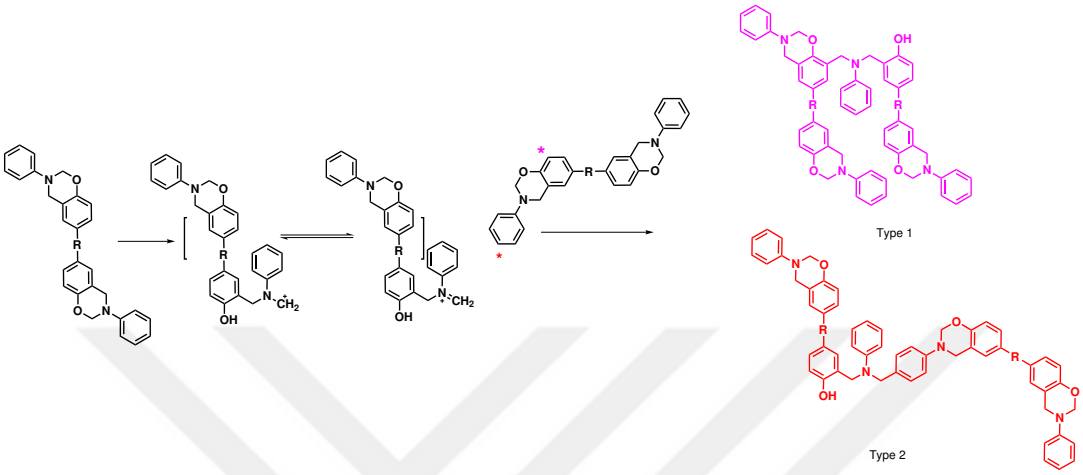


Figure 4.31: Two Types of Polymers of Benzoxazine

As explained in the introduction chapter, polymerization stars with the breakage of C-O bond in the ring forming an iminium carbocation intermediate. In the second part of the polymerization reaction free ortho position of the benzoxazine molecule reacts with the carbocation via electrophylic substitution reaction resulting in Mannich bridge (Type 1). The reactivity of this step depends on the reactivity of the ortho group. As a result electron density of this position increases the probability of the reaction. This probability is highest for BA because of the electron donating alkyl groups at the bridge and it is lowest for BZ due to electron withdrawing carbonyl group at the bridge.

Polymerization mechanism can also proceed with the reaction of para position of aniline and carbocation intermediate (Type 2). The decrease in the probability increases the probability of second reaction. This is highest for BZ and lowest for BA. This additional polymerization probability may be the reason of the increased crosslinking density of BZ. In Figure 4.32 formed benzoxazine infrared spectra are shown.

As shown from the Figure 4.32 the ratio of mono substituted benzene ring around 680 $cm^{-1}$ to the disubstituted benzene ring around 830 $cm^{-1}$ is highest for PBA and lowest for PBZ.

Yet another reason for the highest glass transition temperature for PBZ can be explained with strength of intramoleculer six membered hydrogen bonding shown in Figure 4.33.

The strength of the intramolecular hydrogen bonding depends on either acidity of the OH proton or basicity of the amine. Thus hydrogen bonding is strongest for PBZ due to electron withdrawing group at the para position and lowest for PBA due to an opposite effect. Therefore weakling of the secondary forces is most difficult for PBZ as the thermal load is applied before

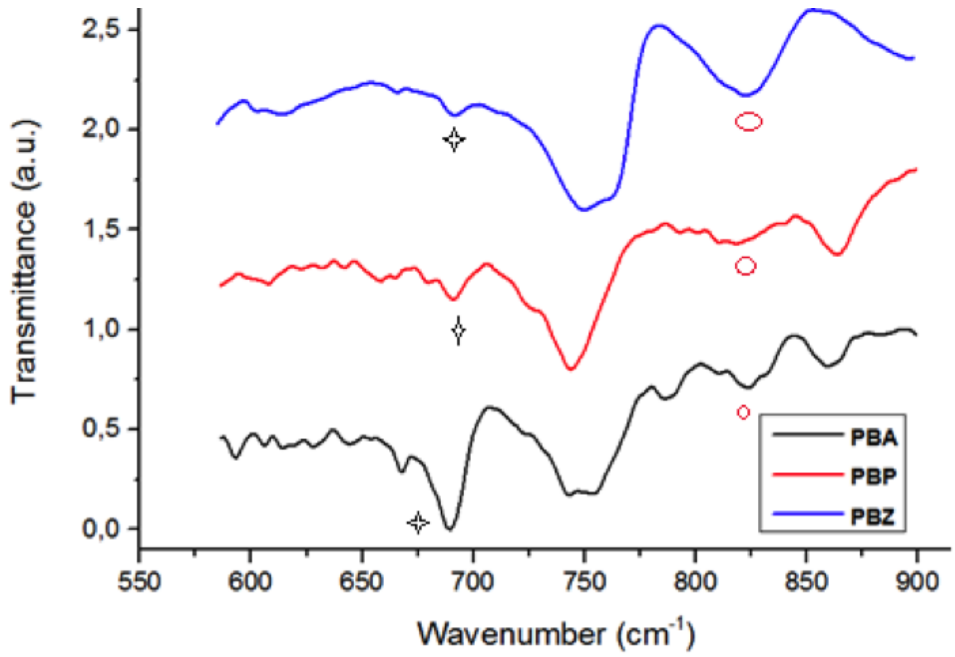


Figure 4.32: FTIR Spectra of PBA, PBP and PBZ

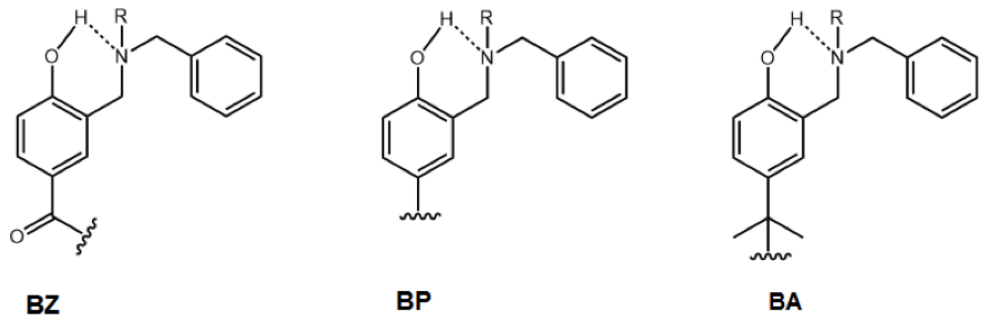


Figure 4.33: Hydrogen Bonding of Polybenzoxazine Derivatives

reaching glass transition.

### 4.6 Properties of Composites

Resin Powder Molding, which is used for solid resin row material has some advantages such as no need use of a solvent and resulting solvent evaporation problems which may result in pore formation within the composite. In addition the solid fillers may be distributed within the powder resin by ball milling. The solubility and aggregation problem of the powder fillers during process are avoided.

In order to investigate thermal insulation performance of the resins, 20x20 $cm^2$ high silica cloth fabric composites were prepared. At around 8 g of the powder resin was distributed onto the single ply of the cloth. According to the thickness requirements for corresponding tests; 8, 20 or 40 plies of the composites were prepared. Cured composites of BA, BP and BZ are shown in Figure 4.34.

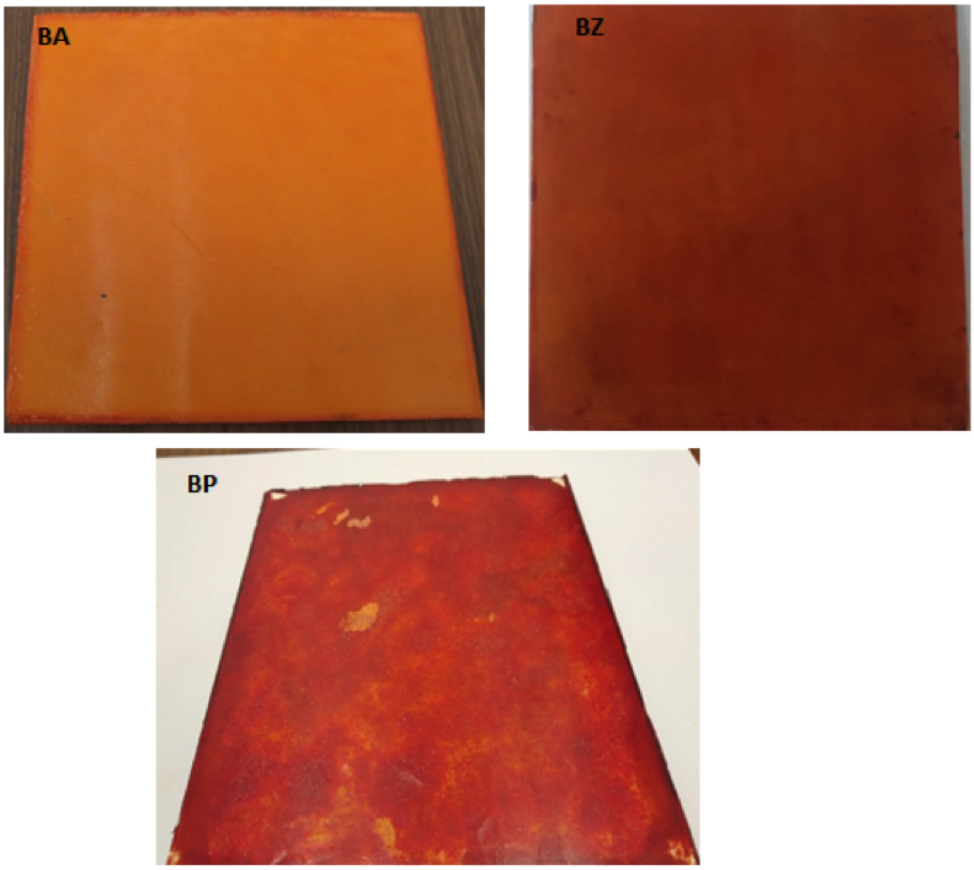


Figure 4.34: BA BP and BZ High Silica Composite Plates

Applicability of the investigated cure cycles of neat resins was tried in composite productions. After optimization studies for composite production cure cycles, appropriate temperature, pressure and time parameters were defined for both BA and BZ. For BA, after leaving the

system at 150 °C and under the pressure of 2 ton for half an hour, the temperature and pressure were increased to 160 °C and 10 ton respectively. The duration time at this temperature was 2 hours, and then the temperature was increased to 180 °C at the same pressure for two hours. Final step of curing was carried out at 200 °C for another 2 hours at the same pressure. At the end of the cycle, the system was left for natural cooling.

For BZ on the other hand, the starting procedures were the same, namely: at 150°C under the pressure of 2 ton and 30 minutes duration was decided to be enough for wetting the reinforcement. Before the completion of gelling, the temperature and pressure were both increased to 170 °C and 10 ton respectively for 2 hours. Under the same pressure, cure cycle of 190 °C 2 hour and 220 °C 2 hour was applied. The material was left for natural cooling.

For BP resin on the other hand, as can be seen from the Figure 4.30 there occurred a significant phase separation between the cured resin and fabric. The reasons may be the processing window of the monomer 4.3.1 Figure 4.8. Just after the melting the resin starts to polymerize, which does not allow resin to interact with the fabric.

Another reason may be lack of sizing agent on the fabric surfaces, which enhances the interaction between hydrophobic resin and hydrophilic fabric [65].

### 4.6.1 Density Measurement of Composites

According to Archimedes Principle measurement, the densities of the produced composites are summarized in Table 4.10. The need for the lightweight materials for current technology is one of the key reasons of using polymer composite materials with desirable performances. Density measurement samples are shown in Figure 4.35 and the averaged measurements are summarized in Table 4.10.

Table4.10: Density Measurements of BA and BZ Composites

| **g/cm$^3$** | **Sample 1** | **Sample 2** | **Sample 3** |
|---|---|---|---|
| BA | 1.736 | 1.697 | 1.740 |
| BZ | 1.627 | 1.620 | 1.636 |

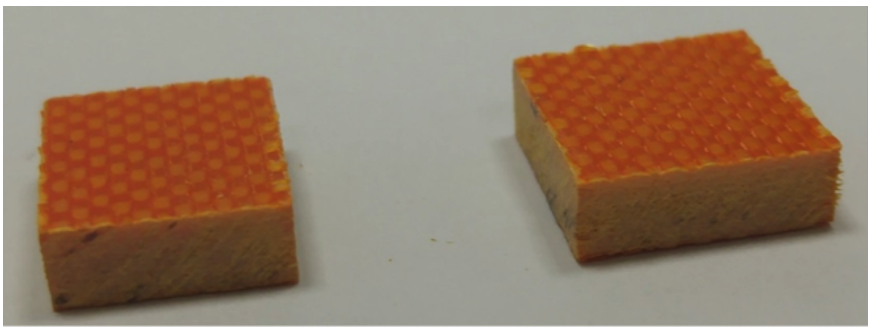

Figure 4.35: Density Measurement Samples

Thermosetting resin materials are used in aeroscope application because of their high strength

and lightweight properties compared to metal alloys counterparts. The values obtained from the measurements of BA and BZ high silica composites indicate that these materials are suitable for rocket/missile application. The current technology used for rocket/missile nozzle thermal insulation is Silica phenolic composites, which have a density of 1.63 g/cm$^3$ [66].

### 4.6.2 Thermal Analysis of Composites

TGA analyses give information about the chemical events such as dehydration decomposition beside physical phenomena such as vaporization, sublimation as a function of increasing temperature. TGA analysis is used to measure the variation in mass of the materials when subjected to heating isothermally or dynamically.

In order to analyze thermal characteristics of composites; thermogravimetric analysis had been conducted (Figure 4.36 and Figure 4.37). Corresponding results are summarized in Table 4.11. The resin/fabric ratio can be deduced from the char yield at oxygen at 800 °C. Because $SiO_2$ is stable at this [67] temperature the lost weight belongs to resin in the composite. The resin content of BA is 35 %. While preparing the composite, BA is melted at 150 °C, the viscosity has reached to its minimum value at this temperature. This value for BA resin is too small and curing onset is very high. As a result too much resin had been lost while pressing it. Although the resin content is below the desired value, the composite has still significant mechanical properties.

The resin content for BZ-high silica composite on the other hand, is calculated as 46 %. This ratio is very desirable for nozzle applications (around 40-50 percent).

BA composite has char yields of 74 %, 65 % at inert and oxygen environments respectively. The values for BZ composite on the other hand are 74 % and 65 % respectively. It can be seen that although BZ has a higher concentration of the resin, its char yield at inert atmosphere is still higher than BA composite. This is because of the higher char forming tendency of BZ as explained in 3.4.2.

The results are summarized in Table 4.11 give the information that these resins have the potential that can be used for ablative nozzle insulation materials.

Table4.11: TGA Results of BA and BZ Composite

| | Char Yield in $N_2$ (%) | Char Yield in $O_2$ (%) | Td in $N_2$ | Td in $O_2$ | % Resin Content |
|---|---|---|---|---|---|
| BA | 74 | 65 | 367 | 390 | 35 |
| BZ | 79 | 54 | 410 | 453 | 46 |

### 4.6.3 Mechanical Characterizations

#### 4.6.3.1 Tensile Tests

Tensile tests were conducted using Instron according to ASTM D3039 [68], in order to study the behavior and ability of the material response under the tensile loads. Tensile test curves

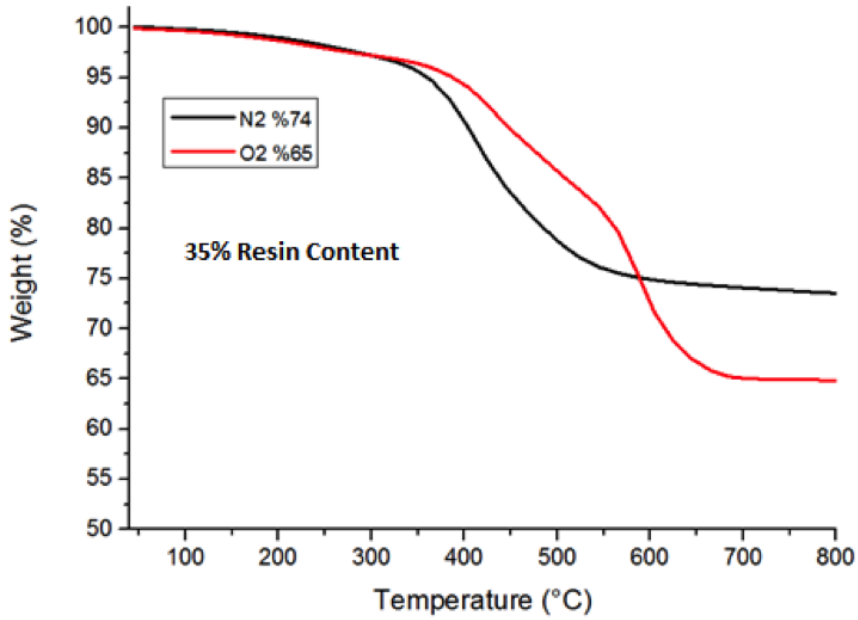


Figure 4.36: TGA of BA Composite at $O_2$ and $N_2$ Enviroment

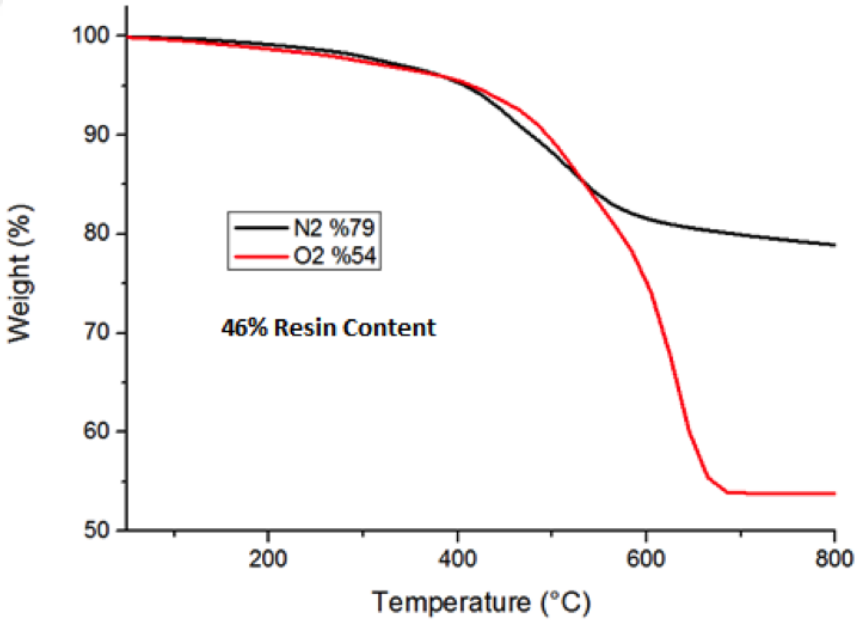


Figure 4.37: TGA of BZ Composite at $O_2$ and $N_2$ Environment

of BA and BZ high silica composites are shown in Figure 4.38 and 4.39.

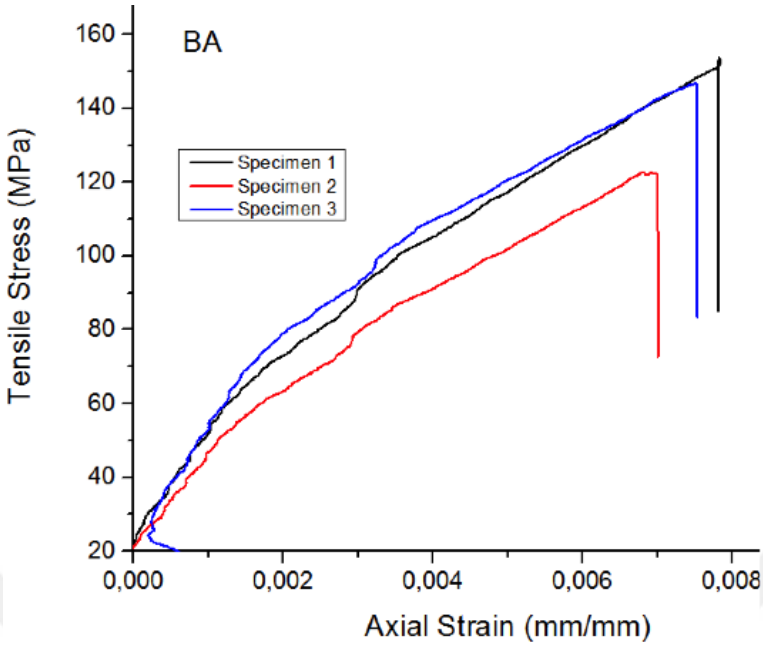


Figure 4.38: Stress strain Curves of BA Composite

After reaching maximum stress values for the samples can hold an immediate decrease of the strength values were observed.

The samples failed immediately after reaching the maximum stress. The absorbed energy under the curve can be explained as the work done against the friction of displacing the resin relative to the cloth or work required to cause elastic de-bonding.

Tensile test of results BA and BZ composites are summarized in Table 4.12.

Table4.12: Tensile Test Results of BA and BZ Composites

| | **BA** | **BZ** |
|---|---|---|
| Tensile Stress | 154 | 36 |
| at Max. Load | 123 | 43 |
| (MPa) | 147 | 72 |
| Tensile Strain | 0. 8 | 0. 2 |
| at Break | 0. 7 | 0. 4 |
| (%) | 0. 8 | 0. 3 |
| Modulus (MPa) | 22198 | 16877 |

The results reveal that, BA has a tensile strength around 150 MPa. Although the structural properties of the high silica fabrics are very low, the strength value for BA is quite high and promising.

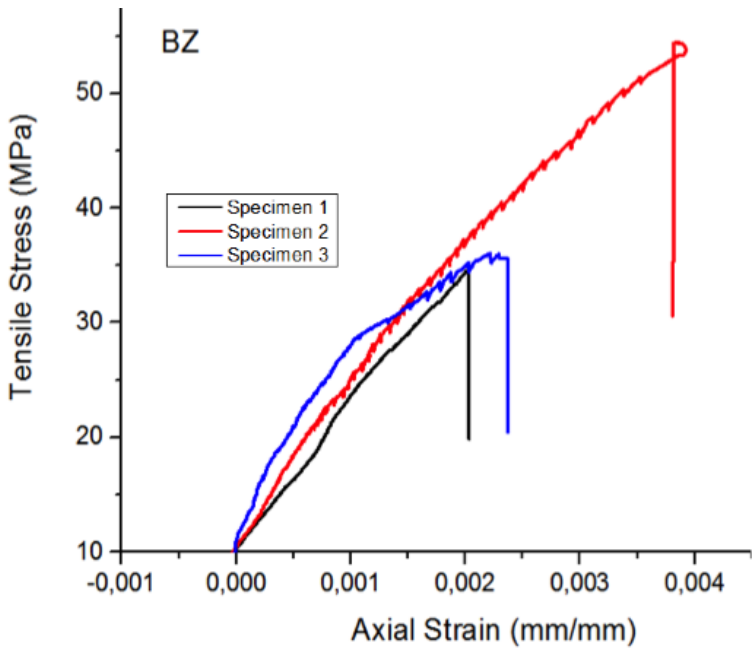


Figure 4.39: Stress strain Curves of BZ Composite

Interfacial adhesion between fiber and resin is a crucial issue, which in turn effect the overall strength of the composite material. A strong interfacial interaction and adhesion is desired in order to perform better stress transfer between fiber and matrix.

BA has more electron density throughout the entire molecule, which results in better intermolecular attraction. As mentioned before benzoxazines can have various types of H-bonding capability. The degree of intra- and intermolecular hydrogen bonding capability depends on the amine basicity and phenol acidity. As the basicity of amine or acidity of the phenol increases, the percentage of intramolecular hydrogen bonding capability increases. Geometrically available hydroxyl groups in BA resin with less intramolecularly hydrogen bonded contributes more to adhesion with silica fabrics, which also has free -OR groups at the surface.

In addition to interface strength between fabric and resin the ability of resistance to tensile force of matrix itself is another critical issue. Higher intermolecular attraction such as $\pi$-$\pi$ stacking Van der Waals interactions and H-bonding, is higher for BA due to its higher electron density. Increased coulombic interaction also enhances the load bearing ability.

In addition to electronic effects, there may be some physical contribution to the differences between BA and BZ tensile strength values. The viscosity of BA is significantly lower than BZ resin. High viscosity decreases the impregnation ability of the resin, which results in wettability capacity. In fact at the end of the test, it is seen that at some points BZ cannot spread smoothly shown in Figure 4.40.

Agglomeration acts as areas of weakness and causes stress concentrations leading to low mechanical properties. These inhomogenities prevent the load transfer behavior of the matrix due to the load-carrying capacity of the composite.

Figure 4.40: Agglomeration of BZ

BZ composite preparation methods need further optimization studies.

#### 4.6.3.2 Compression Tests

The need for insulation material compression strength is one of the key factors especially at the exit cone of nozzle. Insulation compressive strength can be a very important design consideration. The greater the compressive strength, the more durable the insulation is.

Materials which has high compression strength values, can withstand various forms of external pressure. When the insulating material has higher compression strength values, it will perform better insulation properties, and last longer.

Table4.13: Compressive Strength Test Results of BA and BZ Composites

| | **BA** | **BZ** |
|---|---|---|
| Compression Stress | 267.6 | 124.4 |
| at Max. Load | 235.5 | 139.8 |
| (MPa) | 238.1 | 145.3 |

Silica phenolic compression strengths are around 140-150 MPa. This indicates that compressive strengths of both BA and BZ are sufficient for use in this application.

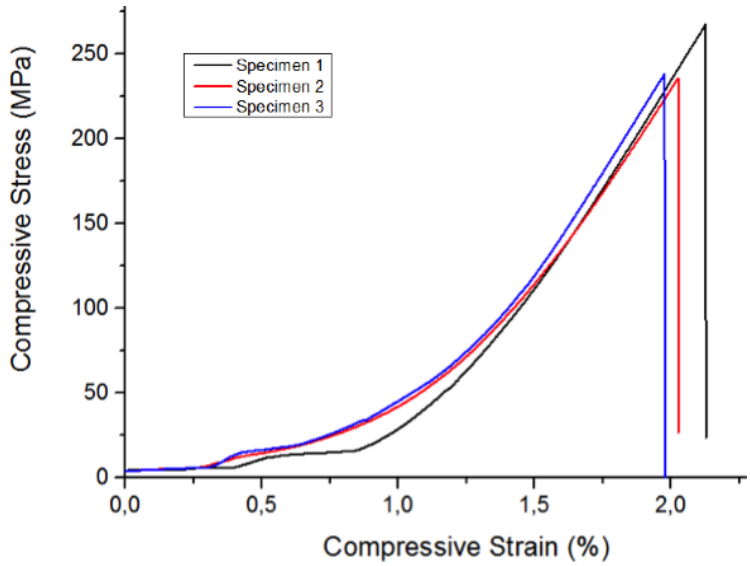


Figure 4.41: Compressive Strength Test of BA Composite

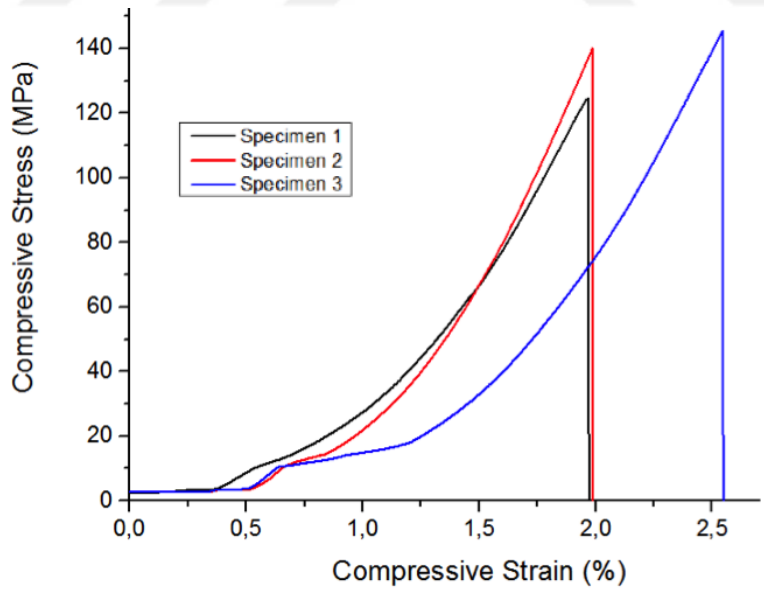


Figure 4.42: Compressive Strength Test of BZ Composite

### 4.6.4 DMA Characterizations

The fiber-reinforced polymeric composites lose their ability to withstand mechanical or thermal loads near their glass transition temperature with softening, decomposition or degradation. The steel or other metals on the other hand, can retain their structural integrity for a long time of period. By dynamic mechanical analysis the change in the storage modulus of the material is measured with temperature increase.

DMA results show that modulus increases and exhibits a value at least double that for neat PBZ (Figure 4.43). Moreover substantial enhancement in the rubbery plateau modulus of the composite also increased significantly compared to neat resin. Glass transition values according to storage modulus are similar with neat resin at around 330 °C. However, the glass transition temperature values according to loss modulus and loss factor values are delayed and increased from around 250 °C to 350 °C. This indicates a good thermal load transfer between resin and fabric.

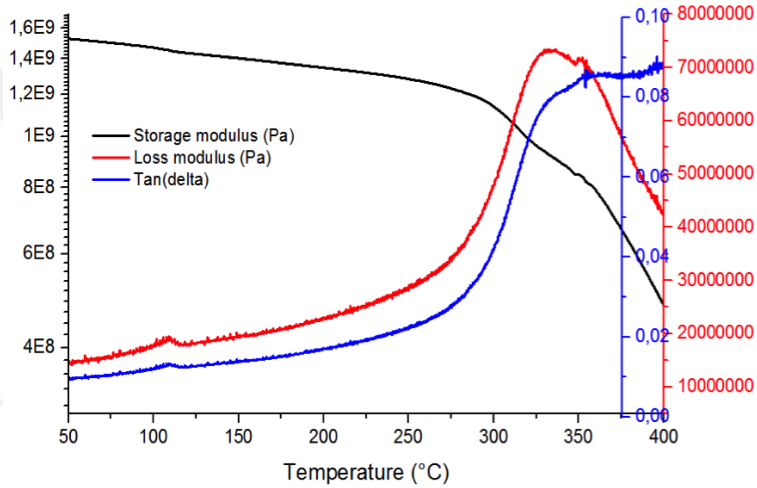


Figure 4.43: DMA graph of BZ High Silica Composite

Table4.14: DMA Results of BA and BZ Composites

| | Tg E' | Tg E'' | Tand Height | $W_{1/2}$ Tand |
|---|---|---|---|---|
| **BA** | 182 | 187 | 0.23 | 20 |
| **BZ** | 323 | 258 | 0.085 | - |

### 4.6.5 Thermomechanical Characterizations

Thermal expansions of the composites were analyzed by thermo-mechanical analyzer (TMA). Coefficient of thermal expansion (CTE) of the materials was measured before and after glass transition temperature (Tg). The significant change in dimension change with time is defined as glass transition temperature in which a significant portion of the material loses intermolecular interaction capability and thus more free to expand.

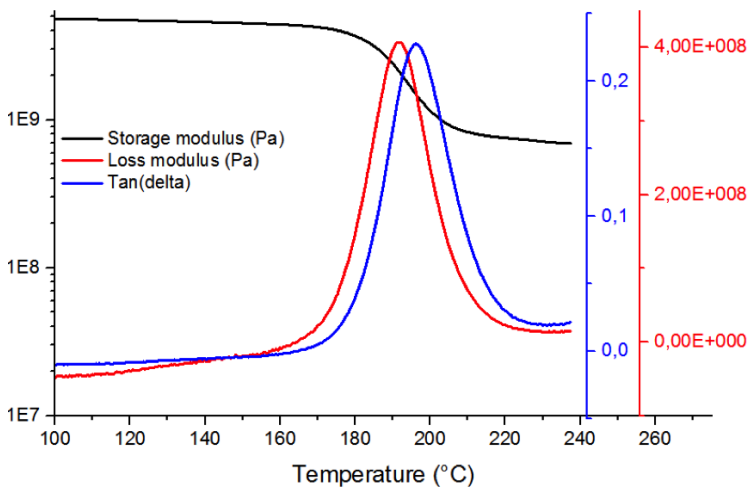


Figure 4.44: DMA graph of BA High Silica Composite

Table 4.15 shows the CTE values of BZ and BA high silica composites before and after Tg.

The results indicated that dimensional change at lower temperature was lower than the dimensional change at higher temperature. The CTE values before and after glass transition were measured from the slope of curves. The point of the sharp change of the thermal expansion behavior was named as glass transition temperature because before this point strong molecular interactions did not allow too much expansion. After the weakening of the intermolecular forces, the expansion capability increases [69].

Table4.15: TMA Results of BA and BZ Composites

| | Tg | CTE @ T<Tg | CTE @ T>Tg | |
|---|---|---|---|---|
| **BA** | 164.17 | 10.72 | 105.69 | 9.86 |
| **BZ** | 285 | 58,6 | 128.4 | 2 |

In both states, thermal expansion coefficient is lower for BA material, which may result better intermolecular interaction between the chains that is in consistent with the previous mechanical, and DMA results. The change in the thermal expansion coefficient on the other hand is much more for BA. This is again in agreement with the previous results. BA composite properties are more dependent to the intermolecular interactions rather than the crosslink property or crosslinking density is higher for BA composite than BZ composite. These secondary force interactions are much more dominant at lower temperatures.

### 4.6.6 Oxyacetylene Torch Characterizations

During the re-entry of a spacecraft vehicle, thermal protection of the components against harsh and short intense thermal and mechanical loads is very important in order to maintain its functionality. In addition while designing the spacecraft vehicles one of the key parameter is the mass gain. For this, increase in the ablation resistance of the materials used with limited

mass is crucial parameter for the design studies.

Oxyacetylene torch test is the most convenient and low cost method and is used for primary evaluation of thermal ablation resistance of materials. The test conditions impart erosive and shear forces on the sample. Oxyacetylene flame test was carried out based on standard ASTME285-08 [70]. Ablation resistance characteristics were measured via volumetric and mass loss manner before and after the ablation. LAR and MAR are defined as the Linear Ablation rate and Mass Ablation rates respectively. LAR and MAR values are defined by the following equations.

$$LAR = dL/dt \tag{4.3}$$

$$MAR = dM/dt \tag{4.4}$$

While calculating the ablation parameters, the difference between initial parameters and final parameters are divided.

The specimens of 30 mm diameter and 10 mm thickness were prepared and they were subjected to a flame torch which has an approximate temperature of 2500 °C for 20 s time duration. The inner diameter of the oxyacetylene torch tip was 2 mm, and the distance between the gun tip and specimen surface was 10 mm. the flow rate ratio of oxygen and acetylene were kept at a constant value of 2.5

The average ablation rate of three samples from each composition is taken as the ultimate ablation rate of BZ and BA composites and the results are shown in Table 4.16.

Table4.16: Oxyacetylene Test Results

| **Sample** | **Mass Ablation Rate g/s** | **Linear Ablation Rate mm/s** |
|---|---|---|
| Silica Phenolic | 0.0638 | - |
| BZ – 1 | 0.054 | 0.095 |
| BZ – 2 | 0,041 | 0.1 |
| BA – 1 | 0,029 | 0.043 |
| BA – 2 | 0,029 | 0.082 |
| BA – 3 | 0,026 | 0.085 |

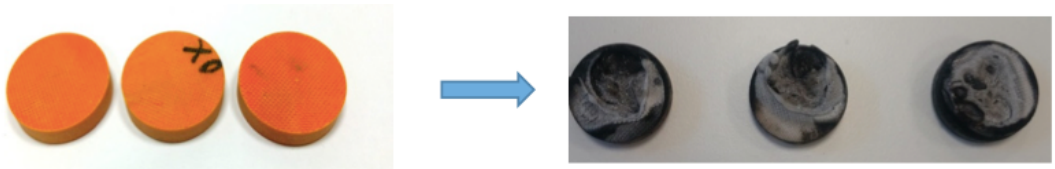

As can be seen from the Figure that, a white coating on the thermoset resin has been occurred. This was result from a consecutive reaction as:

| | | | |
|---|---|---|---|
| $SiO_2$(l) | $\rightarrow$ | $SiO_2$(g) | 1 |
| 1/3 $SiO_2$(l)+C(s) | $\rightarrow$ | 2/3 SiC(s)+ CO(g) | 2 |
| 1/3 $SiO_2$(g)+C(s) | $\rightarrow$ | 2/3 SiC(s)+ CO(g) | 3 |
| 1/3 $SiO_2$(g)+C(s) | $\rightarrow$ | 2/3 SiC(l)+ CO(g) | 4 |
| 1/3 $SiO_2$(l)+C(s) | $\rightarrow$ | 2/3 SiC(s)+ CO(g) | 5 |
| 1/3 $SiO_2$(g)+C(s) | $\rightarrow$ | 2/3 SiC(s)+ CO(g) | 6 |
| 1/3 $SiO_2$(g)+C(s) | $\rightarrow$ | 2/3 SiC(s)+ CO(g) | 7 |
| 1/3 $SiO_2$(l)+C(s) | $\rightarrow$ | 1/2 SiO (l)+ CO(g) | 8 |
| 2 $SiO_2$(l) + SiC(s) | $\rightarrow$ | 3 SiO(g)+ CO(g) | 9 |
| 2 $SiO_2$(l)+ SiC(l) | $\rightarrow$ | 3 SiO(g)+ CO(g) | 10 |

While silicon dioxide melting it absorbs a huge amount of energy cooling the system. The other consecutive reactions are also exothermic result in cooling of the system. Beside the exothermic reactions, a protective layer on the outersurface of the composite has been created which is much stronger than the carboneous char layer and thermally more stable. Although the char yield of BZ composite is higher than the BA composite as discussed in TGA results, the interaction of BA resin with the cloth is stronger than BZ resin composite as explained in the mechanical property discussions. This stronger interaction may result in better efficiency cooling reactions of BA with $SiO_2$.

The results indicate that the ablation performance of BA and BZ high silica composites are quite low and they are both even lower than the reference silica phenolic insulation materials. They have the potential of nozzle insulation materials.

# CHAPTER 5

# CONCLUSION

In the first part of study, synthesis of the designed monomers BA BP and BZ were achieved. BA is a commercial product being sold by some producers, such as HENKEL and HUNTSMAN. Primary characterizations confirm that BA products produced by our laboratory shows similar behaviors with the commercial BA products. The other two monomers BP and BZ are known in literature. But their synthesis methods are quite complex which are not suitable for the large-scale productions. The efficiencies for them are below 60 % and need multi-step purifications. For the new synthetic methods developed in our laboratory, the two monomers can be successfully synthesized with efficiencies more than 90 % without any purification in less than two hours.

DSC thermograms of purified and crude monomers reveal that, the crude products of BA and BZ have wider processing windows compare to purified ones. This allows better processing opportunities with the utilization of the crude products.

Kinetic analysis of the pure monomers shows the theoretical behaviour. The least electron density at the monomer of BZ, which contains electron withdrawing carbonyl group at the para position to phenolic hydroxyl group has the highest tendency toward polymerization. The reason is the destabilized C-O bond.

Thermal analysis of the cured resins shows a general two steps degradation. At first, amine derivatives leave the structure and secondly aromatic backbone degradation occurs. Initial degradation temperature increases with increased strength of six membered intramolecular hydrogen bonding. Char yields are above 30 % for PBA and above 60 % for PBP and PBZ. Mass loss rates indicate the ablation rate behavior and it is the least for PBZ with a broader curve.

Initial characterizations show that BA monomer characteristics are suitable for the structural insulation resin development. For BP and BZ molecule the results indicate that they can be applicable for the nozzle thermal protection systems.

The composite production of BA and BZ can be achieved but due to the lower processing window of BP, the composites could not be produced with resin powder molding method. Solution coating method will be tried for this resin.

Mechanical, thermal and ablation analysis of both BA and BZ high silica composites indicate that corresponding performances of these composites are better than the currently used silica phenolic insulation materials.

# REFERENCES


[1] B. Laub and E. Venkatathy. Thermal protection system technology and facility needs for demanding future planetary missions. In *Proceedings of international workshop on planetary probe atmospheric entry and descent trajectory analysis and science*, Lisbon, Portugal, 2003.

[2] Ashraf Fathy Ahmed and Suong V Hoa. Thermal insulation by heat resistant polymers for solid rocket motor insulation. *Journal of Composite Materials*, 46(13):1549–1559, Jun 2012.

[3] R.P. Nathan and S. Bindu. Low temperature ablative heat shield for re-entry vehicles. In *Proceedings of AIAA thermophysics conference*, Toronto, Ontario, Canada, 2005.

[4] G. Pulci, J. Tirillò, F. Marra, F. Fossati, C. Bartuli, and T. Valente. Carbon–phenolic ablative materials for re-entry space vehicles: Manufacturing and properties. *Composites Part A: Applied Science and Manufacturing*, 41(10):1483–1490, Oct 2010.

[5] E.L. Strauss. *Aspects of polymer degradation and stabilization*, page 528. Elsevier, New York, 1978.

[6] Hatsuo Ishida and Douglas J. Allen. Physical and mechanical characterization of near-zero shrinkage polybenzoxazines. *Journal of Polymer Science Part B: Polymer Physics*, 34(6):1019–1030, Apr 1996.

[7] Hatsuo Ishida and Hong Yee Low. A study on the volumetric expansion of benzoxazine-based phenolic resin. *Macromolecules*, 30(4):1099–1106, Feb 1997.

[8] Frederick W. Holly and Arthur C. Cope. Condensation products of aldehydes and ketones with o-aminobenzyl alcohol and o-hydroxybenzylamine. *Journal of the American Chemical Society*, 66(11):1875–1879, Nov 1944.

[9] H. Schreiber. German Offen, 2,255,504, 1973.

[10] H. Schreiber. German Offen, 2,323,936, 1973.

[11] G. Reiss, J.M. Schwob, G. Guth, M. Roche, and B. Lande. *Advances in Polymer Synthesis*, pages 27–49. Plenum, New York, 1985.

[12] Xin Ning and Hatsuo Ishida. Phenolic materials via ring-opening polymerization: Synthesis and characterization of bisphenol-a based benzoxazines and their polymers. *Journal of Polymer Science Part A: Polymer Chemistry*, 32(6):1121–1129, 1994.

[13] Hajime Kimura, Akihiro Matsumoto, and Keiko Ohtsuka. New type of phenolic resin: Curing reaction of phenol-novolac based benzoxazine with bisoxazoline or epoxy resin using latent curing agent and the properties of the cured resin. *Journal of Applied Polymer Science*, 112(3):1762–1770, May 2009.

[14] Xin Ning and Hatsuo Ishida. Phenolic materials via ring-opening polymerization of benzoxazines: Effect of molecular structure on mechanical and dynamic mechanical properties. *Journal of Polymer Science Part B: Polymer Physics*, 32(5):921–927, 1994.

[15] H. Ishida. Process for preparation of benzoxazine compoundsin solventless systems. U.S. Pat. No. 5,543,516, 1996.

[16] Andrey Chernykh, Jinping Liu, and Hatsuo Ishida. Synthesis and properties of a new crosslinkable polymer containing benzoxazine moiety in the main chain. *Polymer*, 47(22):7664–7669, Oct 2006.

[17] Baris Kiskan, Narendra Nath Ghosh, and Yusuf Yagci. Polybenzoxazine-based composites as high-performance materials. *Polymer International*, 60(2):167–177, Oct 2010.

[18] Tsutomu Takeichi, Koji Nakamura, Tarek Agag, and Hiroyuki Muto. Synthesis of cresol-based benzoxazine monomers containing allyl groups and the properties of the polymers therefrom. *Designed Monomers and Polymers*, 7(6):727–740, 2004.

[19] W.F. Li, S. Shi, R.L. Yu, C.Z. Yao, and Z.H. Feng. Recent development of phenolic resins for rtm processing. *Aerospace. Mater. Technol.*, 34:8–13, 2004.

[20] H. Ishida and Y. Rodriguez. Catalyzing the curing reaction of a new benzoxazine-based phenolic resin. *Journal of Applied Polymer Science*, 58(10):1751–1760, Dec 1995.

[21] Yong-Xia Wang and Hatsuo Ishida. Synthesis and properties of new thermoplastic polymers from substituted 3,4-dihydro-2h-1,3-benzoxazines. *Macromolecules*, 33(8):2839–2847, Apr 2000.

[22] X. Liu and Y. Gu. Study on the volumetric change during ring-opening polymerization of benzoxazines. *Acta. Polym. Sinica.*, pages 612–619, 2000.

[23] Xin Liu and Yi Gu. Study on the volumetric expansion of benzoxazine curing with different catalysts. *Journal of Applied Polymer Science*, 84(6):1107–1113, Feb 2002.

[24] C. Maggana and P. Pissis. Water sorption and diffusion studies in an epoxy resin system. *Journal of Polymer Science Part B: Polymer Physics*, 37(11):1165–1182, Jun 1999.

[25] Sang-Baek Lee, T.J. Rockett, and R.D. Hoffman. Interactions of water with unsaturated polyester, vinyl ester and acrylic resins. *Polymer*, 33(17):3691–3697, Jan 1992.

[26] E.P. Gellert and D.M. Turley. Seawater immersion ageing of glass-fibre reinforced polymer laminates for marine applications. *Composites Part A: Applied Science and Manufacturing*, 30(11):1259–1265, Nov 1999.

[27] S. Ghosh, R. Klett, D. Fink, K.K. Dwivedi, J. Vacik, V. Hnatowicz, and J. Červena. On the penetration of aqueous solutions into pristine and radiation damaged polyimide. *Radiation Physics and Chemistry*, 55(3):271–284, Jul 1999.

[28] M. Kanchanasopa, N. Yanumet, K. Hemvichian, and H. Ishida. The effect of polymerization conditions on the density and tg of bisphenol a and hexafluoroisopropylidene-containing polybenzoxazines. *Polym. Polym. Compos.*, 9(6):367–375, 2001.

[29] G. Wisanrakkit and J.K. Gillham. *The glass transition temperature as a parameter for monitoring the isothermal cure of an amine-cured epoxy system*, pages 143–166. American Chemical Society, Washington D.C., 1990.

[30] K. P. Pang and J. K. Gillham. Anomalous behavior of cured epoxy resins: Density at room temperature versus time and temperature of cure. *Journal of Applied Polymer Science*, 37(7):1969–1991, Mar 1989.

[31] R. A. Venditti, J. K. Gillham, E. Chin, and F. M. Houlihan. Glass transition temperature (tg) versus fractional conversion for a linear thermosetting polyamic acid ester–polyimide system. *Journal of Applied Polymer Science*, 53(4):455–461, Jul 1994.

[32] Fire statistics: Great britain april 2013 to march 2014.

[33] Indrek S. Wichman. Material flammability, combustion, toxicity and fire hazard in transportation. *Progress in Energy and Combustion Science*, 29(3):247–299, Jan 2003.

[34] Hatsuo Ishida and Tarek Agag. *Handbook of Benzoxazine Resins.*

[35] Gamal N. Ahmed, Mark A. Dietenberger, and Water W. Jones. Calculating flame spread on horizontal and vertical surfaces. Technical Report NISTIR 5392, Building and Fire Research Laboratory, National Institute of Standards and Technology, Gaithersburg, April 1994.

[36] Morgan A.B. and Wilkie C.A. *Flame retardant polymer nanocomposites.* Wiley-Interscience, New Jersey, 2007.

[37] Richard E. Lyon and Marc L. Janssens. Polymer flammability. Technical Report DOT/FAA/AR-05/14, Office of Aviation Research, U.S. Department of Transportation, Washington D.C. 20591, May 2005.

[38] C. Martín, J.C. Ronda, and V. Cádiz. Boron-containing novolac resins as flame retardant materials. *Polymer Degradation and Stability*, 91(4):747–754, Apr 2006.

[39] Thomas Hassenklöver, Sabine Predehl, Jyotsna Pilli, Jessica Ledwolorz, Michael Assmann, and Ulf Bickmeyer. Bromophenols, both present in marine organisms and in industrial flame retardants, disturb cellular ca2+ signaling in neuroendocrine cells (pc12). *Aquatic Toxicology*, 76(1):37–45, Jan 2006.

[40] M Sain, S.H Park, F Suhara, and S Law. Flame retardant and mechanical properties of natural fibre–pp composites containing magnesium hydroxide. *Polymer Degradation and Stability*, 83(2):363–367, Feb 2004.

[41] Anna Hermansson, Thomas Hjertberg, and Berntke Sultan. The flame retardant mechanism of polyolefins modified with chalk and silicone elastomer. *Fire and Materials*, 27(2):51–70, 2003.

[42] Xiang-Cheng Bian, Jian-Hua Tang, and Zhong-Ming Li. Flame retardancy of hollow glass microsphere/rigid polyurethane foams in the presence of expandable graphite. *Journal of Applied Polymer Science*, 109(3):1935–1943, 2008.

[43] S. Levchik, A. Piotrowski, E. Weil, and Q. Yao. New developments in flame retardancy of epoxy resins. *Polymer Degradation and Stability*, 88(1):57–62, Apr 2005.

[44] Ging-Ho Hsiue, Shin-Jen Shiao, Hsiao-Fen Wei, Wen-Jang Kuo, and Yi-An Sha. Novel phosphorus-containing dicyclopentadiene-modified phenolic resins for flame-retardancy applications. *Journal of Applied Polymer Science*, 79(2):342–349, 2000.

[45] Jingjing Si, Peijun Xu, Wei He, Shujuan Wang, and Xinli Jing. Bis-benzoxazine resins with high char yield and toughness modified by hyperbranched poly(resorcinol borate). *Composites Part A: Applied Science and Manufacturing*, 43(12):2249–2255, Dec 2012.

[46] Richard N. Walters and Richard E. Lyon. Molar group contributions to polymer flammability. *Journal of Applied Polymer Science*, 87(3):548–563, Nov 2002.

[47] Won-Kook Kim and Wayne L. Mattice. Conformational statistics of a polybenzoxazine. *Computational and Theoretical Polymer Science*, 8(3-4):339–351, Dec 1998.

[48] Ingo Schnell, Steven P. Brown, Hong Yee Low, Hatsuo Ishida, and Hans Wolfgang Spiess. An investigation of hydrogen bonding in benzoxazine dimers by fast magic-angle spinning and double-quantum 1 h nmr spectroscopy. *Journal of the American Chemical Society*, 120(45):11784–11795, Nov 1998.

[49] Gillian R. Goward, Daniel Sebastiani, Ingo Schnell, Hans Wolfgang Spiess, Ho-Dong Kim, and Hatsuo Ishida. Benzoxazine oligomers: Evidence for a helical structure from solid-state nmr spectroscopy and dft-based dynamics and chemical shift calculations. *Journal of the American Chemical Society*, 125(19):5792–5800, May 2003.

[50] Supa Wirasate, Sujitra Dhumrongvaraporn, Douglas J. Allen, and Hatsuo Ishida. Molecular origin of unusual physical and mechanical properties in novel phenolic materials based on benzoxazine chemistry. *Journal of Applied Polymer Science*, 70(7):1299–1306, Nov 1998.

[51] Huntsman. Xu 35610 benzoxazine resin. `https://apps.huntsmanservice.com/WebFolder/ui/browse.do?pFileName=/opt/TDS/Huntsman%20Advanced%20Materials/English%20US/Long/XU%2035610_US_e.pdf`.

[52] Tarek Agag, Jia Liu, Robert Graf, Hans W. Spiess, and Hatsuo Ishida. Benzoxazole resin: A novel class of thermoset polymer via smart benzoxazine resin. *Macromolecules*, 45(22):8991–8997, Nov 2012.

[53] Elliot R. Alexander and Elizabeth J. Underhill. Studies on the mechanism of the mannich reaction. i. ethylmalonic acid, a methynyl compound. *Journal of the American Chemical Society*, 71(12):4014–4019, Dec 1949.

[54] Xiaoying Wang, Feng Chen, and Yi Gu. Influence of electronic effects from bridging groups on synthetic reaction and thermally activated polymerization of bisphenol-based benzoxazines. *Journal of Polymer Science Part A: Polymer Chemistry*, 49(6):1443–1452, 2011.

[55] J. Dunkers and H. Ishida. Vibrational assignments of 3-alkyl-3,4-dihydro-6-methyl-2h-1,3-benzoxazines in the fingerprint region. *Spectrochimica Acta Part A: Molecular and Biomolecular Spectroscopy*, 51(6):1061 – 1074, 1995.

[56] Douglas J. Allen and Hatsuo Ishida. Effect of phenol substitution on the network structure and properties of linear aliphatic diamine-based benzoxazines. *Polymer*, 50(2):613 – 626, 2009.

[57] Douglas J. Allen and Hatsuo Ishida. Polymerization of linear aliphatic diamine-based benzoxazine resins under inert and oxidative environments. *Polymer*, 48(23):6763 – 6772, 2007.

[58] Stephen G. Kuzak and Arun Shanmugam. Dynamic mechanical analysis of fiber-reinforced phenolics. *Journal of Applied Polymer Science*, 73(5):649–658, 1999.

[59] Clarissa Coussirat Angrizani, Heitor Luiz Ornaghi Júnior, Ademir José Zattera, and Sandro Campos Amico. Thermal and mechanical investigation of interlaminate glass/curaua hybrid polymer composites. *Journal of Natural Fibers*, 14(2):271–277, 2017.

[60] Masatsugu Ogata, Noriyuki Kinjo, and Tatsuo Kawata. Effects of crosslinking on physical properties of phenol–formaldehyde novolac cured epoxy resins. *Journal of Applied Polymer Science*, 48(4):583–601, 1993.

[61] Saira Jabeen, Shaukat Saeed, Ayesha Kausar, Bakhtiar Muhammad, Sagheer Gul, and Muhammad Farooq. Influence of chitosan and epoxy cross-linking on physical properties of binary blends. *International Journal of Polymer Analysis and Characterization*, 21(2):163–174, 2016.

[62] Jianxiang Huang, Jian Zhang, Fan Wang, Farong Huang, and Lei Du. The curing reactions of ethynyl-functional benzoxazine. *Reactive and Functional Polymers*, 66(12):1395 – 1403, 2006.

[63] Aravind Dasari, Zhong-Zhen Yu, Gui-Peng Cai, and Yiu-Wing Mai. Recent developments in the fire retardancy of polymeric materials. *Progress in Polymer Science*, 38(9):1357 – 1387, 2013.

[64] Alexander B. Morgan and Jeffrey W. Gilman. An overview of flame retardancy of polymeric materials: application, technology, and future directions. *Fire and Materials*, 37(4):259–279, 2013.

[65] N. Sato, T. Kurauchi, S. Sato, and O. Kamigaito. Microfailure behaviour of randomly dispersed short fibre reinforced thermoplastic composites obtained by direct sem observation. *Journal of Materials Science*, 26(14):3891–3898, 1991.

[66] John J. Brennan and Karl M. Prewo. Silicon carbide fibre reinforced glass-ceramic matrix composites exhibiting high strength and toughness. *Journal of Materials Science*, 17(8):2371–2383, 1982.

[67] G Camino, S.M Lomakin, and M Lazzari. Polydimethylsiloxane thermal degradation part 1. kinetic aspects. *Polymer*, 42(6):2395 – 2402, 2001.

[68] Standard test method for tensile properties of polymer matrix composite materials. ASTM D3039 / D3039M - 14.

[69] W.N. dos Santos, J.A. de Sousa, and R. Gregorio Jr. Thermal conductivity behaviour of polymers around glass transition and crystalline melting temperatures. *Polymer Testing*, 32(5):987 – 994, 2013.

[70] Standard test method for oxyacetylene ablation testing of thermal insulation materials. ASTM E285 - 08(2015), 02 2017.

# APPENDIX A

# SOLVENTLESS WITHOUT CATALYST

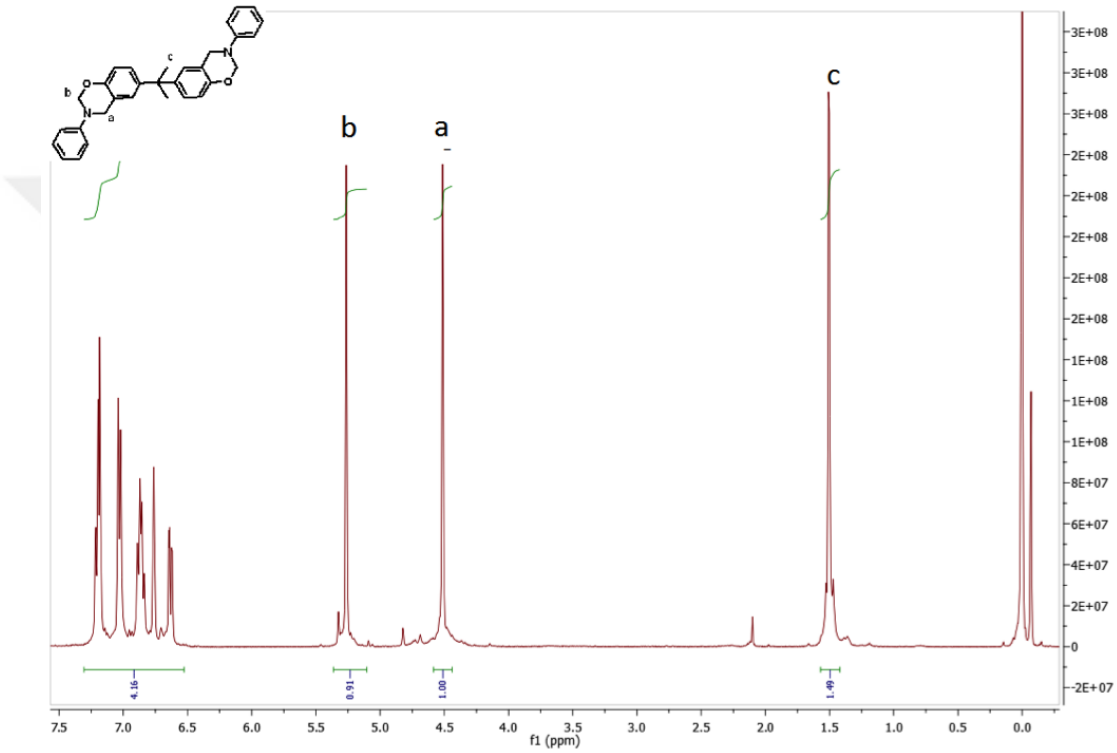


Figure A.1: $^{1}$H NMR spectrum of monomer crude BA synthesized with 20 gr of Bisphenol A, the reaction efficiency is greater than 95 %

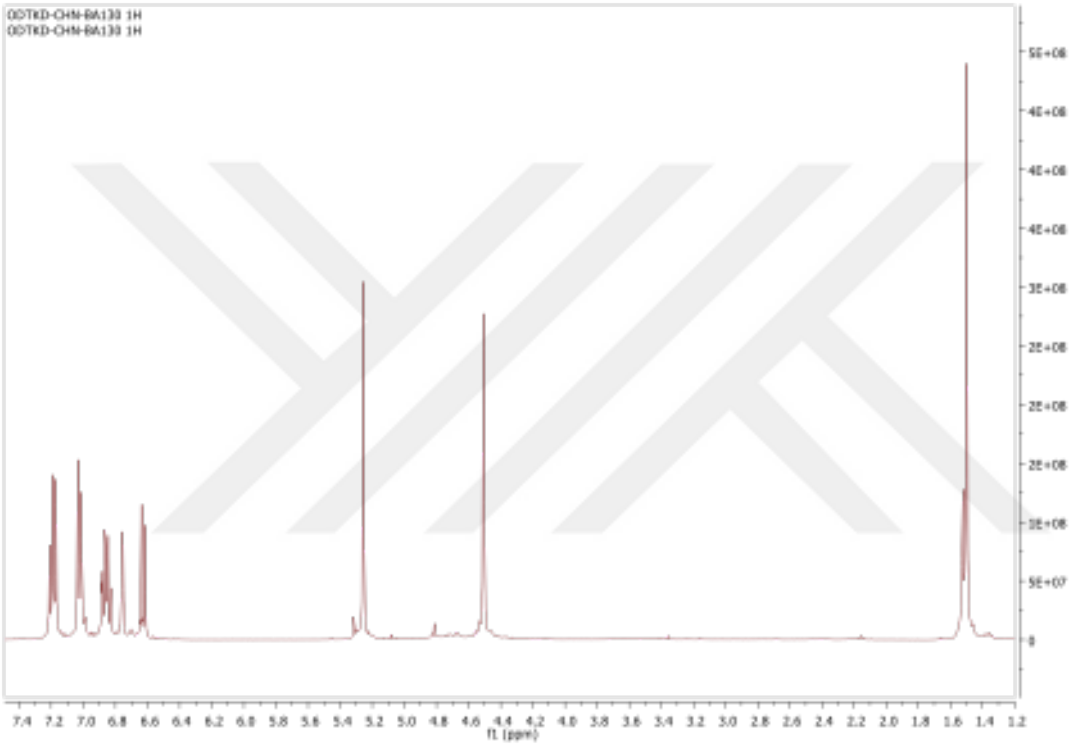


Figure A.2: $^{1}$H NMR spectrum of monomer crude BA synthesized with 100 gr of Bisphenol A, the reaction efficiency is greater than 95 %

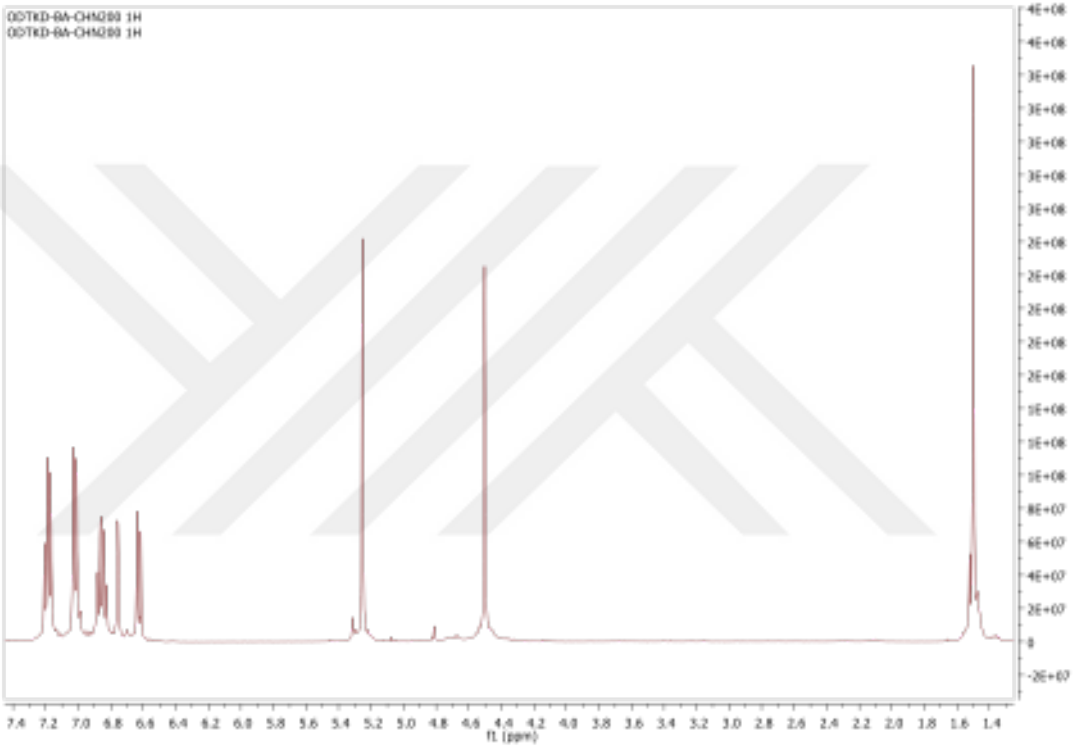


Figure A.3: $^{1}$H NMR spectrum of monomer crude BA synthesized with 200 gr of Bisphenol A, the reaction efficiency is greater than 95 %

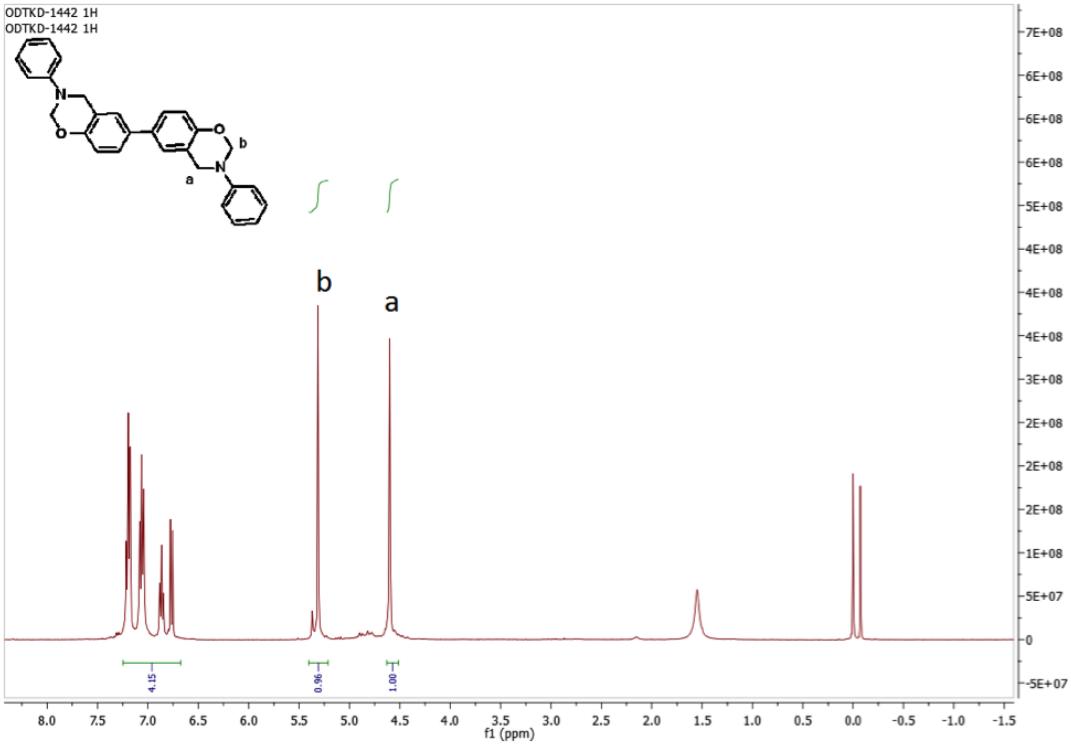


Figure A.4: $^{1}$H NMR spectrum of monomer crude BP synthesized with 10 gr of 4,4-dihydroxybiphenyl, the reaction efficiency is greater than 95 %

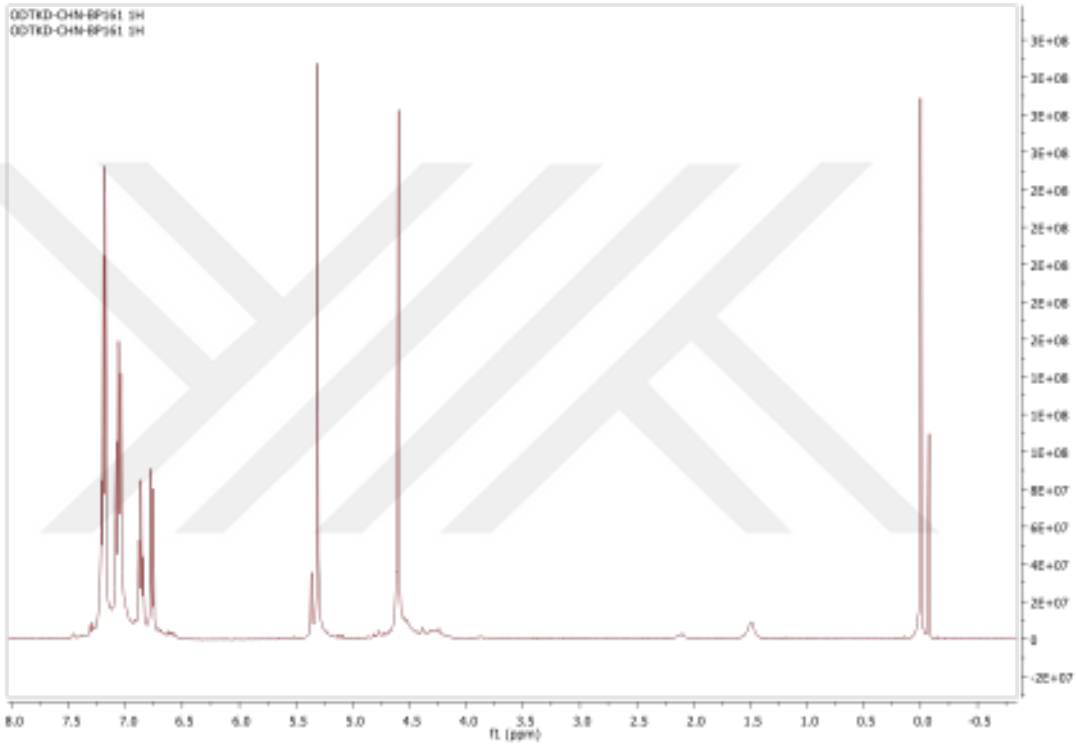


Figure A.5: $^{1}$H NMR spectrum of monomer crude BP synthesized with 20 gr of 4,4-dihydroxybiphenyl, the reaction efficiency is greater than 95 %

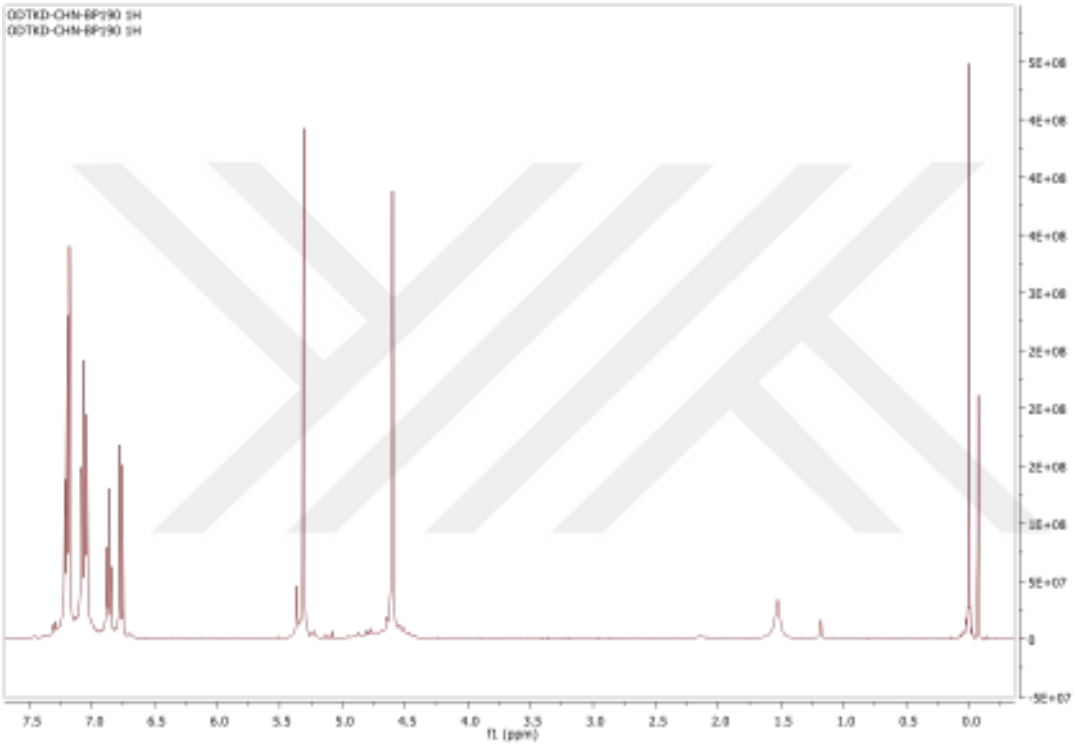


Figure A.6: $^{1}$H NMR spectrum of monomer crude BP synthesized with 100 gr of 4,4-dihydroxybiphenyl, the reaction efficiency is greater than 95 %

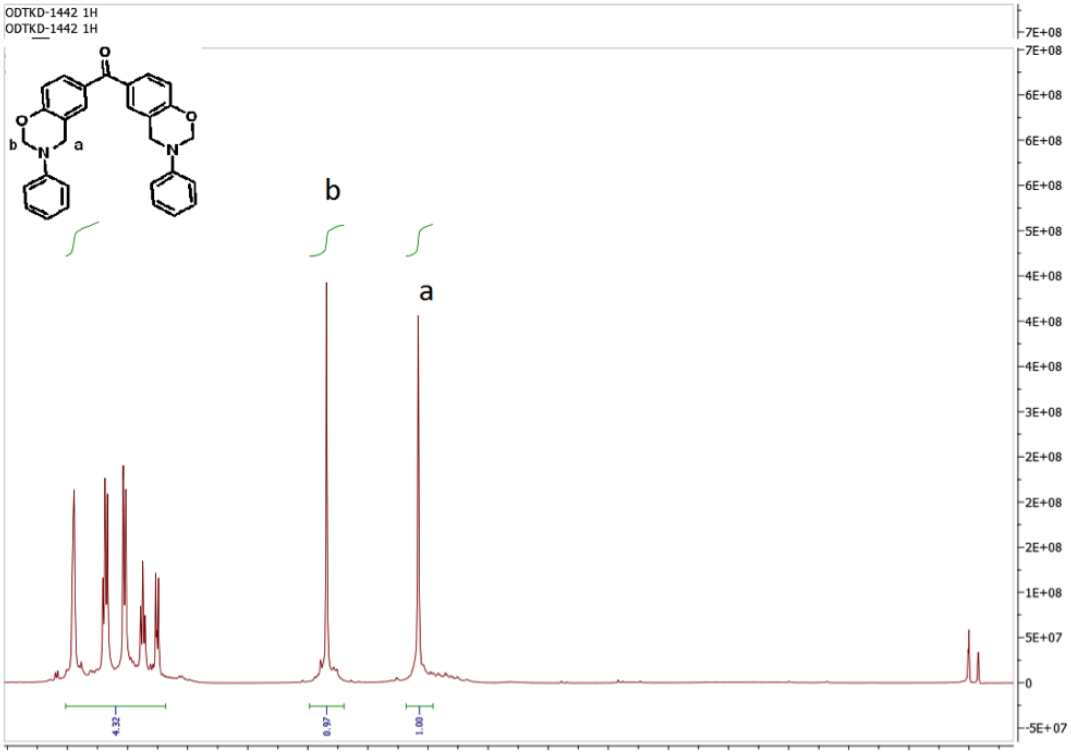


Figure A.7: $^{1}$H NMR spectrum of monomer crude BZ synthesized with gr of 4,4-dihydroxybiphenyl, the reaction efficiency is greater than 95 %

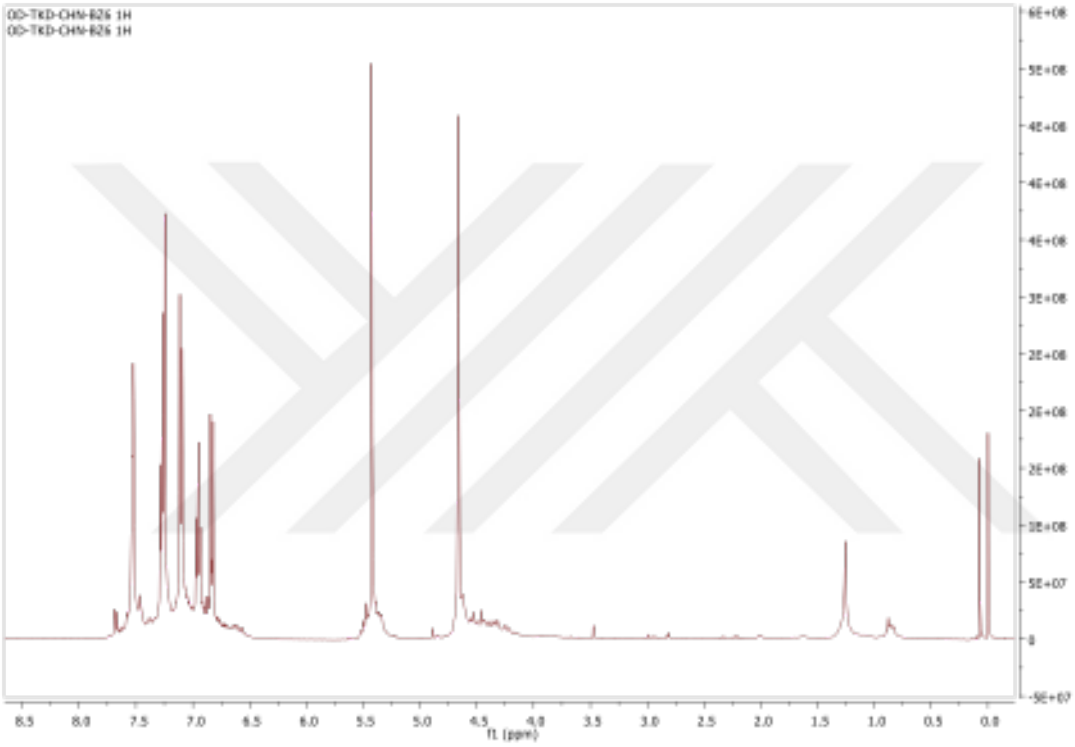


Figure A.8: $^{1}$H NMR spectrum of monomer crude BZ synthesized with 20 gr of 4,4-dihydroxybiphenyl, the reaction efficiency is greater than 95 %

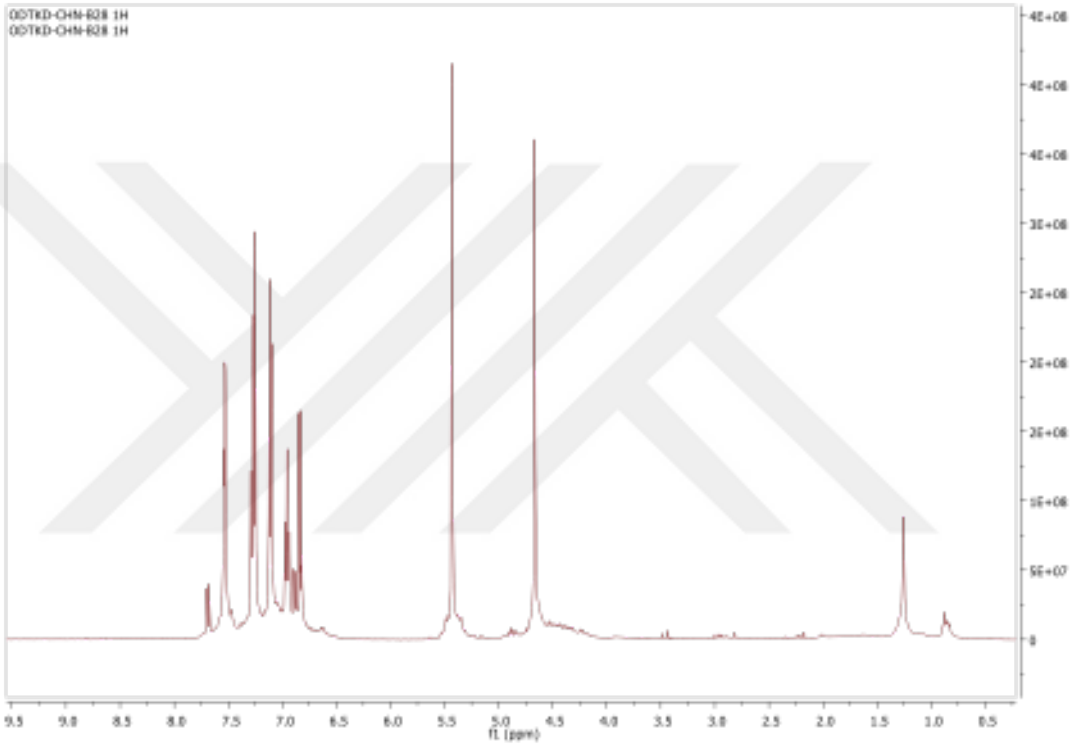


Figure A.9: $^{1}$H NMR spectrum of monomer crude BZ synthesized with 300 gr of 4,4-dihydroxybiphenyl, the reaction efficiency is greater than 95 %

# APPENDIX B

# DSC AND TGA ANALYSIS OF PBA

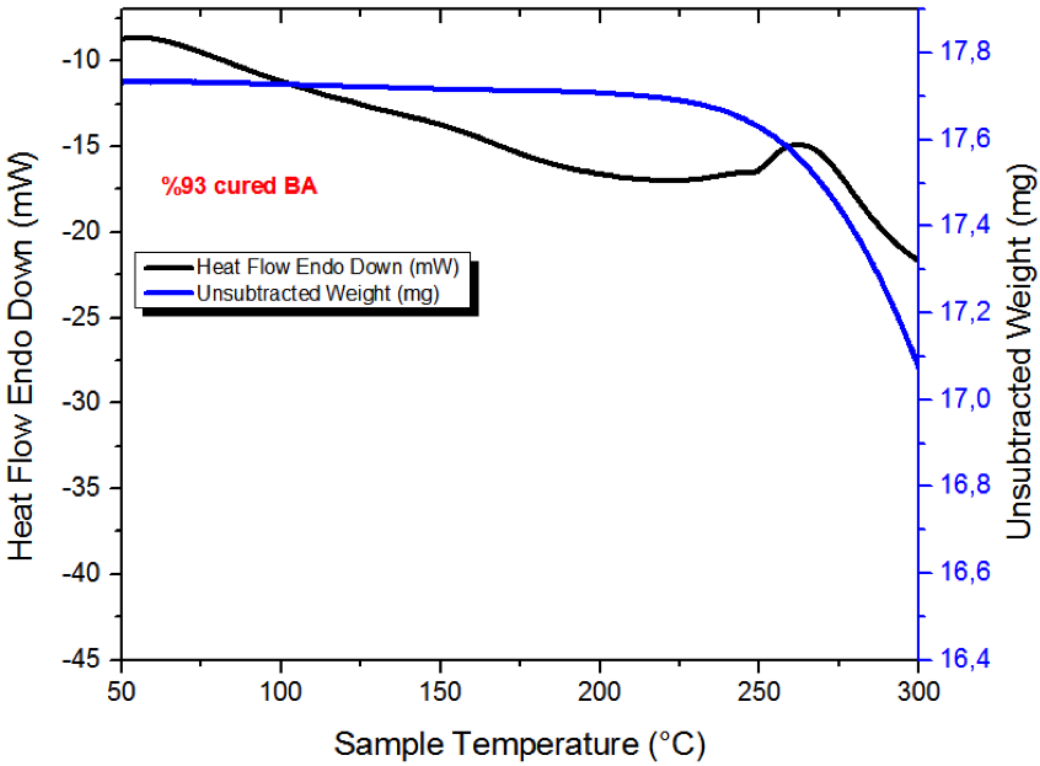


Figure B.1: DSC and TGA analysis of PBA after 93 % curing indicating mass loss during cure

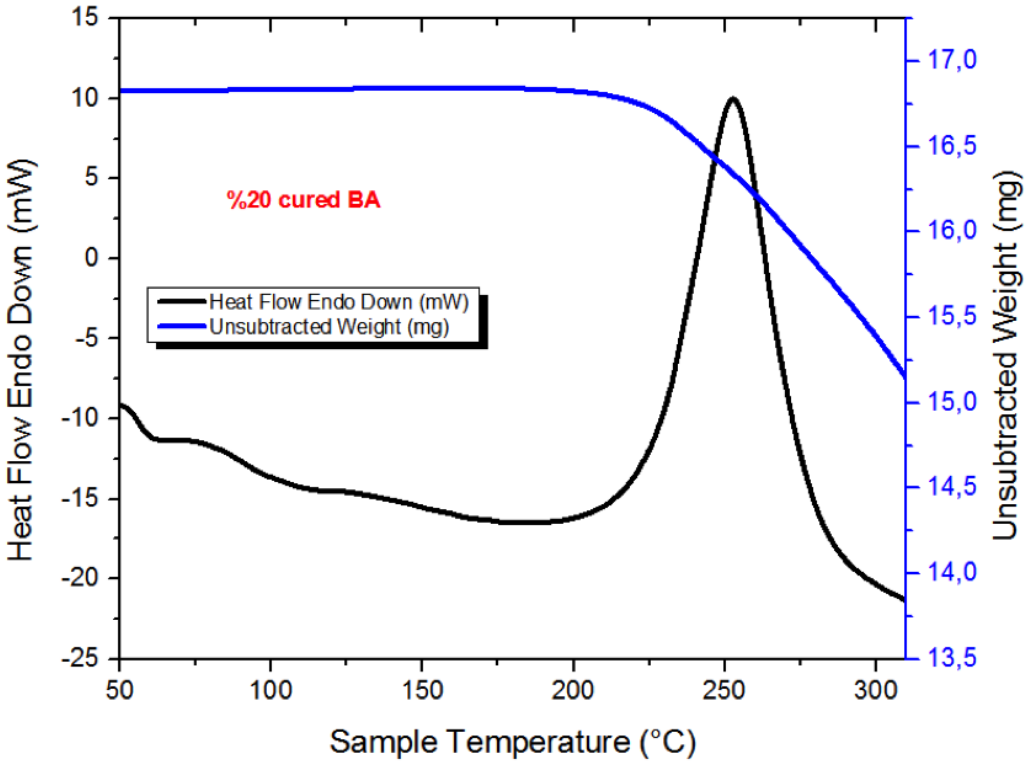


Figure B.2: DSC and TGA analysis of PBA after 20 % curing indicating mass loss during cure

# CURRICULUM VITAE

## PERSONAL INFORMATION

**Surname, Name:** Kaya Deniz, Tuğba
**Nationality:** Turkish (TC)
**Date and Place of Birth:** 3.5.1985, Koyulhisar
**Marital Status:** Married
**Phone:** +905547056665
**e-mail:** tugbakayadeniz@gmail.com

## EDUCATION

| Degree | Institution | Year of Graduation |
|---|---|---|
| M.Sc. | METU - Polymer Science & Technology | 2012 |
| B.Sc. | METU - Chemistry Education | 2010 |
| High School | Edirne Anadolu Öğretmen Lisesi | 2003 |

## PROFESSIONAL EXPERIENCE

| Year | Place | Enrollment |
|---|---|---|
| 07.2007-03.2009 | Prof. Ataman's Research Group - METU Dept. of Chemistry | Researcher |
| 01.2010-10.2012 | Prof. Çırpan's Research Group - METU Dept. of Chemistry | Researcher |
| 10.2012-10.2016 | Prof. Bayramlı's Research Group - METU Dept. of Chemistry | Researcher |
| 10.2016- Present | Roketsan Missiles Industries Inc. | Senior Engineer |

## PUBLICATIONS

### International Conference Publications

Tayfun U., Deniz T.K., Dogan M., Bayramli E., "Investigations on the Short Carbon Fiber Reinforced Polyurethane Elastomer Composites", 4th International Polymeric Composites Symposium (IPC 2015), Izmir/Turkey 2015

Kaya Deniz T., Nurioglu A.G., Unlu N.A., Cirpan A., "Polymer Light Emitting Diode Applications of Biphenyl Containing Conjugated Copolymers", NANOTRVIII, 8th Nanoscience-Nanotechnology Congress & IANM 3rd World Congress, 2012

**National Conference Publications**

Kaya Deniz T., Doğan Ö, Bayramlı E., "Diamin Türevi Benzoksazin Monomer ve Polimerlerin Sentezi, Karakterizasyonu ve Termal Özelliklerinin Araştırılması", 27. Ulusal Kimya Kongresi, Kimya 2015

Kaya Deniz T., Doğan Ö, Bayramlı E., "Yüksek Performanslı Polinaftoksazin Sentezi ve Karakterizasyonu", V. Ulusal Polimer Bilim ve Teknolojisi Kongresi, 2014

**Journal Papers**

Kaya Deniz T., Apaydın D.K., Özelcaglayan A.C., Toppare L., Çırpan A., "Photo- and electroluminescence behavior of biphenyl derivative in blends with poly(vinylcarbazole)", Turkish Journal of Chemistry, 37 (2013) 538-546

Kaya Deniz T., Nurioglu A.G., Ünlü N.A., Şendur M., Toppare L., Çırpan A. "Syntheses, Electrochemical and Photophysical Properties of Biphenyl Containing Conjugated Copolymers" Polymer 2013, 54, 2243-2249

Ünlü N.A., Kaya Deniz T, İendur M., Çırpan A. "Effect Of Dithienopyrrole Unit On Electrochromic And Optical Properties Of Benzotriazole Based Conjugated Polymers" Macromolecular Chemistry and Physics 2012, 213, 1885-1891 (Front Cover)

Savaş L.A., Kaya Deniz T., Tayfun Ü, Doğan M. "Effect of microcapsulated red phosphorus on flame retardant, thermal and mechanical properties of thermoplastic polyurethane composites filled with huntite &hydromagnesite mineral", Polymer Degradation and Stability, 135, December 2016